FILLING OF CARBON *NANO*-TUBES WITH NANO ACTIVE METAL SPECIES AND THEIR STUDIES ON THE PHYSICO-CHEMICAL BEHAVIORS

A DISSERTATION SUBMITTED TO THE DEPARTMENT OF CHEMISTRY IN THE PARTIAL FULFILLMENT OF THE REQUIREMENT FOR THE DEGREE OF MASTER OF PHILOSOPHY IN CHEMISTRY(PHYSICAL-INORGANIC)

M.Phil THESIS

SUBMITTED BY
MD. SYDUR RAHMAN
STUDENT ID: 0413033206
SESSION: APRIL-2013

BANGLADESH UNIVERSITY OF ENGINEERING AND TECHNOLOGY

October 2016
Dhaka, Bangladesh

CHEMISTRY (PHYSICAL-INORGANIC)
DEPARTMENT OF CHEMISTRY

Bangladesh University of Engineering and Technology

Department of Chemistry

Certification of Thesis

A thesis on
FILLING OF CARBON *NANO*-TUBES WITH NANO ACTIVE METAL SPECIES AND THEIR STUDIES ON THE PHYSICO-CHEMICAL BEHAVIORS

By
MD. SYDUR RAHMAN

has been accepted as satisfactory in partial fulfilment of requirements for the degree of master of philosophy (M.Phil) in chemistry and certify that the student has demonstrated a satisfactory knowledge of the field covered by this thesis in an oral examination held on September 7, 2016.

Board of Examiners

1. **Dr. Md. Nazrul Islam**
   Professor
   Department of Chemistry, BUET, Dhaka
   (Supervisor)

   _____
   Chairman

2. **Head**
   Department of Chemistry, BUET, Dhaka

   _____
   Member (Ex-Officio)
   07.09.2016

3. **Dr. Shakila Rahman**
   Professor
   Department of Chemistry, BUET, Dhaka

   _____
   Member

4. **Dr. Md. Shafiul Azam**
   Assistant Professor
   Department of Chemistry, BUET, Dhaka.

   _____
   Member

5. **Dr. Md. Mufazzal Hossain**
   Professor
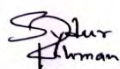   Department of Chemistry, University of Dhaka

   _____
   Member(External)

CANDIDATE'S DECLARATION

It is hereby declare that this thesis or any part of it has not been submitted elsewhere for the award of any degree or diploma.
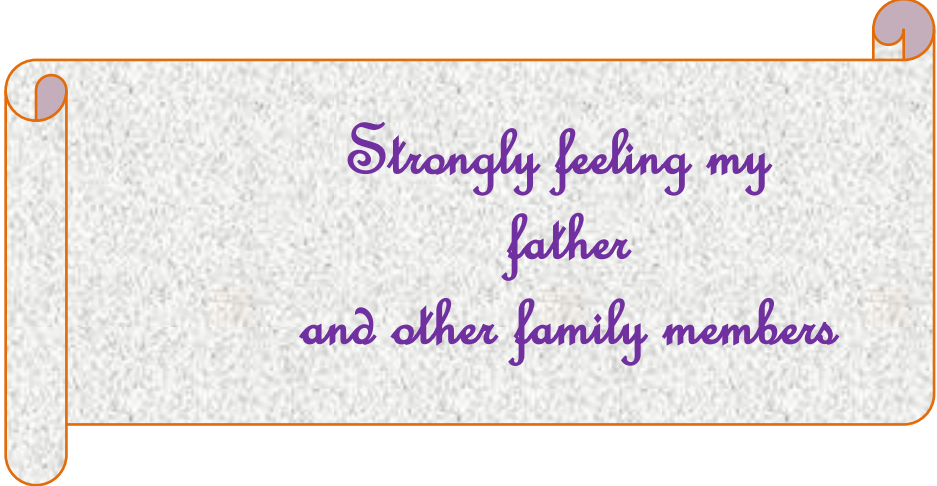
…………………..
Signature

MD. SYDUR RAHMAN
Candidate
M.Phil student
Student ID:0413033206
Department of Chemistry, BUET

Strongly feeling my
father
and other family members

ACKNOWLEDGEMENT

Thesis Content

LIST OF FIGURES

LIST OF TABLES

ABSTRACT

Nanomaterials exhibit interesting physical properties distinct from both the molecular and broad scales, presenting new opportunities for physico-chemical as well as biomedical researches and applications in various areas of chemistry, biology and medicine. The unique chemical, physical and mechanical properties of CNTs have stimulated extensive investigation since their discovery in early1990s by Iijima.The present reserch interest focuses on the development of simple and cost effective way for the synthesis of CNTs and proposes the new idea of bulk chemical method.

Filling hollow CNTs with chosen materials opens new possibilities of generating nearly one dimensional nanostrutures. One simple approach to fill the hollow cavity of CNTs is continuous boiling of the mixture suspension of CNTs and other nanoactive species at 100 ^{o}C for several hours. For the filling purposes four nanoactive metal species (NiO, Ni, Mn$_3$O$_4$, MnO$_2$) were prepared using established conventional methods. NiO nanoparticles were prepared using precipitation method. Ni nanoparticles were prepared by control reduction of NiO nanoparticles. Mn$_3$O$_4$ nanoparticles were prepared from hydrolysis of manganese (ll) acetate. MnO$_2$ were prepared by treating manganese (ll) acetate with potassium permanganate.

Nanoparticles increase chemical activity due to crystallographic surface structure with their large surface to volume ratio. This has promoted research to check the antibacterial activity of the prepared Mn$_3$O$_4$ nanop articles of definite size . Researches have been reported on CNT-based drug delivery. CNT itself don't have any antibacterial activity and can easily release the carring drugs to the target places at definite chemical environments.

Adsorption of methylene blue dyes on the surface of NiO loaded CNTs represents an important and intensively studied phenomenon. From the adsorption studies it was observed that the rate constant(k_2) of CNTs and NiO is 1.82×10^{-5} gμg^{-1}min^{-1} and 1.27×10^{-4} gμg^{-1}min^{-1}. Here it should be clear that the adsorption capacity is higher for CNTs than NiO nanoparticles but it is comperatively time cosuming. The rate constant(k_2) of NiO loaded CNTs is 6.62×10^{-5} gμg^{-1}min^{-1}. The adsorption rate of NiO filled CNTs are slightly higher than CNTs. This is because of the total increasd surface area of NiO nanoparticles loaded CNTs. This excess surface area as well as the overall functionalization did impact on the rate of adsorption.

CHAPTER ONE

INTRODUCTION

INTRODUCTION

1.1. Motivation

Nanotechnology and nanoscience is about controlling and understanding matter on the sub-micrometer and atomic scale. "Nano" refers to the scale of objects measured in nanometers (nm). By definition it is the exciting multidisciplinary field that involves the design and engineering of objects or tools, characterization, production, and application of structures, devices, and systems by controlled manipulation of size and shape at nanometer scale (atomic, molecular, and macromolecular scale) that produces structures, devices, and systems with at least one novel/superior characteristic or property.

Fullerenes and other related graphitic structures have many fascinating electronic, chemical, and mechanical properties. They are particularly interesting for the nanomaterials research in order to develop substances with predefined properties oriented towards specific technological applications. Among the large variety of nanostructures in the fullerene family, recently one particular member has become the focus of a great deal of scientific and technological attention: the carbon nanotube(shortly CNT). The basic structural unit of a CNT is a graphitic sheet rolled into a cylinder, while the tube tip is closed by hemispherical or polyhedral graphitic domes or fullerines. In practice, we can roughly divide CNTs into two different classes, either by considering their structure or synthesis method, these are single-walled carbon nanotubes(SWCNTs) and multi-walled carbon nanotubes (MWCNTs) . The first class includes cylinders formed by a single graphitic layer where the typical diameter is 1–1.5 nm[1]. And sometimes the diameter reaches to 3-4 nm[2]. SWCNTs are recovered from the fluffy carbon powder which coats the vacuum chamber.

The second class of tube includes structures formed by the coaxial arrangement of several (2–50) SWCNTs; their external diameter is of the order of 2-100 nm[3] and if the participation of SWCNTs increases then the outside diameter increases paralally. They are synthesized using a pure carbon arc run in an inert-gas atmosphere and are found in the deposit formed on the cathode. Aside from their nanoscopic dimensions and their remarkable thermal and mechanical robustness, their main attractive feature relates to the predicted electronic properties; theoretical calculations indicate that nanotubes

may be insulators, semiconductors, or metals depending on their radius and helicity. If the tube radius increases, the properties of the tubes approach those of macroscopic planar graphite.

Another fascinating aspect of CNTs is their cavities, which can be used to incorporate atoms or molecules in order to generate novel compounds or nanostructured materials. These nanocavities may even display catalytic activity. Furthermore, the very long cavities of the CNTs may potentially be used as templates for elongated nanostructures. Some successful attempts to form long nanometric filaments were based on the electric-arc method, using composite electrodes impregnated with the filling material. But although these experiments led to the observation of a great variety of interesting filled graphitic structures, the efficiency and control of the process was very low hindering further development. But, since the synthesis methods of CNTs are rather efficient, it is feasible to separate the production and filling procedures. A promising approach exploits the capillary properties of the CNTs.

Since the discovery of CNTs in 1991 by Iijima[4,5] they have been extensively studied by researchers in various fields such as chemical, physical, materials and bio-chemical sciences. CNTs have unique nanostructure with remarkably mechanical, thermal and electrical properties, which made them highly attractive for the use as reinforcement in nano-tube based composite materials.

CNTs exhibit many unique intrinsic physical and chemical properties and have been intensively explored for biological and biomedical applications in the past few years. Nano-materials have sizes ranging from about one nanometer up to several hundred nanometers, comparably to many biological macromolecules such as enzymes, antibodies, and DNA plasmids. Materials in this size range exhibit interesting physical properties, distinct from both the molecular and bulk scales presenting new opportunities for bio-medical research and applications in various including biology and medicine. The emerging field of bio-nanotechnology bridges the physical science with biological sciences via chemical methods in developing novel tools and platforms for understanding biological systems and diseases diagnosis and treatment.

The development of new and efficient drug delivery systems is of fundamental importance to improve the pharmacological profiles of many classes of therapeutic molecules. Many different types of drug delivery systems are currently available. Within the family of nanomaterials, CNTs have emerged as a new alternative and efficient tool for transporting and translocating therapeutic molecules. CNT can be functionalised with bioactive peptides, proteins, nucleic acids and drugs, and used to deliver their cargos to cells and organs. Because functionalised CNTs display low toxicity

and are not immunogenic[6,7], such systems hold great potential in the field of bio-nanotechnology and nanomedicine.

The ultimate goal of this research is to develop the preparation technique of the CNTs(MWCNTs) and some other nanometal and metal oxides and filling these nanometal and metal oxides into CNTs in a suitable way and checkout their various physico -chemical characteristics.

In this chapter basic insight of the structure, chemistry and properties of CNTs, filled matrices of CNTs, the present stages of development on this field and the scope of the future research are discussed.

1.2. Carbon nanotubes(CNTs)

A significant nanoparticle discovery that came to light in 1991 was carbon nanotubes[8]. Where buckyballs are round, nanotubes are cylinders that haven't folded around to create a sphere. CNTs are composed of carbon atoms linked in hexagonal shapes, with each carbon atom covalently bonded to three other carbon atoms. CNTs are allotropes of carbon with a cylindrical nanostructure. CNT has been constructed with length-to-diameter ratio of up to 132,000,000:1, significantly larger than for any other material. These cylindrical carbon molecules have unusual properties, which are valuable for nanotechnology, electronics, optics and other fields of material science and technology. In particular, owing to their extraordinary thermal conductivity and mechanical and electrical properties, CNTs find applications as additives to various structural materials. Although, like buckyballs, CNTs are strong, they are not brittle. They can be bent, and when released, they will spring back to their original shape. The general imaging view of CNTs are illustrated in Figure(1.1).
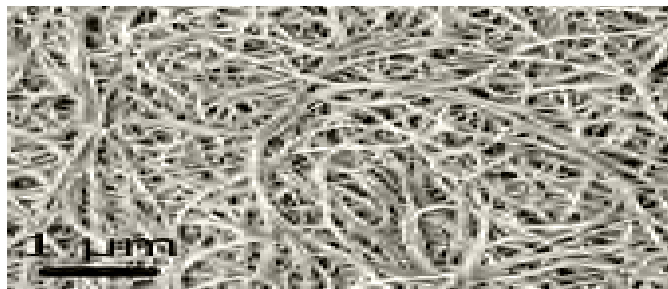
Figure 1.1: Scanning electron microscopic image of carbon nanotubes

1.2.1.   Classification of CNTs

Structurally, CNTs can be viewed as wrapped of graphene sheets. SWCNTs have one layer of graphene sheet, whereas, the MWCNTs contain multi layers of graphene sheets. Individual nanotubes naturally align themselves into "ropes" held together by van der Waals forces, more specifically, pi-stacking.

Applied quantum chemistry, specifically, orbital hybridization best describes chemical bonding in nanotubes. The chemical bonding of nanotubes is composed entirely of sp^2 bonds, similar to those of graphite. These bonds, which are stronger than the sp^3 bonds found in alkanes and diamond, provide nanotubes with their unique strength.

1.2.1.1.   Single walled carbon nanotubes (SWCNTs)
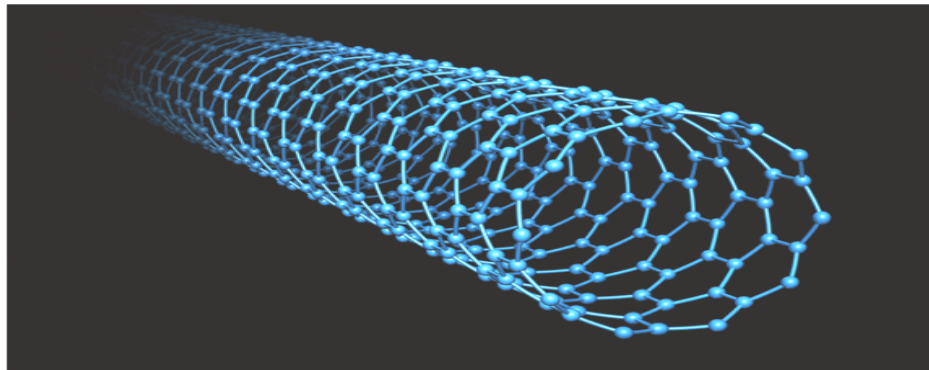
Figure 1.2: Image of single-walled carbon nanotube

Most SWCNTs (Figure 1.2) have a diameter of close to 1-3 nanometers, with a tube length that can be many millions of times longer. The structure of a SWCNT diagramed as Figure(1.3) can be conceptualized by wrapping a one-atom-thick layer of graphite called graphene into a seamless cylinder.
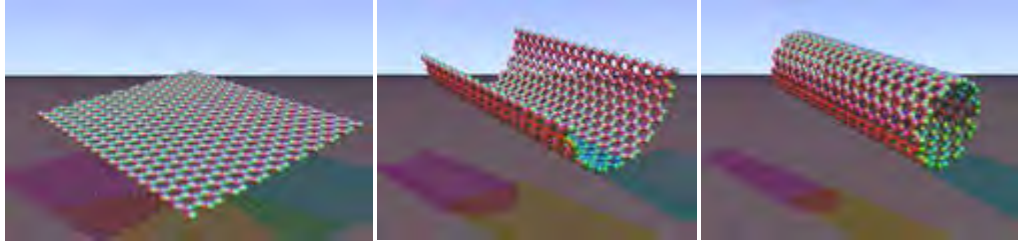
Figure 1.3: "Roll up" the graphene sheet to make the carbon nanotube.

In particular, their band gap can vary from zero to about 2 eV and their electrical conductivity can show metallic or semiconducting behavior. SWCNTs are likely candidates for miniaturizing electronics. The most basic building block of these systems is the electric wire, and SWCNTs with diameters of an order of a nanometer can be excellent conductors. One useful application of SWCNTs is in the development of the first intermolecular field-effect transistors (FET). The first intermolecular logic gate using SWCNT FETs was made in 2001. A logic gate requires both a p-FET and an n-FET. Because SWCNTs are p-FETs when exposed to oxygen and n-FETs otherwise, it is possible to protect half of an SWCNT from oxygen exposure, while exposing the other half to oxygen. This results in a single SWCNT that acts as a non logic gate with both p and n-type FETs within the same molecule.

SWCNTs are too expensive for widespread application but are forecast to make a large impact in electronics applications by 2020 according to The Global Market for CNTs report.

1.2.1.2. Multi-walled carbon nanotubes(MWCNTs)

MWCNTs consist of multiple rolled layers (concentric tubes) of graphene. There are two models that can be used to describe the structures of multi-walled nanotubes. Sheets of graphite are arranged in concentric cylinders, e.g., a SWCNT within a larger SWCNT. But in the Parchment model, a single sheet of graphite is rolled in around itself, resembling a scroll of parchment or a rolled newspaper. The interlayer distance in multi-walled nanotubes is close to the distance between graphene layers in graphite, approximately 3.4 Å. Its individual shells can be described as SWCNTs, which can be metallic or semiconducting. The schematic diagram of MWCNT can be sighted as Figure(1.4).
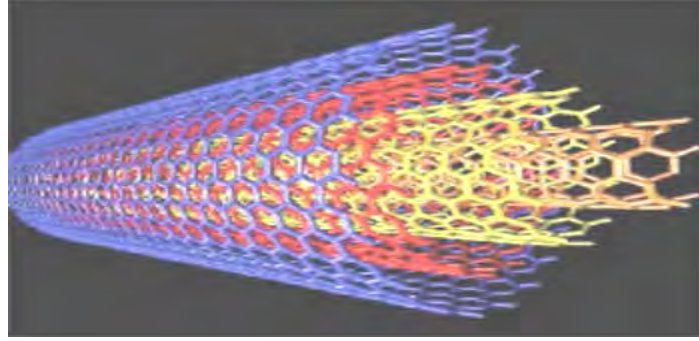
Figure 1.4: Multi-walled carbon nanotube(concentric)

The telescopic motion ability of inner shells and their unique mechanical properties will permit the use of MWCNTs as main movable arms in coming nanomechanical devices. Retraction force that occurs to telescopic motion caused by the <u>Lennard-Jones interaction</u> between shells and its value is about 1.5 nN.

1.2.2. General properties of CNTs

1.2.2.1. Electrical conductivity

CNTs can be highly conducting, and hence can be said to be metallic. Their conductivity has been shown to be a function of their chirality, the degree of twist as well as their diameter. CNTs can be either metallic or semi-conducting in their electrical behavior. Conductivity in MWCNTs is quite complex. Some types of "armchair"-structured CNTs appear to conduct better than other metallic CNTs. Furthermore, interwall reactions within MWCNTs have been found to redistribute the current over individual tubes non-uniformly. However, there is no change in current across different parts of metallic SWCNTs. The behavior of the ropes of semi-conducting SWCNTs is different, in that the transport current changes abruptly at various positions on the CNTs.

The conductivity and resistivity of ropes of SWCNTs **[9,10]** has been measured by placing electrodes at different parts of the CNTs. It has been reported that individual single walled nanotubes may contain defects. Fortuitously, these defects allow the SWCNTs to act as transistors. Likewise, joining CNTs together may form transistor-like devices. A CNT with a natural junction (where a straight metallic section is joined to a chiral semiconducting section) behaves as a rectifying diode – i.e., a

half-transistor in a single molecule. It has also recently been reported that SWCNTs can route electrical signals at speeds up to 10 GHz when used as interconnects on semi-conducting devices.

1.2.2.2. Strength and elasticity

The carbon atoms of a single sheet of graphite form a planar honeycomb lattice, in which each atom is connected via a strong chemical bond to three neighboring atoms. Because of these strong bonds, the basal plane elastic modulus of graphite is one of the largest of any known material. For this reason, CNTs are expected to be the ultimate high-strength fibers[11]. SWCNTs are stiffer than steel, and are very resistant to damage from physical forces. Pressing on the tip of a nanotube will cause it to bend, but without damage to the tip. When the force is removed, the CNT returns to its original state. This property makes CNTs very useful as probe tips for very high-resolution scanning probe microscopy. Quantifying these effects has been rather difficult, and an exact numerical value has not been agreed upon.

Using atomic force microscopy, the unanchored ends of a freestanding CNT can be pushed out of their equilibrium position, and the force required to push the CNT can be measured. The current Young's modulus value of single-walled nanotubes is about 1 teraPascal, but this value has been widely disputed, and a value as high as 1.8 Tpa has been reported. Other values significantly higher than that have also been reported. The differences probably arise through different experimental measurement techniques.

1.2.2.3. Thermal conductivity and expansion

All CNTs are expected to be very good thermal conductors[12] along the tube, exhibiting a property known as "ballistic conduction", but good insulators laterally to the tube axis. Measurements show that a SWCNT has a room-temperature thermal conductivity along its axis of about 3500 $W \cdot m^{-1} \cdot K^{-1}$, compare this to copper, a metal well known for its good thermal conductivity, which transmits 385 $W \cdot m^{-1} \cdot K^{-1}$. A SWCNT has a room-temperature thermal conductivity across its axis (in the radial direction) of about 1.52 $W \cdot m^{-1} \cdot K^{-1}$, which is about as thermally conductive as soil. The temperature stability of CNTs is estimated to be up to 2800 °C in vacuum and about 750 °C in air.

Many applications of CNTs, such as in nanoscale molecular electronics, sensing and actuating devices, or as reinforcing additive fibers in functional composite materials, have been proposed. Reports of several recent experiments on the preparation and mechanical characterization of CNT-polymer composites have also appeared. These measurements suggest modest enhancements in strength of characteristics of CNT-embedded matrixes as compared to bare polymer matrixes. It is expected, therefore, that CNT reinforcements in polymeric materials may also significantly improve the thermal and thermomechanical properties of the composites.

1.2.2.4. Field emission

Field emission results from the tunneling of electrons from a metal tip into vacuum, under application of a strong electric field. The small diameter and high aspect ratio of CNTs is very favorable for field emission. Even for moderate voltages, a strong electric field develops at the free end of supported CNTs because of their sharpness. It is remarkable that some years later Samsung actually realized a very bright color display, which will be shortly commercialized using this technology. Studying the field emission properties of MWCNTs, Bonard and co-workers at EPFL observed that together with electrons, light is emitted as well. This luminescence is induced by the electron field emission, since it is not detected without applied potential. This light emission occurs in the visible part of the spectrum, and can sometimes be seen with the naked eye.

1.2.2.5. High aspect ratio

CNTs represent a very small, high aspect ratio conductive additive for plastics of all types. Their high aspect ratio means that a lower loading of CNTs is needed compared to other conductive additives to achieve the same electrical conductivity. This low loading preserves more of the polymer resin's toughness, especially at low temperatures, as well as maintaining other key performance properties of the matrix resin. CNTs have proven to be an excellent additive to impart electrical conductivity in plastics. Their high aspect ratio, about 1000:1 imparts electrical conductivity at lower loadings, compared to conventional additive materials such as carbon black, chopped carbon fiber, or stainless steel fiber.

1.2.2.6. Highly adsorbency

The large surface area and high adsorbency of CNTs **[13,14,15]** make them ideal candidates for use in air, gas, and water filtration. A lot of research is being done in replacing activated charcoal with CNTs in certain ultra high purity applications.

1.2.2.7. Hardness

Standard single-walled carbon nanotubes can withstand a pressure up to 25 GPa without deformation. They then undergo a transformation to superhard phase nanotubes**[16]**. Maximum pressures measured using current experimental techniques are around 55 GPa. However, these new superhard phase nanotubes collapse at an even higher, albeit unknown, pressure.

The bulk modulus of superhard phase nanotubes is 462 to 546 GPa, even higher than that of diamond (420 GPa for single diamond crystal).

1.2.2.8. Kinetic properties

MWCNTs are multiple concentric nanotubes precisely nested within one another. These exhibit a striking telescoping property whereby an inner nanotube core may slide, almost without friction, within its outer nanotube shell, thus creating an atomically perfect linear or rotational bearing. This is one of the first true examples of molecular nanotechnology, the precise positioning of atoms to create useful machines. Already, this property has been utilized to create the world's smallest rotational motor. Future applications such as a gigahertz mechanical oscillator are also envisioned.

1.2.3. Functionalization of CNTs

CNTs are unfortunately insoluble in many liquids such as water, polymer resins, and most solvents. Thus they are difficult to evenly disperse in a liquid matrix such as epoxies and other polymers. This complicates efforts to utilize the nanotubes outstanding physical properties in the manufacture of

composite materials, as well as in other practical applications which require preparation of uniform mixtures of CNTs with many different organic, inorganic, and polymeric materials.

To make nanotubes more easily dispersible in liquids, it is necessary to physically or chemically attach certain molecules, or functional groups, to their smooth sidewalls without significantly changing the CNTs' desirable properties. This process is called functionalization. The production of composite materials requires strong covalent chemical bonding between the filler particles and the polymer matrix, rather than the much weaker van der Waals physical bonds which occur if the CNTs are not properly functionalized.

Functionalization methods such as filling, oxidation, and "wrapping" of the CNTs in certain polymers can create more active bonding sites on the surface of the nanotubes. For biological uses, CNTs can be functionalized by attaching biological molecules, such as lipids, proteins, biotins, etc. to them[17,18]. Then they can usefully mimic certain biological functions, such as protein adsorption, and bind to DNA and drug molecules. This would enable medially and commercially significant applications such as gene therapy[19] and drug delivery[20-24]. In biochemical and chemical applications such as the development of very specific biosensors, molecules such as carboxylic acid (-COOH), poly m-aminobenzoic sulfonic acid (PABS), polyimide, and polyvinyl alcohol (PVA) have been used to functionalize CNTs, as have amino acid derivatives, halogens, and compounds. Some types of functionalized CNTs are soluble in water and other highly polar, aqueous solvents.

1.2.4. Applications of functionalized & filled CNTs

1.2.4.1. Conductive or reinforced plastics

Much of the history of plastics over the last half-century has involved their use as a replacement for metals. For structural applications, plastics have made tremendous headway, but not where electrical conductivity is required, because plastics are very good electrical insulators. This deficiency is overcome by loading plastics up with conductive fillers, such as carbon black and larger graphite fibers. The loading required to provide the necessary conductivity using conventional fillers is typically high, however, resulting in heavy parts, and more importantly, plastic parts whose structural

properties are highly degraded. It is well-established that the higher the aspect ratio of the filler particles, the lower the loading required to achieve a given level of conductivity.

CNTs are ideal in this sense, since they have the highest aspect ratio of any carbon fiber. In addition, their natural tendency to form ropes provides inherently very long conductive pathways even at ultra-low loadings. Applications that exploit this behavior of CNTs include EMI/RFI shielding composites; coatings for enclosures, gaskets, and other uses such as electrostatic dissipation; antistatic materials, transparent conductive coatings; and radar-absorbing materials for stealth applications. A lot of automotive plastics companies are using CNTs as well. CNTs have been added into the side mirror plastics on automobiles in the US since the late 1990s.

1.2.4.2.   Biomedical applications

The exploration of CNTs in biomedical applications is just underway, but has significant potential. Due to their extraordinary physical and chemical properties CNTs reveal a promising potential as biomedical agents for heating, temperature sensoring and drug delivery on the cellular level. Filling CNTs with nanoactive materials realises nanoscaled containers in which the active content is encapsulated by a protecting carbon shell. Since a large part of the human body consists of carbon, it is generally thought of as a very biocompatible material. Cells have been shown to grow on CNTs, so they appear to have no toxic effect. The cells also do not adhere to the CNTs, potentially giving rise to applications such as coatings for prosthetics and surgical implants. The ability to functionalize the sidewalls of CNTs also leads to biomedical applications such as neuron growth and regeneration. It has also been shown that a single strand of DNA can be bonded to a nanotube, which can then be successfully inserted into a cell; this has potential applications in gene therapy. Here the biomedical applications of CNTs are illustrated by Figure(1.5).
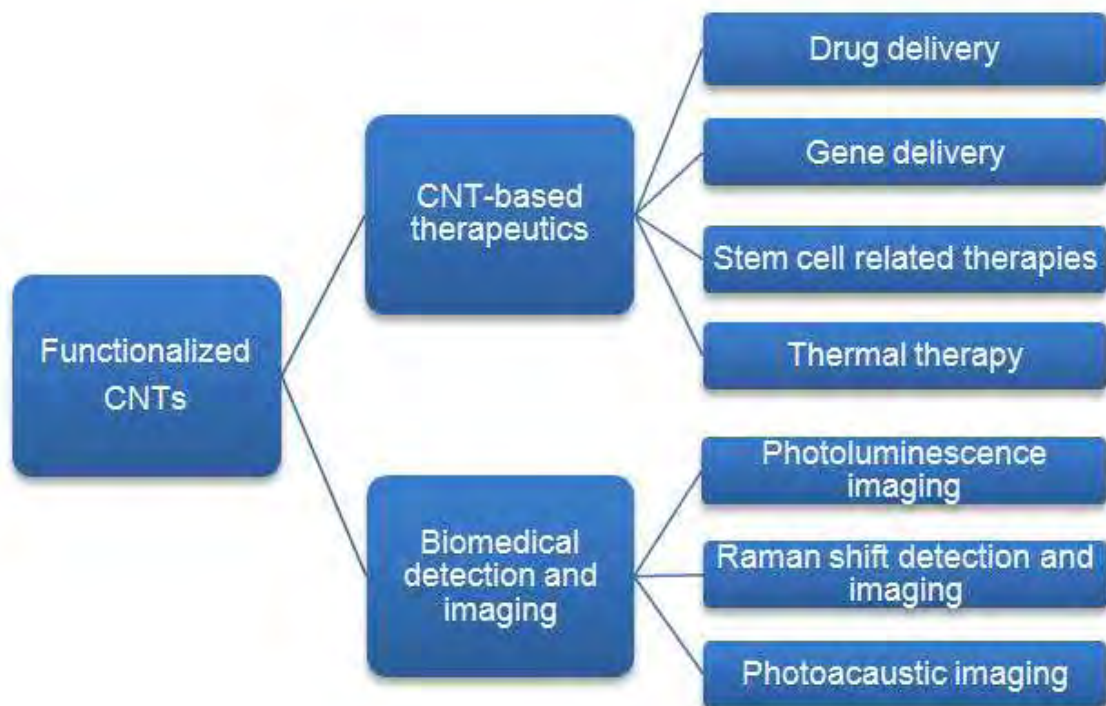
Figure 1.5: Biomedical applications of functionalized CNTs

1.2.4.3.   Nanobiotechnological applications of Filled CNTs

With the great development in new filling methodologies for preparing endohedral CNTs, encapsulation strategies employing biomedically relevant molecular guests have emerged rapidly in recent years. All of these hybrid nanomaterials feature distinct properties and potential applications depending on both the chemical nature and spatial arrangement of the encapsulated molecular guests. The most significant examples in which CNT hybrids, filled with suitable molecular species, are used for biomedical applications[25,26]. CNTs containing strongly emitting molecules hold great promises for diagnostic devices, whereas those filled with radioactive species and magnetically-active nanoparticles are attracting considerable attention for theranostic applications. The use of the CNT's tubular cavity as an active reservoir for the controlled release of drugs is also significant.

1.2.4.4.   Energy storage

CNTs have the intrinsic characteristics desired in material used as electrodes in batteries and capacitors, two technologies of rapidly increasing importance. CNTs have a tremendously high surface area, good electrical conductivity, and very importantly, their linear geometry makes their surface highly accessible to the electrolyte.

Research has shown that CNTs have the highest reversible capacity of any carbon material for use in lithium ion batteries. In addition, CNTs are outstanding materials for super capacitor electrodes and are now being marketed for this application. CNTs also have applications in a variety of fuel cell components. They have a number of properties, including high surface area and thermal conductivity, which make them useful as electrode catalyst supports in PEM fuel cells. Because of their high electrical conductivity, they may also be used in gas diffusion layers, as well as current collectors. CNT's high strength and toughness-to-weight characteristics may also prove valuable as part of composite components in fuel cells that are deployed in transport applications, where durability is extremely important.

1.2.4.5. Conductive adhesives and connectors

The same properties that make CNTs attractive as conductive fillers for use in electromagnetic shielding, ESD materials, etc., make them attractive for electronics packaging and interconnection applications, such as adhesives, potting compounds, coaxial cables, and other types of connectors.

1.2.4.6. Molecular electronics

The idea of building electronic circuits out of the essential building blocks of materials - molecules - has seen a revival the past few years, and is a key component of nanotechnology. In any electronic circuit, but particularly as dimensions shrink to the nanoscale, the interconnections between switches and other active devices become increasingly important. Their geometry, electrical conductivity, and ability to be precisely derived, make CNTs the ideal candidates for the connections in molecular electronics. In addition, they have been demonstrated as switches themselves.

There are already companies such as Nantero from Woburn, that is already making CNT based non-volitle random access memory for PC's. A lot of research is being done to design CNT based transistors as well.

1.2.4.7.   Structural composites

The superior properties of CNTs are not limited to electrical and thermal conductivities, but also include mechanical properties, such as stiffness, toughness, and strength. These properties lead to a wealth of applications exploiting them, including advanced composites requiring high values of one or more of these properties.

1.2.4.8.   Fibers and fabrics

Fibers spun of pure CNTs have recently been demonstrated and are undergoing rapid development, along with CNT composite fibers. Such super-strong fibers will have many applications including body and vehicle armor, transmission line cables, woven fabrics and textiles.

1.2.4.9.   Catalyst support

CNTs intrinsically have an enormously high surface area; in fact, for SWCNTs every atom is not just on one surface - each atom is on two surfaces, the inside and the outside of the nanotube! Combined with the ability to attach essentially any chemical species to their sidewalls this provides an opportunity for unique catalyst supports. Their electrical conductivity may also be exploited in the search for new catalysts and catalytic behavior.

1.2.4.10.   CNT ceramics

A ceramic material reinforced with CNTs has been made by materials scientists at UC Davis. The new material is far tougher than conventional ceramics, conducts electricity and can both conduct heat and act as a thermal barrier, depending on the orientation of the CNTs. Ceramic materials are very hard and resistant to heat and chemical attack, making them useful for applications such as coating turbine blades, but they are also very brittle.

The researchers mixed powdered alumina (aluminum oxide) with 5 to 10 percent CNTs and a further 5 percent finely milled niobium. The researchers treated the mixture with an electrical pulse in a process called spark-plasma sintering. This process consolidates ceramic powders more quickly and at lower temperatures than conventional processes.

The new material has up to five times the fracture toughness, resistance to cracking under stress of conventional alumina. The material shows electrical conductivity seven times that of previous ceramics made with CNTs. It also has interesting thermal properties, conducting heat in one direction, along the alignment of the nanotubes, but reflecting heat at right angles to the CNTs, making it an attractive material for thermal barrier coatings.

1.2.4.11. Air, water and gas filtration

Many researchers and corporations have already developed CNT based air and water filtration devices. It has been reported that these filters can block the smallest particles. This is another area where CNTs have already been commercialized and products are on the market now. Someday CNTs may be used to filter other liquids such as fuels and lubricants as well.

A lot of research is being done in the development of CNT based air and gas filtration. Filtration has been shown to be another area where it is cost effective to use CNTs already. The research suggests that 1 gram of MWCNTs can be dispersed onto 1 sq ft of filter media. Manufacturers can get their cost down to 35 cents per gram of purified MWCNTs when purchasing ton quantities.

1.2.4.12. Thermal materials

The record-setting anisotropic thermal conductivity of CNTs is enabling many applications where heat needs to move from one place to another. Such an application is found in electronics, particularly heat sinks for chips used in advanced computing, where uncooled chips now routinely reach over 100°C. The technology for creating aligned structures and ribbons of CNTs is a step toward realizing incredibly efficient heat conduits. In addition, composites with CNTs have been shown to dramatically increase their bulk thermal conductivity, even at very small loadings.

1.2.4.13. Other applications

Some commercial products on the market today utilizing CNTs include stain resistant textiles, CNT reinforced tennis rackets and baseball bats. Companies like Kraft foods are heavily funding CNT based plastic packaging. Food will stay fresh longer if the packaging is less permeable to atmosphere. Coors Brewing Company has developed new plastic beer bottles that stay cold for longer periods of

time. Samsung already has CNT based flat panel displays on the market. A lot of companies are looking forward to being able to produce transparent conductive coatings and phase out ITO coatings. Samsung uses align SWCNTs in the transparent conductive layer of their display manufacturing process.

1.2.5. Carbon nanotubes production & purification methods

There are a number of methods of making CNTs and fullerenes. CNTs have probably been around for a lot longer than was first realized, and may have been made during various carbon combustion and vapor deposition processes, but electron microscopy at that time was not advanced enough to distinguish them from other types of tubes. Some well recognized synthesis methods are..

1.2.5.1. Arc Discharge Method
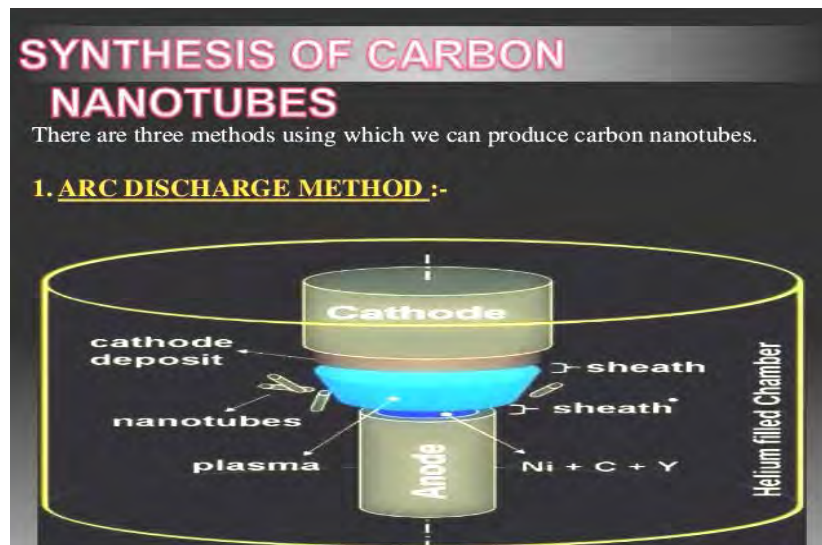
Figure 1.6: Arc discharge method to prepare CNTs

The carbon arc discharge method, initially used for producing C60 fullerenes, is the most common and perhaps easiest way to produce CNTs, as it is rather simple[27-32]. However, it is a technique that produces a complex mixture of components, and requires further purification - to separate the CNTs from the soot and the residual catalytic metals present in the crude product. This method

creates CNTs through arc-vaporization of two carbon rods (Figure 1.6) placed end to end, separated by approximately 1mm, in an enclosure that is usually filled with inert gas at low pressure. Recent investigations have shown that it is also possible to create CNTs with the arc method in liquid nitrogen. A direct current of 50 to 100 A, driven by a potential difference of approximately 20 V, creates a high temperature discharge between the two electrodes. The discharge vaporizes the surface of one of the carbon electrodes, and forms a small rod-shaped deposit on the other electrode. Producing CNTs in high yield depends on the uniformity of the plasma arc, and the temperature of the deposit forming on the carbon electrode.

1.2.5.2.   LaserAblation Method
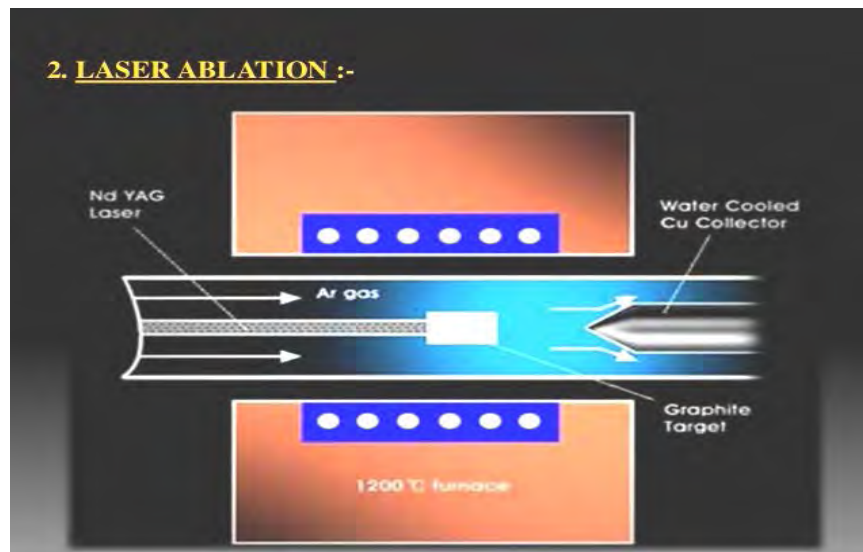
Figure 1.7: Laser ablation method to prepare CNTs

In 1996 CNTs were first synthesized using a dual-pulsed laser and achieved yields of >70wt% purity. Samples were prepared by laser vaporization (Figure 1.7) of graphite rods with a 50:50 catalyst mixture of Cobalt and nickel at 1200°C in flowing argon, followed by heat treatment in a vacuum at 1000°C to remove the C60 and other fullerenes. The initial laser vaporization pulse was followed by a second pulse, to vaporize the target more uniformly. The use of two successive laser pulses minimizes the amount of carbon deposited as soot. The second laser pulse breaks up the larger particles ablated by the first one, and feeds them into the growing nanotube structure.

The material produced by this method appears as a mat of "ropes", 10-20nm in diameter and up to 100μm or more in length[33-37]. Each rope is found to consist primarily of a bundle of SWCNTs, aligned along a common axis. By varying the growth temperature, the catalyst composition, and other process parameters, the average nanotube diameter and size distribution can be varied. Arc-discharge and laser vaporization are currently the principal methods for obtaining small quantities of high quality CNTs. However, both methods suffer from drawbacks. The first is that both methods involve evaporating the carbon source, so it has been unclear how to scale up production to the industrial level using these approaches. The second issue relates to the fact that vaporization methods grow CNTs in highly tangled forms, mixed with unwanted forms of carbon and/or metal species. The CNTs thus produced are difficult to purify, manipulate, and assemble for building nanotube-device architectures for practical applications.

1.2.5.3.   Chemical Vapor Deposition(CVD) Method
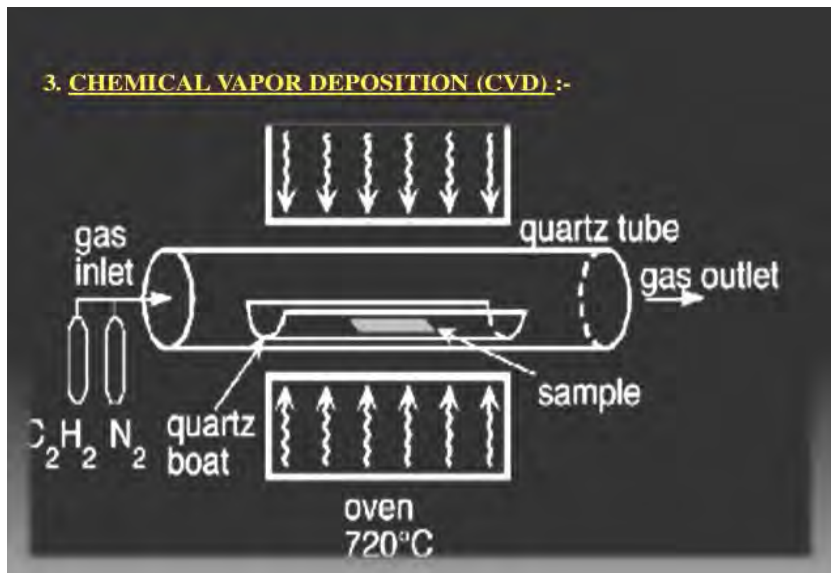
Figure 1.8: Chemical vapor deposition method to prepare CNTs

Chemical vapor deposition (Figure 1.8) of hydrocarbons over a metal catalyst is a classical method that has been used to produce various carbon materials such as carbon fibers and filaments for over twenty years[38-43]. Large amounts of CNTs can be formed by catalytic CVD of acetylene over cobalt and iron catalysts supported on silica or zeolite. The carbon deposition activity seems to relate to the cobalt content of the catalyst, whereas the CNTs' selectivity seems to be a function of the pH

in catalyst preparation. Fullerenes and bundles of single walled nanotubes were also found among the multi walled nanotubes produced on the carbon/zeolite catalyst. Some researchers are experimenting with the formation of CNTs from ethylene. Supported catalysts such as iron, cobalt, and nickel, containing either a single metal or a mixture of metals, seem to induce the growth of isolated SWCNTs or SWCNTs in the ethylene atmosphere. The production of single walled nanotubes, as well as double-walled CNTs, on molybdenum and molybdenum-iron alloy catalysts has also been demonstrated. CVD of carbon within the pores of a thin alumina template with or without a Nickel catalyst has been achieved. Ethylene was used with reaction temperatures of 545°C for Nickel-catalyzed CVD, and 900°C for an uncatalyzed process. The resultant carbon nanostructures have open ends, with no caps. Methane has also been used as a carbon source. In particular it has been used to obtain 'nanotube chips' containing isolated single walled nanotubes at controlled locations. High yields of single walled nanotubes have been obtained by catalytic decomposition of an H_2/CH_4 mixture over well-dispersed metal particles such as Cobalt, Nickel, and Iron on magnesium oxide at 1000°C. It has been reported that the synthesis of composite powders containing well-dispersed CNTs can be achieved by selective reduction in an H_2/CH_4 atmosphere of oxide solid solutions between a non-reducible oxide such as Al_2O_3 or $MgAl_2O_4$ and one or more transition metal oxides. The reduction produces very small transition metal particles at a temperature of usually >800°C. The decomposition of CH_4 over the freshly formed nanoparticles prevents their further growth, and thus results in a very high proportion of SWCNTs and fewer MWCNTs. The following instrumental arrangement (Figure 1.9) used for the deposition of the vaporized CNTs.

Figure 1.9: Instrumental arrangements of Chemical Vapor Deposition method

1.2.5.4.   Ball Milling Method

Ball milling and subsequent annealing is a simple method**[44,45]** for the production of CNTs. Although it is well established that mechanical attrition of this type can lead to fully nanoporous microstructures, it was not until a few years ago that CNTs of carbon and boron nitride were produced from these powders by thermal annealing. Essentially the method consists of placing graphite powder into a stainless steel container along with four hardened steel balls. The container is purged, and argon is introduced. The milling is carried out at room temperature for up to 150 hours. Following milling, the powder is annealed under an inert gas flow at temperatures of 1400°C for six hours. The mechanism of this process is not known, but it is thought that the ball milling process forms nanotube nuclei, and the annealing process activates nanotube growth. Research has shown that this method produces more MWCNTs and few SWCNTs.

1.2.5.5.   Other preparation methods

CNTs can also be produced by diffusion flame synthesis, electrolysis, use of solar energy, heat treatment of a polymer, and low-temperature solid pyrolysis. In flame synthesis, combustion of a portion of the hydrocarbon gas provides the elevated temperature required, with the remaining fuel conveniently serving as the required hydrocarbon reagent. Hence the flame constitutes an efficient source of both energy and hydrocarbon raw material. Combustion synthesis has been shown to be scalable for high-volume commercial production.

1.2.6.   Carbon nanotubes purification methods

Purification of CNTs generally refers to the separation of CNTs from other entities, such as carbon nanoparticles, amorphous carbon, residual catalyst, and other unwanted species. Generally, a centrifugal separation is necessary to concentrate the single walled nanotubes in low-yield soot before the micro filtration operation, since the nanoparticles easily contaminate membrane filters. The advantage of this method is that unwanted nanoparticles and amorphous carbon are removed

simultaneously and the CNTs are not chemically modified. However 2-3 mol nitric acid is useful for chemically removing impurities[46,47].

It is now possible to cut CNTs into smaller segments, by extended sonication in concentrated acid mixtures. The resulting CNTs form a colloidal suspension in solvents. They can be deposited on substrates, or further manipulated in solution, and can have many different functional groups attached to the ends and sides of the CNTs.

Gas phase

The first successful technique for purification of CNTs was developed by Thomas Ebbesen and coworkers. Following the demonstration that nanotubes could be selectively attached by oxidizing gases these workers realized that nanoparticles, with their defect rich structures might be oxidised more readily than the relatively perfect CNTs. They found that a significant relative enrichment of nanotubes could be achieved this way, but only at the expense of losing the majority of the original sample.

A new gas-phase method has been developed at the NASA Glenn Research Center to purify gram-scale quantities of single-wall CNTs. This method, a modification of a gas-phase purification technique previously reported by Smalley and others, uses a combination of high-temperature oxidations and repeated extractions with nitric and hydrochloric acid. This improved procedure significantly reduces the amount of impurities such as residual catalyst, and non-nanotube forms of carbon within the CNTs, increasing their stability significantly.

Liquid phase

The current liquid-phase purification procedure follows certain essential steps:

- preliminary filtration- to get rid of large graphite particles;
- dissolution- to remove fullerenes (in organic solvents) and catalyst particles (in concentrated acids)
- centrifugal separation-
- microfiltration- and

- chromatography

It is important to keep the CNTs well-separated in solution, so the CNTs are typically dispersed using a surfactant prior to the last stage of separation.

Intercalation

An alternative approach to purifying multi walled nanotubes was introduced in 1994 by a Japanese research group. This technique made use of the fact that nanoparticles and other graphitic contaminants have relatively "open" structures and can therefore be more readily intercalated with a variety of materials that can close nanotubes. By intercalating with copper chloride, and then reducing this to metallic copper, the research group was able to preferentially oxidize the nanoparticles away, using copper as an oxidation catalyst. Since 1994, this has become a popular method for purification of nanotubes. "The first stage is to immerse the crude cathodic deposit in a molten copper chloride and potassium chloride mixture at 400°C and leave it for one week. The product of this treatment, which contains intercalated nanoparticles and graphitic fragments, is then washed in ion exchanged water to remove excess copper chloride and potassium chloride. In order to reduce the intercalated copper chloride-potassium chloride metal, the washed product is slowly heated to 500°C in a mixture of Helium and hydrogen and held at this temperature for 1 hour. Finally, the material is oxidized in flowing air at a rate of 10°C/min to a temperature of 555°C. Samples of cathodic soot which have been treated this way consist almost entirely of nanotubes. A disadvantage of this method is that some amount of nanotubes are inevitably lost in the oxidation stage, and the final material may be contaminated with residues of intercalates. A similar purification technique, which involves intercalation with bromine followed by oxidation, has also been described.

1.3. Dye adsorption studies

In industrial water pollution the color produced by minute, amount of organic dyes in water is considered very important because, besides having possible harmful effects, the color in water is aesthetically unpleasant. Colored water can affect plant life, and thus an entire ecosystem can be destroyed by the contamination of various dyes in water. Some dyes are also toxic and even

carcinogenic. This dictates the necessity of dye containing water to undergo treatment before disposal to the environment. The conventional methods for color removal are biological oxidation and chemical precipitation. But these processes are not always effective and economic where the solute concentrations are very low. Moreover, most of the synthetic organic dyes undergo very slow biodegradation. Currently the sorption technique is proved to be an effective and attractive process for the treatment of dye containing waste water. Also the method will become inexpensive, if the sorbent material used is of cheaper cost and does not require any expensive additional pretreatment step.

Removal of dye from colored wastewater using adsorbent is interesting because specific substances are transferred from liquid onto solid surface. The traditional adsorbents have some disadvantages such as relatively limited pollutant removal capacity and poor separation ability.

The pollutant removal using nanoparticles as adsorbents is an emerging field of water and wastewater treatment. These adsorbents could be separated based on their nanostructures. It is important for the release of nanoparticles after adsorption process. Several materials have been used to remove dyes from aqueous solution[48]. Nanoparticles have low adsorption capacity of anionic dyes due to repulsion of the negative charge of nanoparticles surface and anionic dyes.

The adsorption characteristics of MB on various adsorbents have previously been extensively investigated for many purposes of purification and separation[49,50]. Although MB is seen in some medical uses in large quantities, it can also be widely used in coloring paper, dyeing cottons, wools, coating for paper stocks, etc. Though MB is not strongly hazardous, it can cause some harmful effects. Acute exposure to MB will cause increased heart rate, vomiting, shock, Heinz body formation, cryanosis, jaundice and quadriplegia and tissue necrosis in human. Many researcher have investigated the adsorptive properties of unconventional adsorbents. They studied the adsorption mechanisms of MB on to these adsorbents.

In the present work, methylene blue(cationic dye) was selected as a model compound in order to evaluate the capacity of the adsorbent for the removal of methylene blue from its aqueous solution.

1.3.1. Color in compounds and its sensation

If a substance absorbs visible light, it appears to have a color, if not it appears white. So in order for a compound to be colored light absorbing system (chromophore) must be present in it. Various theories have been put forward to establish a relationship between color and constitution. Some important theories are Witts theory, quinoid theory, resonance theory, molecular orbital theory.

1.3.2. Types of adsorption

Forces of attraction exist between adsorbate and adsorbent. These forces of attraction can be due to Vanderwaal forces of attraction which are weak forces or due to chemical bond which are strong forces of attraction. On the basis of type of forces of attraction existing between adsorbate and adsorbent, adsorption can be classified into two types:

i. Physical Adsorption

ii. Chemical Adsorption.

1.3.2.1. Physical adsorption or Physisorption

When the force of attraction existing between adsorbate and adsorbent are weak Vanderwaal forces of attraction, the process is called Physical Adsorption or Physisorption. Physical adsorption takes place with formation of multilayer of adsorbate on adsorbent. It has low enthalpy of adsorption i.e. ΔH adsorption is 20-40KJ/mol. If the temperature is raised, the kinetic energy of the gas molecules increases and they leave the surface of the adsorbent. Thus, rise in temperature lowers the extent of adsorption. Moreover, in physical adsorption, the equilibrium (between adsorption and desorption) is reversible and can be established rapidly. Physical adsorption does not depend upon the chemical nature of substance which is adsorbed. Physical adsorption increases with increase in pressure.

It takes place at low temperature below boiling point of adsorbate. As the temperature increases in, process of Physisorption decreases.

1.3.2.2. Chemical adsorption or Chemisorption

Unlike physical adsorption chemical adsorption involves formation of surface compound i.e. chemical linkage is formed between adsorbed molecule and the surface of adsorbent. The force of attraction existing between adsorbate and adsorbent are chemical forces of attraction or chemical bond, the process is called Chemical Adsorption or Chemisorption. Thus it is highly selective. It is found that only particular type of molecules are adsorbed by a solid in chemisorption. In other words,

this type of adsorption depends upon the chemical properties of gas and the adsorbent. When Chemisorption takes place with formation of unilayer of adsorbate on adsorbent, It has high enthalpy of adsorption.

i.e., $\Delta H_{adsorption}$ is 200-400 kj/mol

Chemisorption is not reversible. In many cases it is found that physical adsorption takes place at low temperature. But as the temperature is raised, it changes into chemical adsorption. Chemical adsorption is often called as *Activated Adsorption*. With the increases in temperature, first increases and then decreases.

1.3.3. Adsorption kinetics

Kinetic modeling not only allows estimation of sorption rates but also leads to suitable rate expressions characteristic of possible reaction mechanisms. In this respect, several kinetic models including the pseudo-first-order kinetics model, pseudo-second-order kinetics models (four linear forms)[51,52], and the intraparticle diffusion model were described.

1.3.3.1. Pseudo-first order model

A pseudo-first-order kinetic equation is given as

$$\ln(q_e - q_t) = \ln q_e - k_1 t_1 \qquad \text{...1.1}$$

where q_t is the amount of lead ions removed at time t (mg/g), q_e is the adsorption capacity at equilibrium (mg/g), k_1 is the pseudo-first-order rate constant (1/min), and t is the contact time (min). Using equation, $ln\ (q_e - q_t)$ versus t can be plotted to determine the rate constant.

1.3.3.2. Pseudo-second order model

Pseudo-second-order kinetic equation is given as

$$\frac{1}{q_e-q_t} = \frac{1}{q_e} + k_2t \quad\quad\quad \text{...1.2}$$

In this model, the rate-limiting step is the surface adsorption that involves chemisorption, where the removal from a solution is due to physicochemical interactions between the two phases. The model is usually represented by its linear form (Table 1.1).

Table 1.1: Pseudo-second-order kinetic model in linearized forms

Type	Linearized form	Plot	Equation no.
Linear 1	$\dfrac{t}{q_t} = \dfrac{1}{K_2 q_e^2} + \dfrac{1}{q_e}t$	t/q vs. t	1.2(1)
Linear 2	$\dfrac{t}{q_e} = \dfrac{1}{q} + \left(\dfrac{1}{K_2 q_e^2}\right)\dfrac{1}{t}$	$1/q$ vs. $1/t$	1.2(2)
Linear 3	$q_e = q_t - \left(\dfrac{1}{k q_t}\right)\dfrac{q}{t}$	q vs. q/t	1.2(3)
Linear 4	$\dfrac{q_e}{t} = k q_t^2 - k q_e q_t$	q/t vs. q	1.2(4)

1.3.3.3. Intraparticle diffusion model

The intraparticle diffusion model describes adsorption processes, where the rate of adsorption depends on the speed at which adsorbate diffuses towards adsorbent (i.e., the process is diffusion-controlled), which is presented by the following equation.

$$q_e = k_3 t^{1/2} + c_1 \qquad\qquad ....1.3$$

where, k_3 is the rate constant of the intraparticle transport (g/mg/min) and c is the intercept.

1.4. Antibacterial activity studies

Antibacterials are used to treat bacterial infections. The discovery, development and clinical use of antibacterials during the 20th century has substantially reduced mortality from bacterial infections. The antibiotic era began with the pneumatic application of nitroglycerine drugs, followed by a "golden" period of discovery from about 1945 to 1970, when a number of structurally diverse and highly effective agents were discovered and developed. However, since 1980 the introduction of new antimicrobial agents for clinical use has declined, in part because of the enormous expense of developing and testing new drugs. Paralleled to this there has been an alarming increase in resistance of bacteria, fungi, viruses and parasites to multiple existing agents.

Antibacterials are among the most commonly used drugs. For example 30% or more patients admitted to hospital are treated with one or more courses of antibacterials. However antibacterials are also among the drugs commonly misused by physicians, such as usage of antibiotic agents in viral respiratory tract infections. The inevitable consequence of widespread and injudicious use of antibacterials has been the emergence of antibiotic-resistant pathogens, resulting in a serious threat to global public health. The resistance problem demands that a renewed effort be made to seek antibacterial agents effective against pathogenic bacteria resistant to current antibacterials. Possible strategies towards this objective include increased sampling from diverse environments and application of metagenomics to identify bioactive compounds produced by currently unknown and uncultured microorganisms as well as the development of small-molecule libraries customized for bacterial targets.

The toxicity to humans and other animals from antibacterials is generally considered low. However, prolonged use of certain antibacterials can decrease the number of gut flora, which may have a

negative impact on <u>health</u>. After prolonged antibacterial use consumption of <u>probiotics</u> and reasonable eating can help to replace destroyed gut <u>flora</u>. <u>Stool transplants</u> may be considered for patients who are having difficulty recovering from prolonged antibiotic treatment, as for recurrent <u>clostridium difficile</u> infections.

A clinically effective antimicrobial agent has several important requirements and characteristics. First, it must target the microbial infection leading to concentrations that can eradicate or even prevent the polyferation. Second, the agent must stand the microbial drug resistance. Third, it's toxicity must be kept to a very minimum.

A key medication that has significant toxicity yet is very effective for lethal infections, particularly fungal. Over the past few decades, inorganic nanoparticles, whose structures exhibit significantly novel and improved physical, chemical, and biological properties, phenomena, and functionality due to their nanoscale size, have elicited much interest. Nanophasic and nanostructured materials are attracting a great deal of attention because of their potential for achieving specific processes and selectivity, especially in biological and pharmaceutical applications[53].

Recent studies have demonstrated that specially formulated metal oxide nanoparticles have good antibacterial activity, and antimicrobial formulations comprising nanoparticles could be effective bactericidal materials.

Among inorganic antibacterial agents, manganese can be employed most extensively since to fight infections and control spoilage next after silver [54-56]. The antibacterial and antiviral actions of manganese compounds have been thoroughly investigated. However, in minute concentrations, manganese is nontoxic to human cells. The epidemiological history of manganese has established its nontoxicity in normal use. Catalytic oxidation by metallic manganese and reaction with dissolved monovalent manganese ion probably contribute to its bactericidal effect. Microbes are unlikely to develop resistance against manganese, as they do against conventional and narrow-target antibiotics, because the metal attacks a broad range of targets in the organisms, which means that they would have to develop a host of mutations simultaneously to protect themselves. Thus, manganese ions have been used as an antibacterial component in dental resin composites, in synthetic zeolites and in coatings of medical devices.

Recent literature reports encouraging results about the bactericidal activity of manganese nanoparticles of either a simple or composite nature. For these reason, the antibacterial activity of Mn_3O_4 nanoparticles was investigated against 7 bacterial microorganisms . Mn_3O_4 nanoparticles were synthesized by solution phase routes, and their interactions with these bacterial microorganisms were studied.

Various biomedical applications of nanomaterials have been proposed in the last few years leading to the emergence of a new field in diagnostics and therapeutics. Most of these applications involve the administration of nanoparticles into patients. CNTs are enjoying increasing popularity as building blocks for novel drug delivery systems as well as for bioimaging and biosensing. The recent strategies to functionalize CNTs have resulted in the generation of biocompatible that are well suited for high treatment efficacy and minimum side effects for future cancer therapies with low drug doses. The toxicological profile of such CNT systems developed as nanomedicines will have to be determined prior to any clinical studies undertaken. To check the activity of the CNT as a drug delivery agent the test for antibacterial activity of the Mn_3O_4 nanoparticles loaded CNTs were also accomplished in the same time.

1.4.1. Microorganisms(Bacteria) utilized

1.4.1.1. *Pseudomonas aeruginosa*
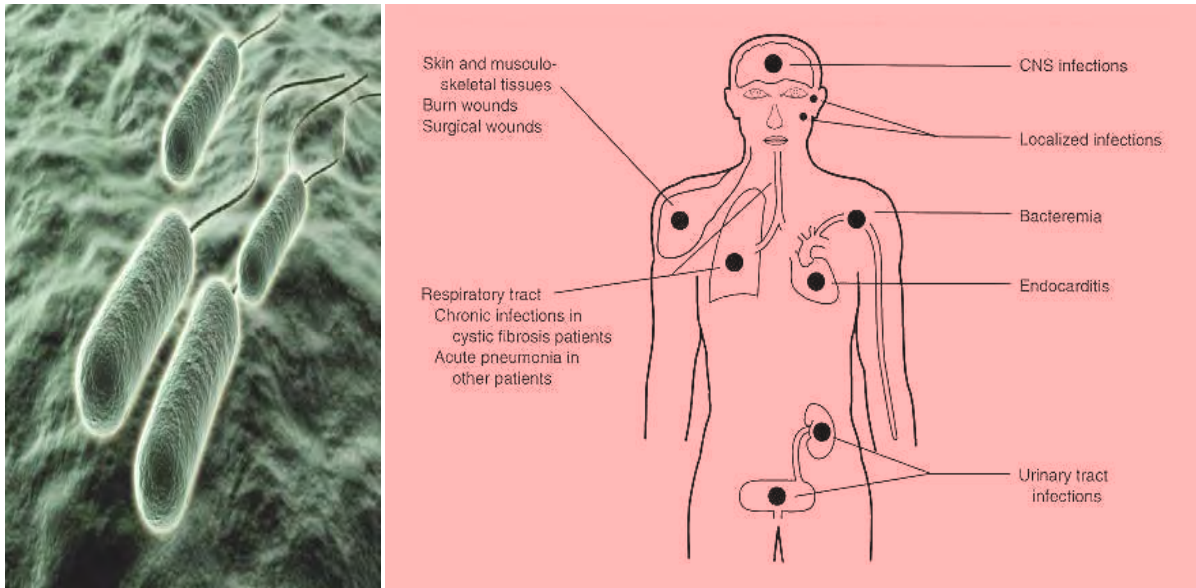
Figure 1.10: *Pseudomonas aeruginosa* and it's harmful effects

Pseudomonas bacteria can be found in many different environments such as soil, water, and plant and animal tissue. Many different species of this bacteria are opportunistic pathogens that affect humans, animals, and plants. *Pseudomonas ae ruginosa*, called the "epitome" of opportunistic pathogens, almost never infects uncompromised tissues; however, it can infect practically any type of tissue if that tissue has some type of compromised defenses. The schematic diagram of and it's harmful effect in the human body are sighted in Figure(1.10)

Pseudomonas bacteria are generally aerobic rod-shaped bacteria that are known for their metabolic diversity. Some species of this bacteria, such as *P. a eruginosa*, are opportunistic pathogens that secrete extracellular proteases and adhere and invade host tissue. More than half of the clinical isolates of Pseudomonas bacteria produce pyocyanin, a blue-green pigment. The Pseudomonas fluorescens group are nonpathogenic saprophytes that also produce a pigment, particularly under conditions of low iron availability. This pigment is a soluble, greenish, fluorescent pigment that led to the group's name. These bacteria are generally obligate aerobes; however, some strains can utilize NO_3 instead of O_2 as an electron acceptor. They have multiple polar flagella that assist in the bacteria's movement. Because they have simple nutritional requirements, they "grow well in mineral salts media supplemented with any of a large number of carbon sources". Several strains of this bacteria also have the ability to suppress plant diseases by "protecting the seeds and roots from fungal infection". This ability is due to secondary metabolites produced by these bacteria such as antibiotics, siderophores, and hydrogen cyanide as well as the ability of these bacteria to rapidly colonize the rhizosphere and out-compete some of pathogens.

1.4.1.2. *Streptococcus pneumoniae*
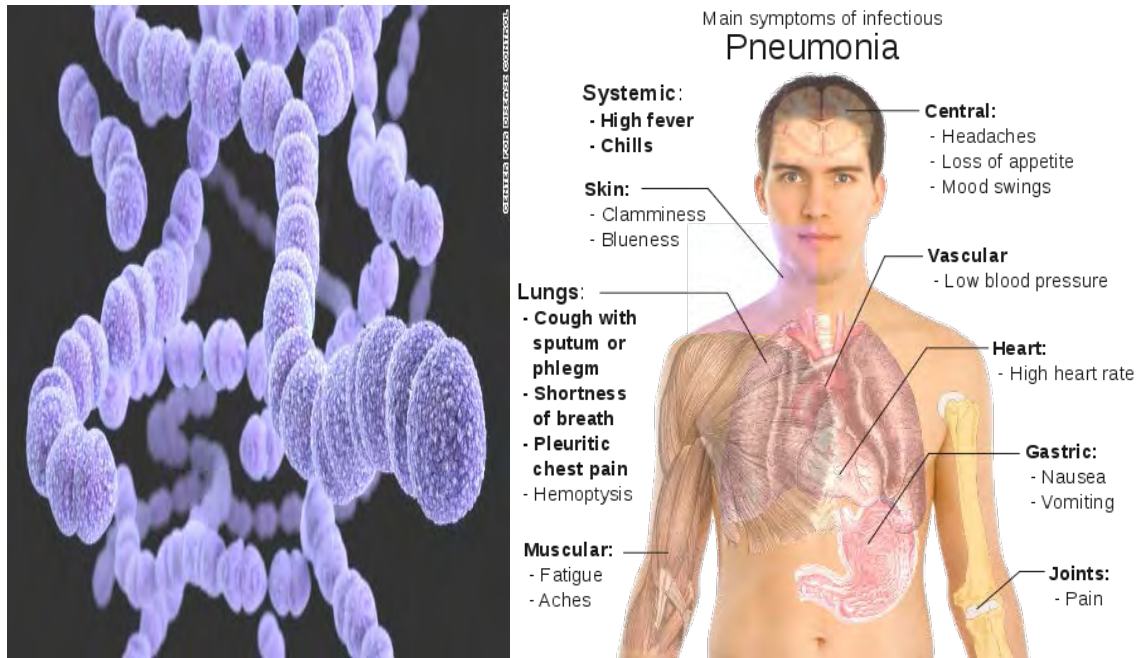
Figure 1.11: *Streptococcus pneumoniae and it's harmful effects*

Streptococcus pne umoniae, or pneumococcus (Figure 1.11) is a Gram-positive, alpha-hemolytic, facultative anaerobic member of the genus *Streptococcus*. A significant human pathogenic bacterium, *S. pneumoniae* was recognized as a major cause of pneumonia in the late 19th century, and is the subject of many humoral immunity studies.

S. pneumoniae resides asymptomatically in the nasopharynx of healthy carriers. The respiratory tract, sinuses, and nasal cavity are the parts of host body that are usually infected. However, in susceptible individuals, such as elderly and immunocompromised people and children, the bacterium may become pathogenic, spread to other locations and cause disease. *S. pneumoniae* is the main cause of community acquired pneumonia and meningitis in children and the elderly, and of septicemia in HIV-infected persons. The methods of transmission include sneezing, coughing, and direct contact with an infected person.

Despite the name, the organism causes many types of pneumococcal infections other than pneumonia. These invasive pneumococcal diseases include bronchitis, rhinitis, acute sinusitis, conjunctivitis, meningitis, bacteremia, sepsis, osteomyelitis, septicarthritis, endocarditisperit onitis, pericarditis, cellulitis, and brain abscess.

S. pneumoniae is one of the most common causes of bacterial meningitis in adults and young adults, along with *Neisseria meningitidis*, and is the leading cause of bacterial meningitis in adults in the USA. It is also one of the top two isolates found in ear infection, otitis media. *Pneumococcal* pneumonia is more common in the very young and the very old.

1.4.1.3. *Vibrio cholerae*
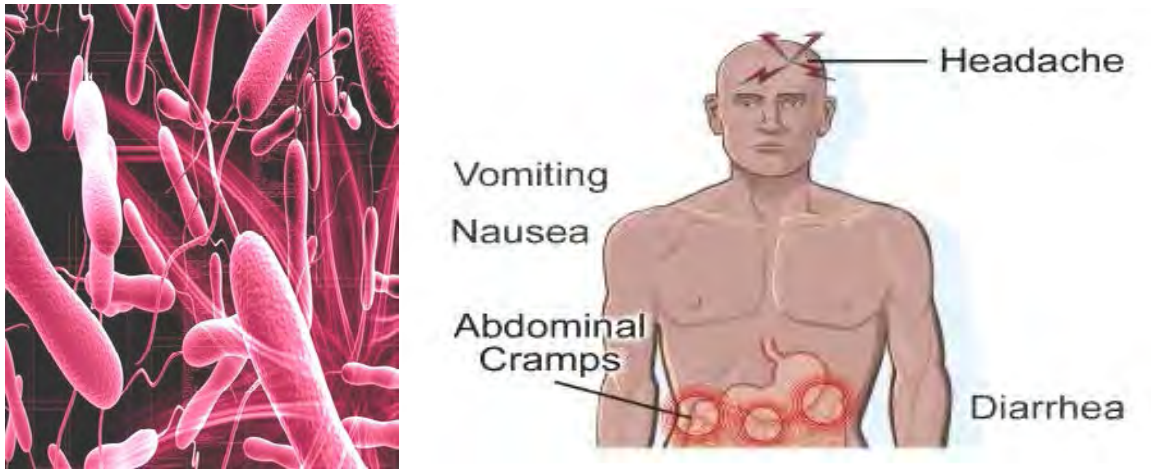
Figure 1.12: *Vibrio cholerae* and it's harmful effects

Vibrio c holerae (Figure 1.12) is a gram-negative, comma-shaped bacterium. Some strains of *V. cholerae* cause the disease cholera. *V. c holerae* is a facultative anaerobic organism and has a flagellum at one cell pole. *V. c holerae* was first isolated as the cause of cholera by Italian anatomist Filippo Pacini in 1854, but his discovery was not widely known until Robert Koch, working independently 30 years later, publicized the knowledge and the means of fighting the disease.

V. c holerae pathogenicity genes code for proteins directly or indirectly involved in the virulence of the bacteria. During infection, *V. c holerae* secretes cholera toxin, a protein that causes profuse, watery diarrhea. Colonization of the small intestine also requires the toxin coregulated pilus (TCP), a thin, flexible, filamentous appendage on the surface of bacterial cells. *Vibrio c holerae* can cause syndromes ranging from asymptomatic to cholera gravis. In endemic areas, 75% of cases are asymptomatic, 20% are mild to moderate, and 2-5% are severe forms like cholera gravis. Symptoms include abrupt onset of watery diarrhea (a grey and cloudy liquid), occasional vomiting and abdominal cramps. Dehydration ensues with symptoms and signs such as thirst, dry mucous

membranes, decreased skin turgor, sunken eyes, hypotension, weak or absent radial pulse, tachycardia, tachypnea, hoarse voice, oliguria, cramps, renal failure, seizures, somnolence, coma and death. Death due to dehydration can occur in a few hours to days in untreated children. The disease is also particularly dangerous for pregnant women and their fetus during late pregnancy, as it may cause premature labor and fetal death. In cases of cholera gravis involving severe dehydration, up to 60% of patients can die; however, less than 1% of cases treated with rehydration therapy are fatal. The disease typically lasts from 4–6 days. Worldwide, diarrhoeal disease, caused by cholera and many other pathogens, is the second leading cause of death for children under the age of 5 and at least 120,000 deaths are estimated to be caused by cholera each year. In 2002, the WHO deemed that the case fatality ratio for cholera was about 3.95%. The main reservoirs of *V. cholerae* are people and aquatic sources such as brackish water and estuaries, often in association with copepods or other zooplankton, shellfish, and aquatic plants.

1.4.1.4. *Escherichia coli*
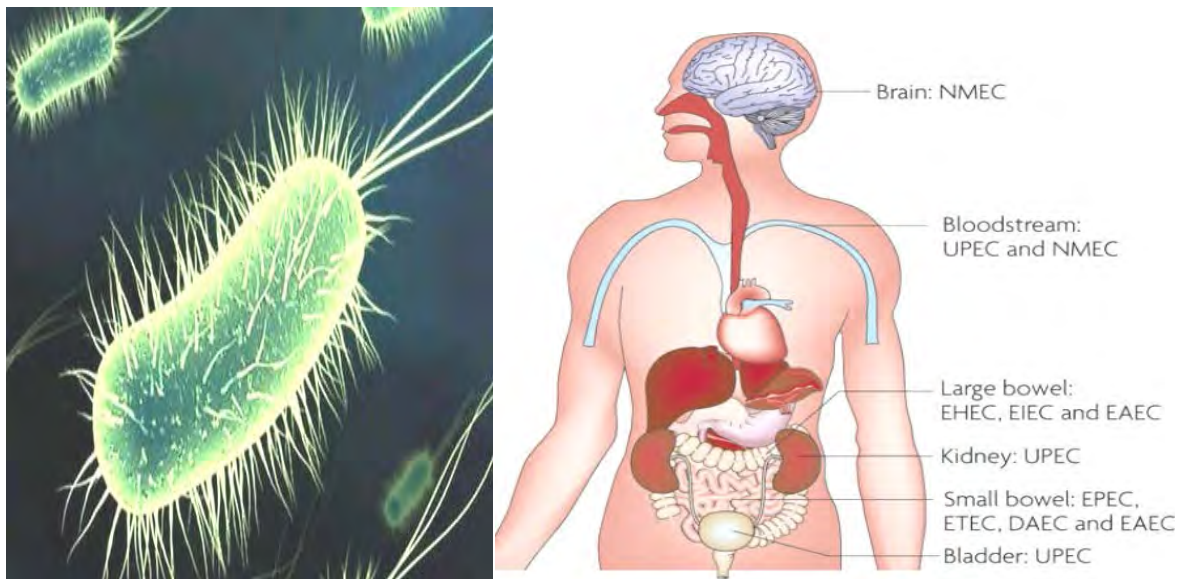
Figure 1.13: *Escherichia coli* and it's harmful effects

Escherichia coli (Figure 1.13) is a Gram-negative, facultatively anaerobic, rod-shaped bacterium of the genus *Escherichia* that is commonly found in the lower intestine of warm-blooded organisms (endotherms). Most *E.coli* strains are harmless, but some serotypes can cause serious food poisoning in their hosts, and are occasionally responsible for product recalls due to food

contamination. The harmless strains are part of the <u>normal flora</u> of the <u>gut</u>, and can benefit their hosts by producing <u>vitamin K$_2$</u>, and preventing colonization of the intestine with <u>pathogenic</u> bacteria.

E. c oli and other facultative <u>anaerobes</u> constitute about 0.1% of <u>gut flora</u>, and <u>fecal–oral transmission</u> is the major route through which pathogenic strains of the bacterium cause disease. Cells are able to survive outside the body for a limited amount of time, which makes them potential <u>indicator organisms</u> to test environmental samples for <u>fecal contamination</u>. A growing body of research, though, has examined environmentally persistent *E. c oli* which can survive for extended periods outside of a host.

The bacterium can be grown and cultured easily and inexpensively in a laboratory setting, and has been intensively investigated for over 60 years. *E.coli* is the most widely studied <u>prokaryotic</u> <u>model organism</u>, and an important species in the fields of <u>biotechnology</u>and <u>microbiology</u>, where it has served as the <u>host organism</u> for the majority of work with <u>recombinant DNA</u>. Under favourable conditions, it takes only 20 minutes to reproduce.

1.4.1.5. *Salmonella Typhi*
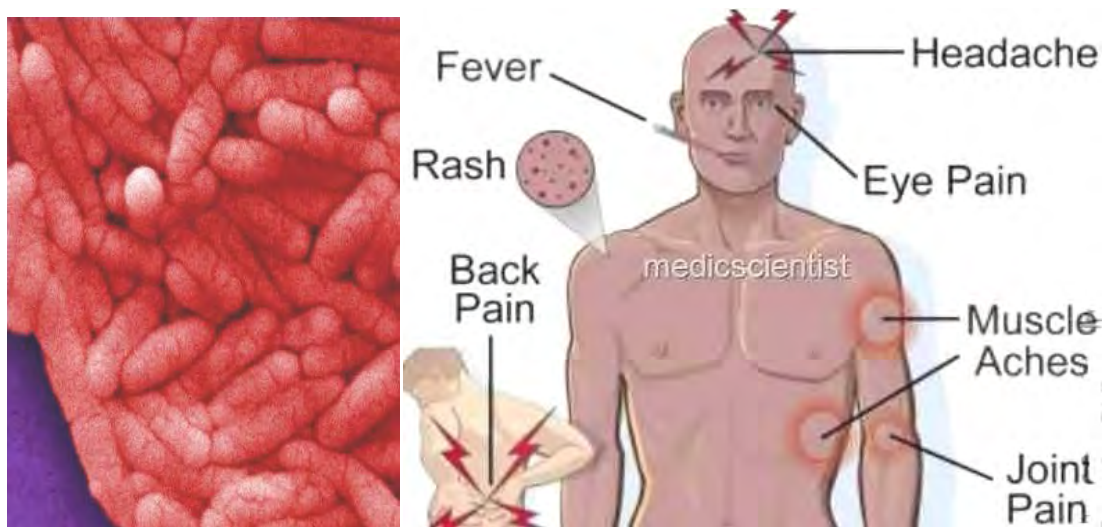
Figure 1.14: *Salmonella typhi* and it's harmful effects

Typhoid fever, also known simply as typhoid, is a symptomatic bacterial infection due to *Salmonella typhi* (Figure 1.14). Symptoms may vary from mild to severe and usually begin six to thirty days after exposure. Often there is a gradual onset of a high <u>fever</u> over several days. Weakness, <u>abdominal</u>

pain, constipation, and headaches also commonly occur. Diarrhea and vomiting are uncommon. Some people develop a skin rash with rose colored spots. In severe cases there may be confusion. Without treatment symptoms may last weeks or months. Other people may carry the bacteria without being affected; however, are still able to spread the disease to others. Typhoid fever is a type of enteric fever along with paratyphoid fever.

The cause is the bacteria *Salmonella typhi*, also known as Salmonella enterica serotype typhi, growing in the intestines and blood. Typhoid is spread by eating or drinking food or water contaminated with the feces of an infected person. Risk factors include poverty as a result of poor sanitation and poor hygiene. Those who travel to the developing world are also at risk. Humans are the only animal infected. Diagnosis is by either culturing the bacteria or detecting the bacteria's DNA in the blood, stool, or bone marrow. Culturing the bacteria can be difficult. Bone marrow testing is the most accurate. Symptoms are similar to that of many other infectious diseases. Typhus is a different disease. It is recommended for those at high risk or people travelling to areas where the disease is common. Other efforts to prevent the disease include providing clean drinking water, better sanitation, and better hand washing. Until it has been confirmed that a person's infection is cleared they should not prepare food for others.

1.4.1.6. *Enterobacter cloacae*
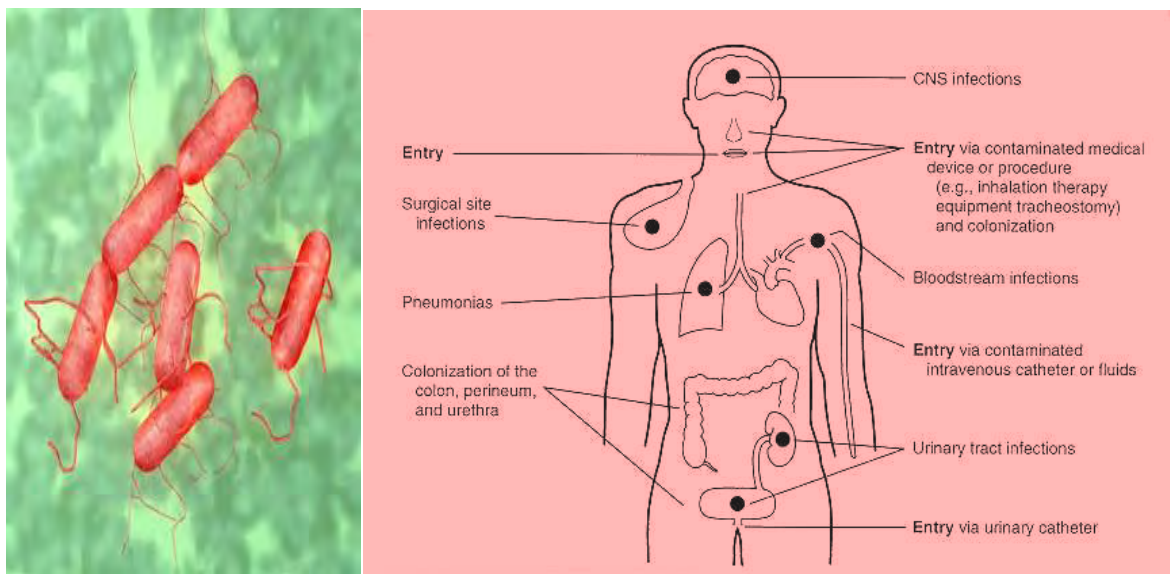
Figure 1.15: *Enterobacter cloacae* and it's harmful effects

Enterobacter cloacae (Figure 1.15) are nosocomial pathogens that can cause a range of infections such as bacteremia, lower respiratory tract infection, skin and soft tissue infections, urinary tract infections, endocarditis, intra-abdominal infections, septic arthritis, osteomyelitis, and ophthalmic infections. This organism affects mostly the vulnerable age groups such as the elderly and the young and can cause prolonged hospitalization in the intensive care unit (ICU). ICU pathogens can cause morbidity and mortality and the management of this bacteria infection is complicated by the organism's multiple antibiotic resistance. These bacteria contain beta-lactamase, which is undetectable in vitro and is highly resistant to antibiotics such as third generation cephalosporins.

This organism is mainly isolated as nosocomial infections in the ICU for those who stay in the hospital for prolonged periods. The infection may be contracted through the skin, gastrointestinal tract, urinary tract, or cross-contamination. Outbreaks can also be traced back to hands of personnel, endoscopes, blood products, total parenternal nutrition solutions, albumin, and hospital equipment such as stethoscopes and dialysis. A genome of *Enterobacter cloacae* has now been <u>fully sequenced</u>. This organism produces chromosomally encoded Beta-lactamases also called cephalosporinases. Many of the Enterobacter species have multiple antibiotic resistance that are undetectable in vitro, which makes it difficult to treat in patients. Some are resistant to fluoroquinolones.

1.4.1.7. *Acinetobacter baumannii*
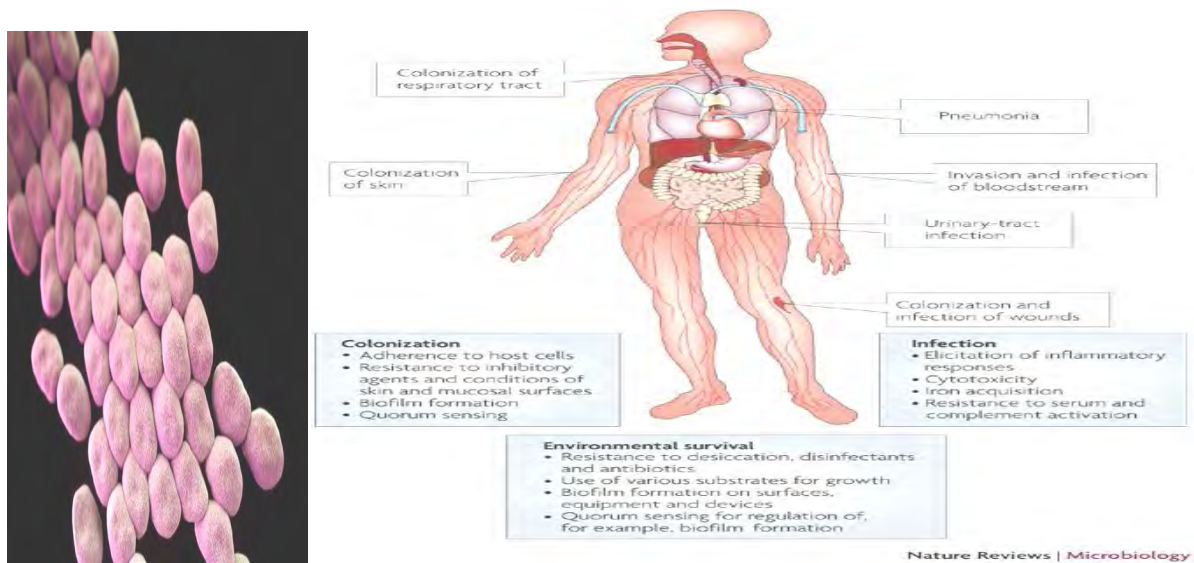
Figure 1.16: *Acinetobacter baumannii* and it's harmful effects

Acinetobacter is a genus of opportunistic pathogens in the proteobacteria group, species of which are distributed in widespread, diverse habitats. It has garnered media attention because of an outbreak among soldiers in Iraq who contracted the species *Acinetobacter baumannii* (Figure 1.16). While it was initially thought that the bacteria had come from the Iraqi soil, it turns out that the bacteria were actually contracted in the military's evacuation chain.

These bacteria can often be found as the cause of pneumonia in hospitalized patients, especially those dependent on ventilators in Intensive Care Units. The bacteria are most often contracted through the exposure of open wounds to contaminated soil. In healthy humans, it is normal to have some amount of Acinetobacter on the skin surface; as many as 25% of healthy adults do in fact harbor these bacteria.

While there is much information available on the types of infections Acinetobacter causes, relatively few studies have been performed on the bacteria's genetics. Because Acinetobacters are very resistant to antibiotics and are difficult to differentiate between species when isolated from patients, learning more about their DNA will help develop better drugs to control outbreaks of the infection.

1.5. Background and objectives of this research work

As yet, with all of the progress, many medications, even those discovered using the most advanced molecular biology strategies, have unacceptable side effects due to the drug interacting with parts of the body that are not the target of the drug. Side effects limit our ability to design optimal medications for many diseases such as cancer, neurodegenerative diseases, and infectious diseases. Scientists now use nanotechnology to approach classical and novel drug delivery applications. Controlled and targeted deliveries are the most enviable requirements expected from a carrier, which involves multi-disciplinary site specific or targeted approach. Pharmaceutical nanoparticles are subnanosize based structure, contain drug or bioactive substances within them and constituted of several tens or hundreds of atoms or molecules with a variety of sizes. CNTs have become strongest candidates mainly in the field of biomedical engineering; biotechnology and pharmaceutical nanotechnology after their discovery in 1991.These are an important new class of technological materials that have numerous novel and useful properties. They have received very much attention as new classes of nanomaterials .These are the long hollow seamless cylinders of graphene. The diameter of these tubes is in the range of 1-100 nm. CNTs are cylinders of one or several coaxial graphite layers with a diameter in the order of nanometers these shows unique chemical, physical and electrical properties. Nanomaterials have sizes ranging from about one nanometer up to several hundred nanometers, comparable to many biological macromolecules such as enzymes, antibodies, and DNA plasmids.

CNTs have the potential to address the challenges of combating infectious agents by both minimizing toxicity by dose reduction of standard therapeutics and allowing a multiple payload capacity to achieve both targeted activity and combating infectious strains, resistant strains in particular. One of their unique characteristics is the network of carbon atoms in the nanometer scale, allowing the creation of nano-channels via cellular membranes. This review focuses on the characterization, development, integration and application of CNTs as nanocarrier-based delivery systems and their appropriate design for achieving the desired drug delivery results in the different areas of infectious diseases. While a more extensive toxicological and pharmacological profile must be obtained, this review will focus on existing research and pre-clinical data concerning the potential use of CNTs.

Reasons behind CNTs can be used efficiently as drug delivery materials-

- ✓ CNTs contain a significant hollow spaces compared to the dimensions of the tube that can be encapsulated wth different desired chemicals as well as biological species.
- ✓ CNTs cosists of open mouths which make the inner space accessible for the easy insertion of the nanoactive species inside the tube.
- ✓ CNTs have the distinct inner and outer surfaces that can be differentially modified for functionalization. As a result outer surface of CNTs can be immobilized with bio compatible materials and inside can be filled with the desired biochemical play load.
- ✓ Molecular dynamics simulation shows that van der waals and hydrophobic forces are impotant for the insertion process. The van der waals forces have a dominant role in the CNT species.

CNTs, as newly emerging carbonaceous materials, have attracted considerable interests as potential adsorbents for water treatment application due to their high specific surface area, distinct structure, and modifiable surface chemistry. CNTs have been observed to be more efficient carbonaceous adsorbents than conventional, with higher adsorption capacity, shorter equilibrium time, and less weight loss in reactivation. CNTs have been proven to possess great potential for removing many kinds of pollutants such as resorcinol, aniline, ethyl benzene, and phenol.

For the purpose of synthesis CNTs(MWCNTs) various techniques were analysed which includes arc discharge method, laser evaporation method, thermal chemical vapor deposition method, catalytic synthesis and the like. In these methods , CNTs are synthesized under severe reaction conditions, for example, at high temperature of several hundred degrees to several thousands degrees in celcius, or in vacuum. Further the type of reactions used is a batch type reaction, instead of a continuous flow type reaction, such that continuous preparation of CNTs is impossible., and only small amounts of CNTs are produced in batch reactions. accordingly, these methods have the problem of facing limitations in mass production of nanotubes at low costs, and therefore it is desired to develop a suitable process for synthesis , especially a process for continuous synthesis which is industrially useful.

The present research work relates to a process enabling continuous bulk preparation of CNTs in which catalytic metal nanoparticles having priliminerally controlled composition, particle size and particle distribution are continuously introduced. More specifically, the present invention is to provide a process for the preparation of CNTs, which comprises introducing in a gaseous phase a colloidal solution of metal nanoparticles, preferably containing an optional surfactant, together with carbon source into a heated reactor and finally CNTs are obtained. So the present synthesis process is highly effective and industrially promising.

The filling or encapsulation of CNTs is another challenge. The hollow interior of CNTs offers confined space that can be filled with various materials or be used to carry out chemical reactions. In this research work four nanoactive metal species (NiO, Mn_3O_4, MnO_2 and Ni nanoparticles) were used as a filling agents. These four nanoparticles were prepared by established conventional methods. Finally the physico-chemical properties which includes individual characterization of every synthesized and filled matrices were analysed and as a delivery agent antibacterial and dye decolorization through adsorption experiments were done.

So the overall objectives with specific aims and possible outcome of this research work are the following:

i. To develop a unique method to prepare CNTs.
ii. To establish a suitable way for the filling of CNTs with nanoactive metal species, eg., Ni, Mn_3O_4, MnO_2, NiO nanoparticles etc.
iii. To study the influence of the metal/metal oxides on the physico-chemical functionalities of CNTs.
iv. To explore the efficiency of CNTs in drug delivery.
v. To explore the adsorption and antibacterial effectiveness of the metal/metal oxides loaded CNTs.

CHAPTER TWO

MATERIALS & EXPERIMENTAL

MATERIALS & EXPERIMENTAL

2.1. Materials

Analytical grade chemicals and solvents were used throughout the work. Deionized water (H_2O) was used as solvent to prepare most of the solutions. The important chemicals and solvents utilized throughout the experiments are listed below(Table 2.1):

Table 2.1: Chemicals utilized in the overall research purposes

No.	Chemicals	Company name	Quoted purity
1	Benzene	Merck	98%
2	m-Xylene	Sigma-Aldrich	99%
3	Cetyl trimethyl-ammoniumbromide (CTAB)	Merck	98%
4	$FeCl_3$	Merck	98±.5%
5	Hydrazene	Merck	98±.5%
6	Deionized water	Labmade	Pure
7	Ethanol	Merck	98%
8	$Mn(CH_3COO)_2$	Merck	98±.5%
9	NH_4HCO_3	Merck	98%
10	Urea	Merck	98%
11	$NiCl_2$	Merck	98%

2.2. Apparatus & Instruments

a. Tube furnace (Inert atmosphere maintained furnace)

b *EDX*.modified **s**canning electron microscopy (SEM) machine

c. Ultra-violet ray (UV-ray) machine

d. Centrifuge machine

e. Shaker

f. High temperature controlled furnace

g. General oven

h. Vacuum oven

i. Magnetic Stirrer

j. Digital balance

k. Decicator

l. Centrifugal machine

m. Electric drier

2.3. Preparation of nanoparticles

2.3.1. Preparation of CNTs

CNT was prepared chemically, in brief as follows:

To the solution of 20 ml of m-Xylene and 30 ml   of benzene, 5g (10% by weight of benzene & m-xylene) of cetyl trimethyl-ammoniumbromide(CTAB) and 1 g of $FeCl_3$ was added and the mixture was stirred for 24 hours. CTAB is a cationic surfactant which played a role of stabilizing nanoparticles to be formed. 0.5g of hydrazene hydrate was added as a reducing agent to the above obtained solution and the mixture was stirred again for 24 hours to get a solution containing iron nanoparticles. Reaction was carried out by introducing the obtained solution together with a carrier gas (Ar) into a reactor at 600^oC for 20 minutes. The product CNTs were obtained as black powder. Figure(2.1) shows the tube furnace used in this experiment.

Figure 2.1: Argon gas controlled high temperature furnace

2.3.2. Preparation of NiO nanoparticles

All the reagents used in this study were analytical graded and used without further purification. $NiCl_2$ and $Ni(NO_3)_2$ were used as n ickel salts. The precipitation agents were $CO(NH_2)_2$, NH_4HCO_3 and $(NH_4)_2CO_3$. Stock solutions containing 0.5mol/L of nickel salts as precipitation agents were prepared by dissolving appropriate amount of corresponding chemicals in distilled water. The precipitation experiments were carried out in the following procedure. 100 ml of precipitation solution was dipped in 50 ml of Ni^{2+} solution at the rate of 5 .0 ml/min. During addition the suspension was kept at constant temperature (80^oC) with constant stirring (800 rpm). The stirring was kept running for 1 hour. Finally the precipitate was washed with distilled water and with alcohol for three times, respectively to remove the possible adsorbed ions such as Ni^{2+}, Cl^-, NH_4^+, NO_3^{2-}, CO_3^{2-}, OH^-, After oven dried at 105 ^oC for 12 hour, the precipitates were heated in air in 400 ^oC for 1 hour. The sintering product was then pulverized and used for analysis.

2.3.3. Preparation of Ni nanoparticles

Nickel nanometal can be prepared by reduction treatment of fixed amount of nanonickel oxides by hydrazine hydrate. Hydrazine hydrate is a well established reducing agent. First, 1.5gm of freshly prepared nanonickel oxide was taken in 50 ml beaker. Then 1 ml of hydrazine hydrate was added to

the beaker and placed the beaker in the vacuum oven at $80^{o}C$ for 1 hour. The nickel nanoparticles were formed by reduction and were separated by filter paper**.**

2.3.4. Preparation of Mn_3O_4 nanoparticles

About 500 ml 0.2 molar   chemical graded hydrated manganese(ll) acetate **[Mn(CH3COO)2.H2O]** solution was heated in the oven for 3 hours at 80 ^{o}C. Brown precipitates of p orous Mn_3O_4 nanoparticles thus synthesized by hydrolysis. Then they were   washed several times by double distilled water and then by ethanol. After drying them at $100^{o}C$ for 10 hours they were preserved.

2.3.5. Preparation of MnO_2 nanoparticles

Chemical graded hydrated manganese(ll) acetate $Mn(CH_3COO)_2.H_2O$ and potassium permanganate $(KMnO_4)$ were used as starting materials. The concentrations of both $Mn(CH_3COO)_2.H_2O$ and $(KMnO_4)$ were 0.1M. Porous MnO_2 nanoparticles were synthesized by redox reaction in aqueous medium, 5L of 0.1M $(KMnO_4)$ was slowly bumped into 5L of 0.1 M $Mn(CH_3COO)_2.H_2O$ solution and stirred continuously for 10 hours. A dark brown precipitate thus formed. It was washed then several times by double distilled water, centrifuged and dried at 110 ^{o}C for 10 hour.Thus the pure MnO_2 nanoparticles were obtained.

2.4. Filling of CNTs with nanoactive metal species

2.4.1. Filling of CNTs with NiO and Ni metal nanoparticles

An approach for filling the CNTs with nanometal species (NiO, Ni nanoparticles) is controlled boiling of the mixture suspension   . An efficient homogenously aqueous dispersed nanograins of (NiO,Ni) first prepared by adding of 1g of   nanoparticles (NiO, Ni) in 100 mL deionized water through continuos stirring at 40 ^{o}C and filling of the CNTs cavity with nanoparticles was demonstrated by incorporation of 0.1g of CNTs in suspension beaker of (NiO,Ni)   nanoparticles and boiled the mixture solution at 100 ^{o}C for 2 hours with continuous stirring   . At this temperature the blocked mouth of CNTs turned open if there were any.   Then the residue was washed by ethanol and deionized water several times and finally dried at room temperature. Then it should be further heated so that to block the CNTs mouth. Then the residue should be washed by ethanol and deionized water several times and finally dried at room temperature.

2.4.2. Filling of CNTs with MnO_2, Mn_3O_4 nanoparticles

Encapsulation of MnO_2 and Mn_3O_4 nanoparticles in the CNTs were done following aqueous in-situ CNT's cavity stabilization that prevents pollution and agglomeration of metal oxide nanoparticles and can lead to nanomaterial filled CNTs . For this a t the time of formation of these metallic oxides CNTs were added to the preparation beaker of these nanometal oxides and then heated the overall solution for 2 hours with 100 ^{o}C temperature maintaining. Then the metallic oxide sticked outside the tube were washed by etha nol and deionized water for several times. The metallic oxide loaded CNTs were precipitated down and the fine nanoparticles of the metaloxides were dispersed in the water. Finally metal oxides loaded CNTs were dried at room temperature. But to get the better filled CNTs fullerine treatment that was explained above should be done.

2.5. Characterization

Figure 2.2: Images of EDX integrated SEM, XRD, FTIR instruments(from left)

- ❑ Scanning Electron Microscopy (SEM) analysis to know the external morphology (texture) of the synthesized nanoparticles and filled matrices

- ❑ Energy Dispersive X-ray (EDX) analysis to get the elemental identification of the synthesized nanoparticles and filled matrices

- ❑ X-ray Crystallographic Diffraction (XRD) analysis to check the crystalinity of the synthesized nanoparticles

❑ Fourier Transform Infrared Spectroscopy (FTIR) analysis to check the unwanted functional groups in the sidewalls of the synthesized CNTs

2.6. Experimental section of dye adsorption studies

Decolorization of MB dye through dye adsorption using synthesized CNTs, NiO nanoparticles and NiO loaded CNTs(MWCNTs) and studies their adsorption kinetics.

2.6.1. Preparation of dye solution

A. Stock MB solution

100 ppm of stock solution of MB(methylene blue) was prepared as stock solution. First 500 ml of deionized water was taken in a volumetric flask. Then accurately 0.05 gm of methylene blue was weighted by a weighing machine and added to the water of the volumetric flask and dissolved the solution completely by shaking the flask. We know methylene blue is a powderish dye and it easily dissolves itself in water.

B. Dilution of MB stock solution

To make 30, 40, 50, 60, 70 ppm dye solution 15, 20, 25, 30, 35 mL of MB solution were taken in 5 reagent bottles. Then added there 35, 30, 25, 20, 15 ml deionized water respectively. Then each reagent bottles were shaked by shaking machine for few minutes.

2.6.2. Adsorption (Batch) process

0.01 g of adsorbents(CNTs, NiO and NiO encapsulated CNTs) were added to every different concentration of solutions. To determine the extinction coefficient first absorbance of individual MB solution of different concentrations were measured. Then absorbance were taken for every MB solution by a time interval of 30 minutes. The change on the absorbance of all solution samples were monitored and determined. The maximum absorbance were then noted for every solution of different concentrations. At the end of the adsorption experiments, the dye concentration was determined. UV–vis spectrophotometer was employed for overall absorbance measurements of the samples.

2.7. Experimental section for antibacterial activity studies

The study was carried out at the Department of Bacteriology, ICDDR,B.

2.7.1. Required materials

a. Muller-Hintonagar
b. Tryptic-soy broth
c. Deionized water
d. Microorganisms(bacteria) colony

2.7.2. Apparatus & Instruments

a. Oven
b. Autoclave machine
c. Micro pipette
d. Culture plate
e. Swab with applicator
f. Burner
g. Forcep

2.7.3. Culture medium

Of the many media available[57], NCCLS recommends Mueller-Hinton agar due to its results in good batch-to-batch reproducibility; it is low in sulfonamide, trimethoprim, and tetracycline inhibitors; it results in satisfactory growth of most bacterial pathogens; and a large amount of data has been collected concerning susceptibility tests performed with this medium. Only media from manufacturers following the NCCLS standards are to be used. The agar medium should have pH 7.2 to 7.4 at room temperature. The surface should be moist but without droplet of moisture. The antibiotic disks should be maintained at 8°C or lower or freeze at -14°C or below until needed, according to the manufacturer's recommendations.

2.7.4. Working procedure

- At first 7 well-isolated colonies(described above) of the same morphological type were selected from agar plates. Then each colony of bacteria were transfered with a wire loop to a test tube containing 4 to 5 mL of a suitable broth medium, such as tryptic-soy broth. The broth culture was allowed to incubate at 35°C until it achieves or exceeds the turbidity of 0.5 McFarland standard.
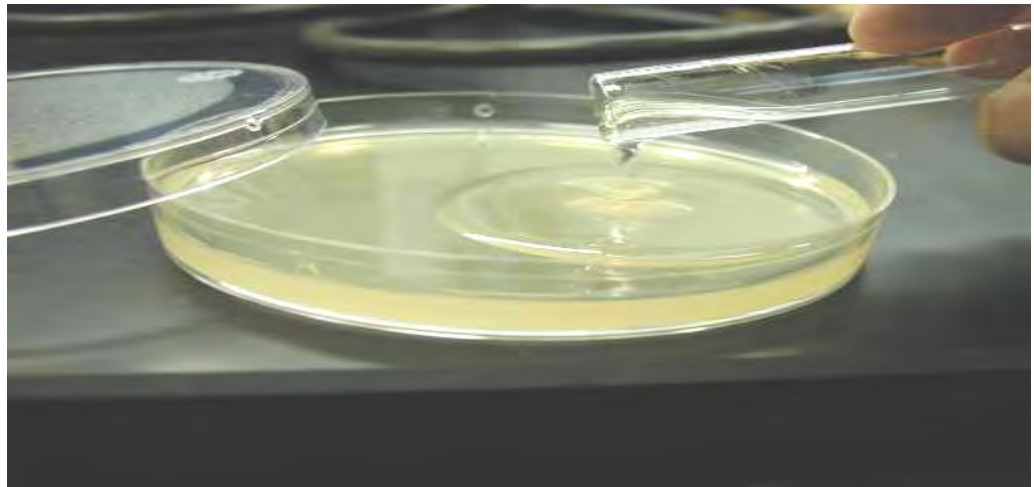
Figure 2.3: Agar plate preparation

- The turbidity was adjusted with sterile saline or broth in adequate light and to aid in the visual comparison, read the tube against a white background with contrasting black lines.
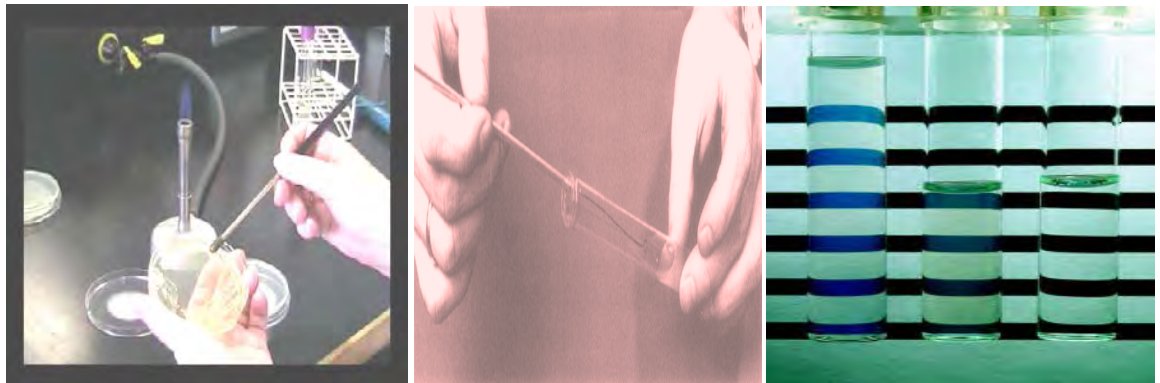
Figure 2.4: Culturing of bacterial micro-organisms in test tube

- Within 15 minutes after adjusting the turbidity of the inoculum suspension, a sterile non-toxic swab with an applicator was dipped into the adjusted suspension. The swab was rotated

several times, pressed firmly on the inside wall of the tube above the fluid level to remove excess inoculum from the swab.
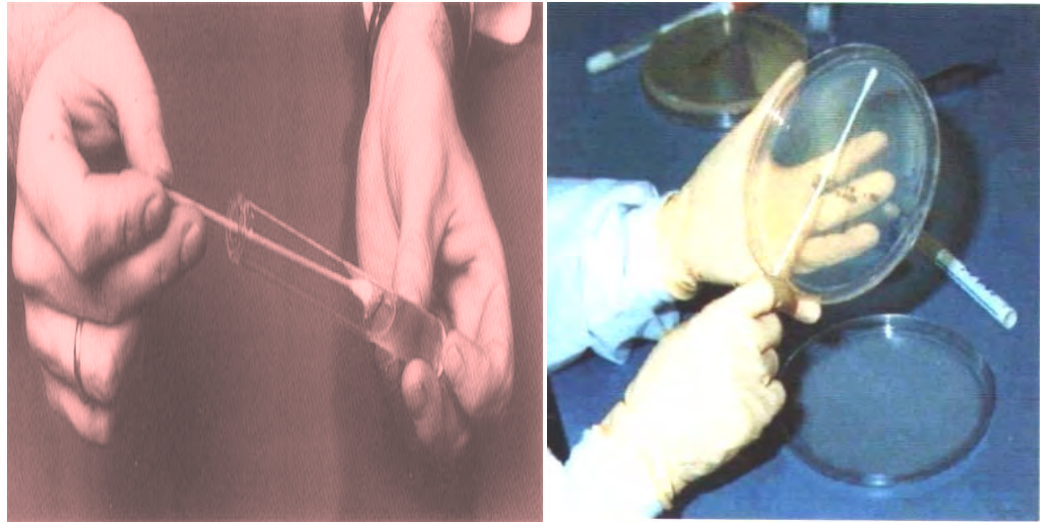
Figure 2.5: Transfering bacterial micro-organisms to experimental agar plate

- The dried surface of a Muller-Hintonagar plates were inoculated by streaking the swab over the entire sterile agar surface. This procedure was repeated two more times, and rotated the plate 60° each time to ensure an even distribution of inoculum. Then the plates were replaced to the top and allowed 3 to 5 minutes, but no longer than 15 minutes, for any excess surface moisture to be absorbed before applying the antibiotic materials. There should be an almost confluent lawn of growth when done properly. If only isolated colonies grown, the inoculum would be too light and the test should be repeated. To avoid extremes in inoculum density, we should never use undiluted overnight broth cultures for streaking plates.

- Instead of disk appropriate well (no closer than 35 mm from center to center) were cut on the surface of the agar plate by using a sterile forceps. No more than 6 wells should be cut on one 150 mm plate. the previously prepared suspension of Mn_3O_4 was poured by 50, 100 and 150 micro liters. In the case of Mn_3O_4 encapsulated CNTs the suspension was kept steady for 30 minutes to come out the filled Mn_3O_4. Then the suspension was poured in the well. Figure(2.3, 2.4, 2.5) describes the necessary experimental steps of antibacterial susceptibility measuring procedures.

- The plates were then placed in an incubator at 37 °C within 15 minutes after wells were cut properly. The plates should be incubated aerobically (no CO_2). After 16-18 hrs. of incubation, each plate were examined   and measured the diameters of the zones of complete inhibition, including the diameter of the well. Measured the zones to the nearest millimeter using a ruler.

- Then the zone sizes were interpreted by referring to the standard table and reported the organism to be either susceptible, intermediate, or resistant.

CHAPTER THREE

RESULTS & DISCUSSION

RESULTS & DISCUSSION

The field of nanoscience and nanotechnology push the investigation forward to produce CNTs with suitable parameters for future applications and our new approaches of their synthesis maintaining uniformity may be a developed and optimized idea. As there are significant hollow spaces **[58, 59]** (showed by Figure 3.1 for both of SWCNTs and MWCNTs) so the possibilities of filling CNT with different nanoparticles is a demanding matter to use it as a carrier in delivery or in various functional issues. In our experiment the other nanoparticles Mn_3O_4, NiO, Ni, MnO_2 which were used for these encapsulation purposes were prepared by conventional method. The total filling of CNTs were done by the controlled boiling of the CNTs with nanoactive metal species.
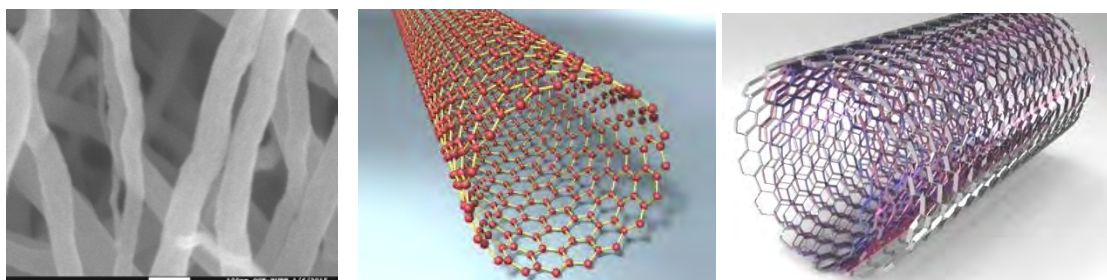
Figure 3.1: Cylindrical structure of CNT(SEM image) clearly demonstrate the hollow space inside it by schemetic diagram for both SWCNT & MWCNT

CNTs and the above nanometal/metal oxides as well as the filled matrices were characterized by Energy Dispersive X-Ray spectroscopy(EDX), Scanning Electron Microscopy(SEM), X-Ray Diffraction(XRD), Fourier Transform Infra-red(FTIR) spectroscopy analysis. The particle size and morphology of synthesized nanomaterials and filled matrices were analysed by the Scannig Electron Microscopic(SEM) experiment. EDX spectroscopy provided the information about the chemical composition. By XRD analysis crystalline structure and crystal size of the synthesized nanoparticles were confirmed. IR analysis provided the presense of functional groups if any in the smooth sidewalls of CNTs.

3.1. Characterization

3.1.1. Scanning Electron Microscopic (SEM) anaysis of the synthesized nanoparticles and the filled matrices
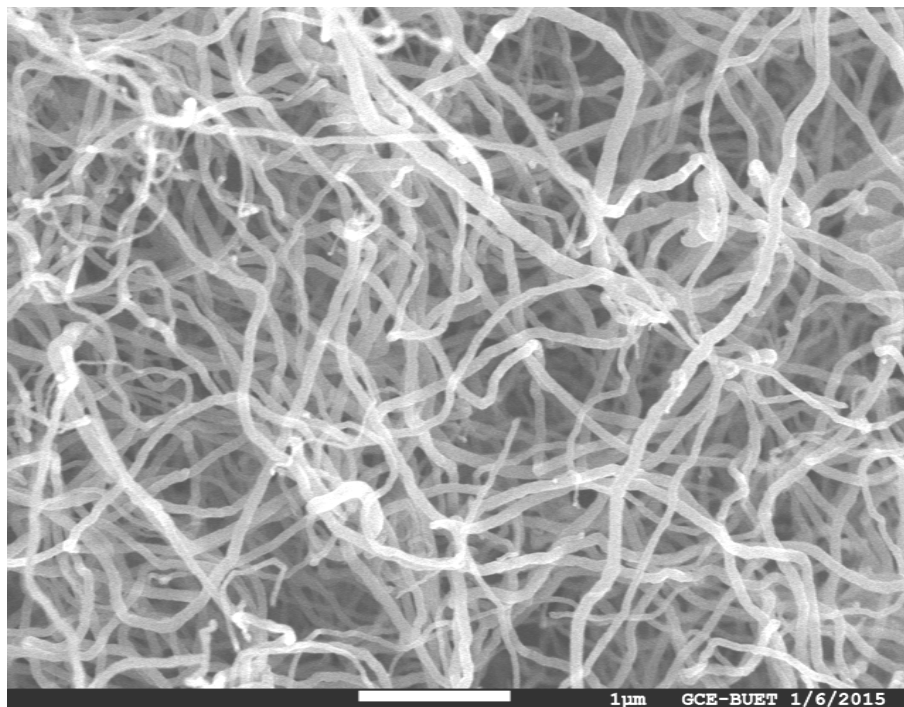
Figure 3.2: SEM image of CNTs to observe the tube diameter of the synthesized CNTs
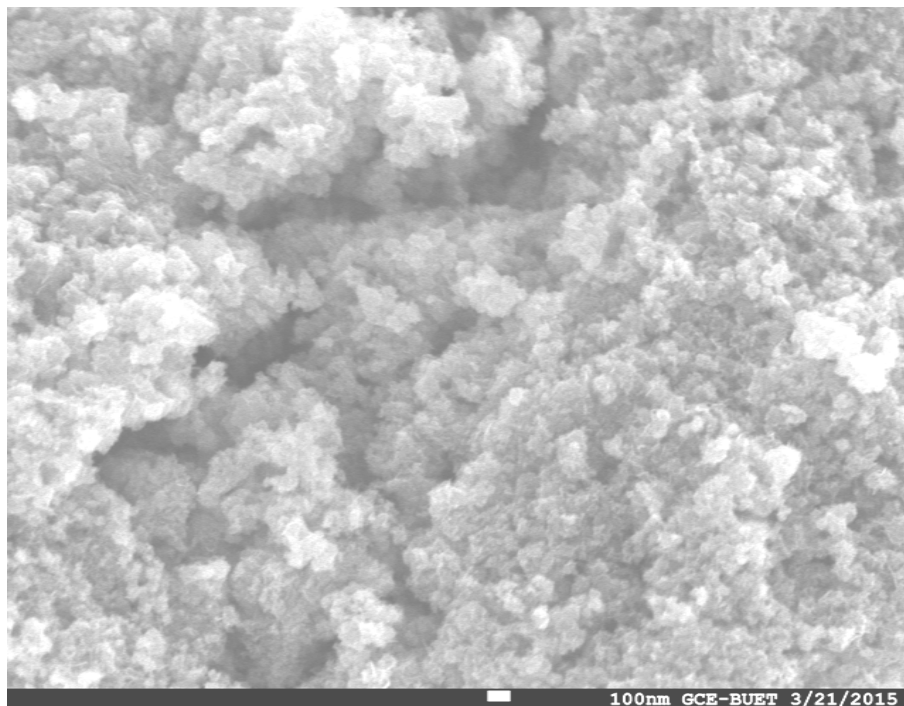
Figure 3.3: SEM image of Ni nanoparticles to observe the grain size of the synthesized particles
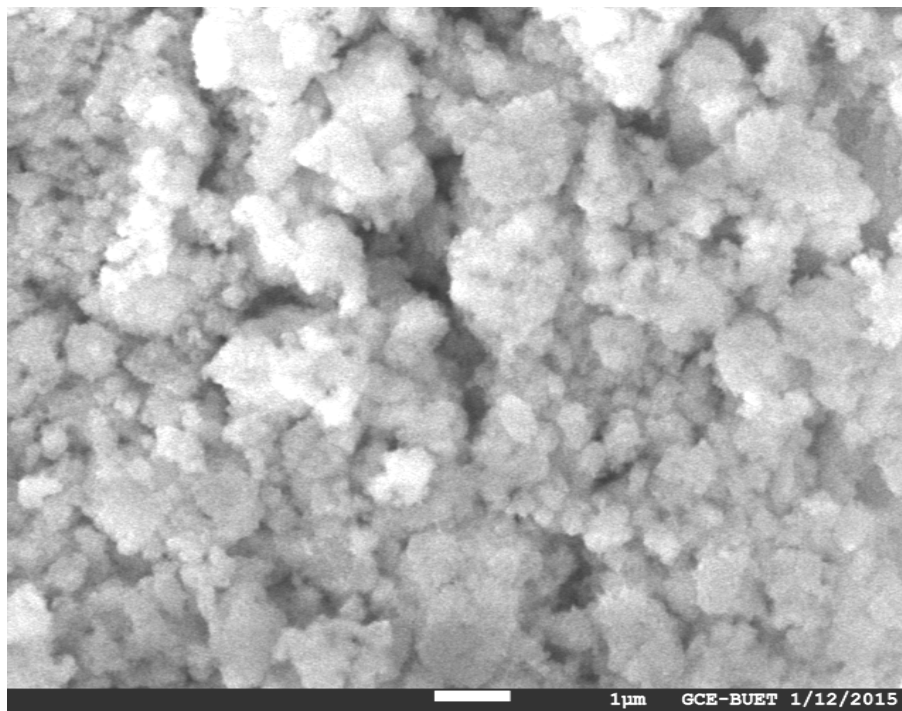
Figure 3.4: SEM image of NiO nanoparticles to observe the grain size of the synthesized particles
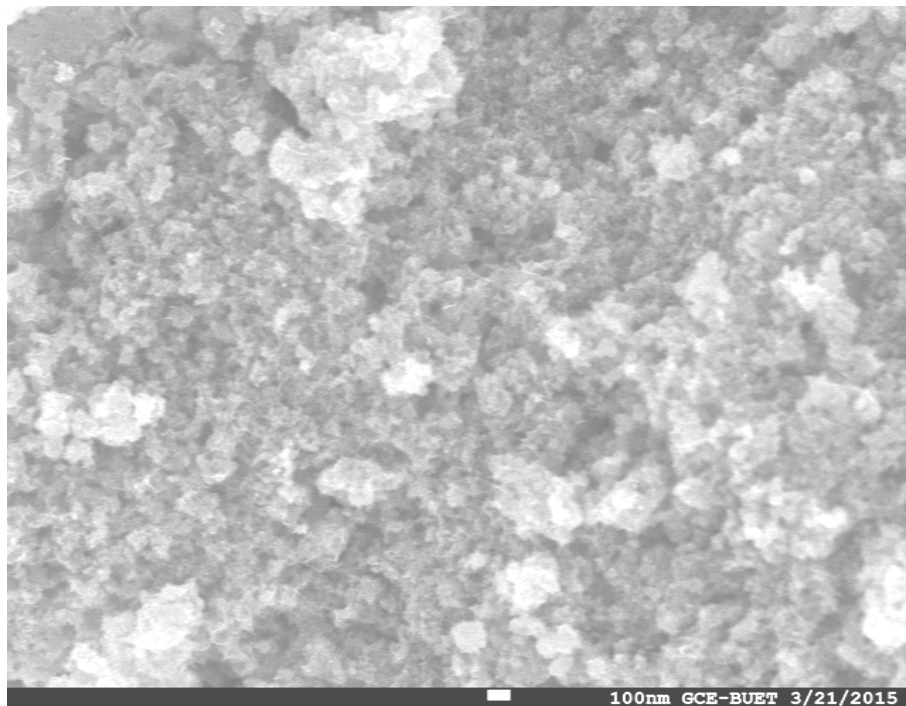
Figure 3.5: SEM image of MnO_2 nanoparticles to observe the grain size of the synthesized particles
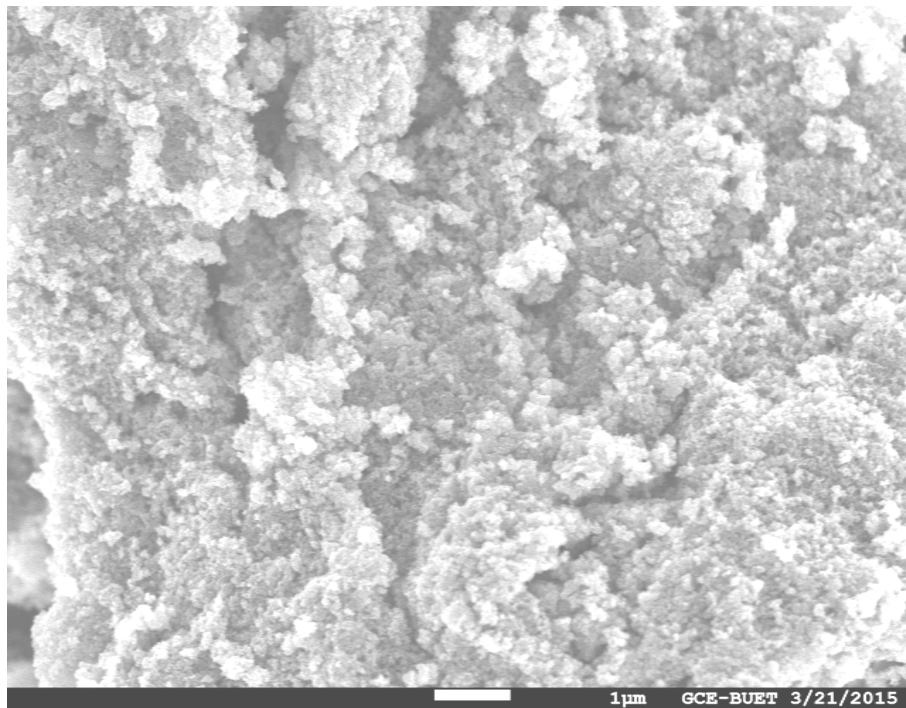
Figure 3.6: SEM image of Mn_3O_4 nanoparticles to observe the grain size of the synthesized particles
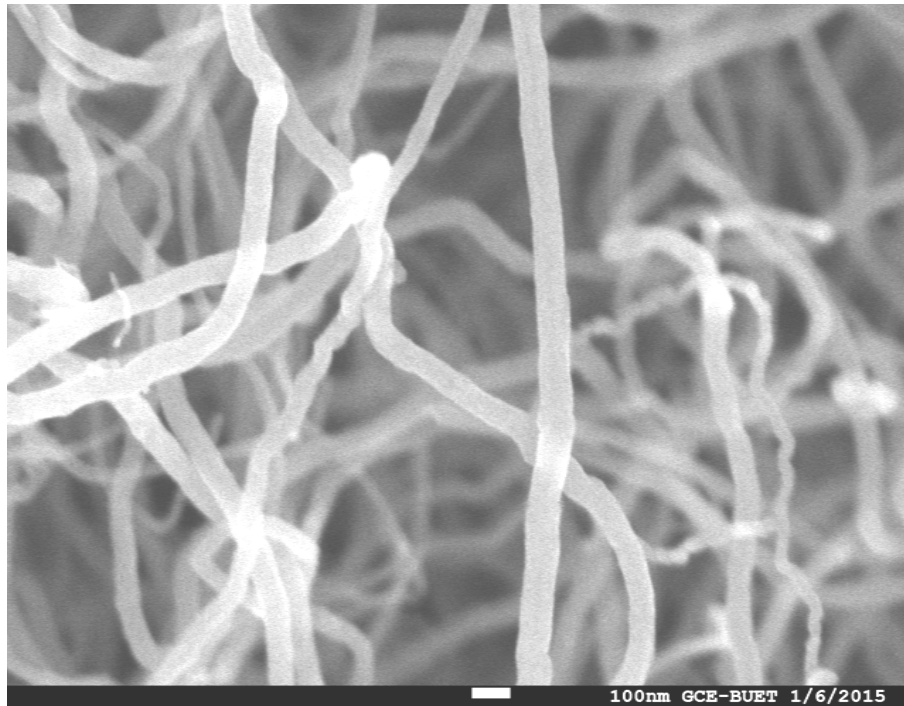
Figure 3.7: SEM image of Ni nanoparticles filled CNTs to observe the percentage of particles attached to the sidewalls of CNTs after filling treatment
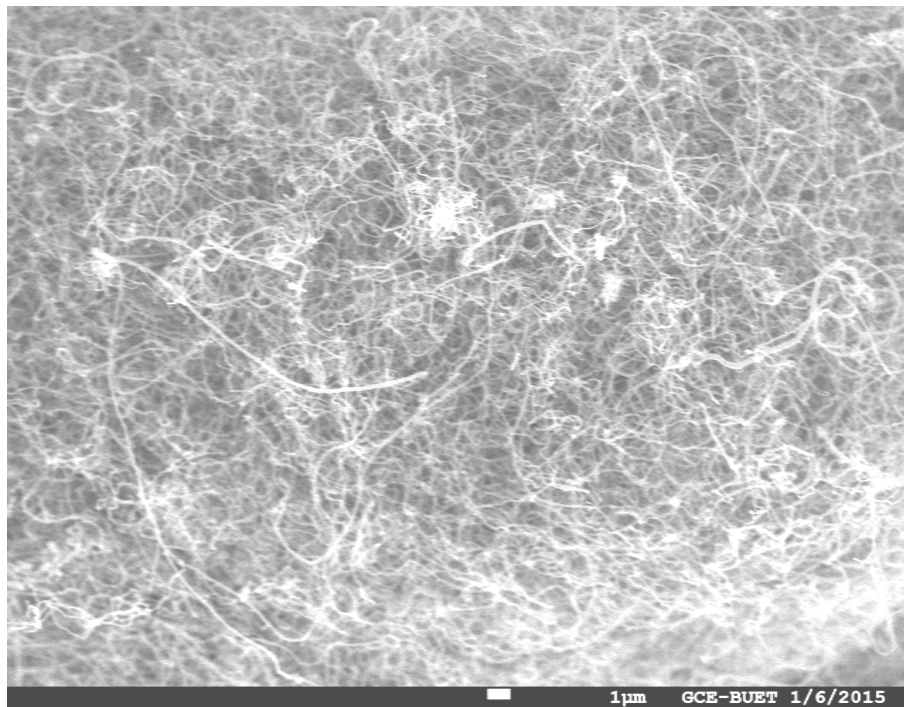
Figure 3.8: SEM image of NiO nanoparticles filled CNTs to observe the percentage of particles attached to the sidewalls of CNTs after filling treatment
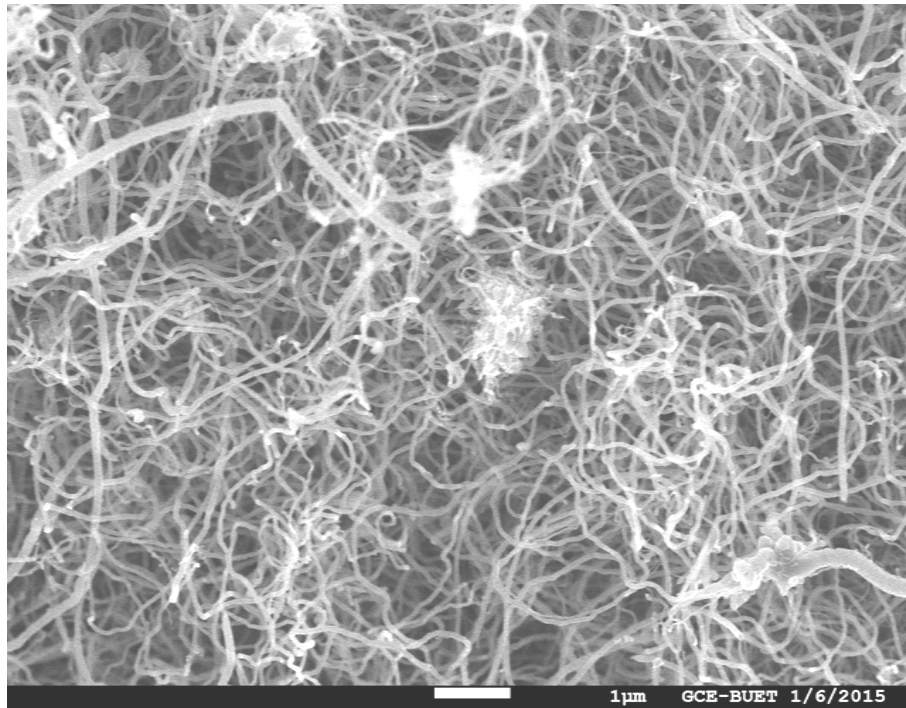
Figure 3.9: SEM image of MnO_2 nanoparticles filled CNTs to observe the percentage of particles attached to the sidewalls of CNTs after filling treatment
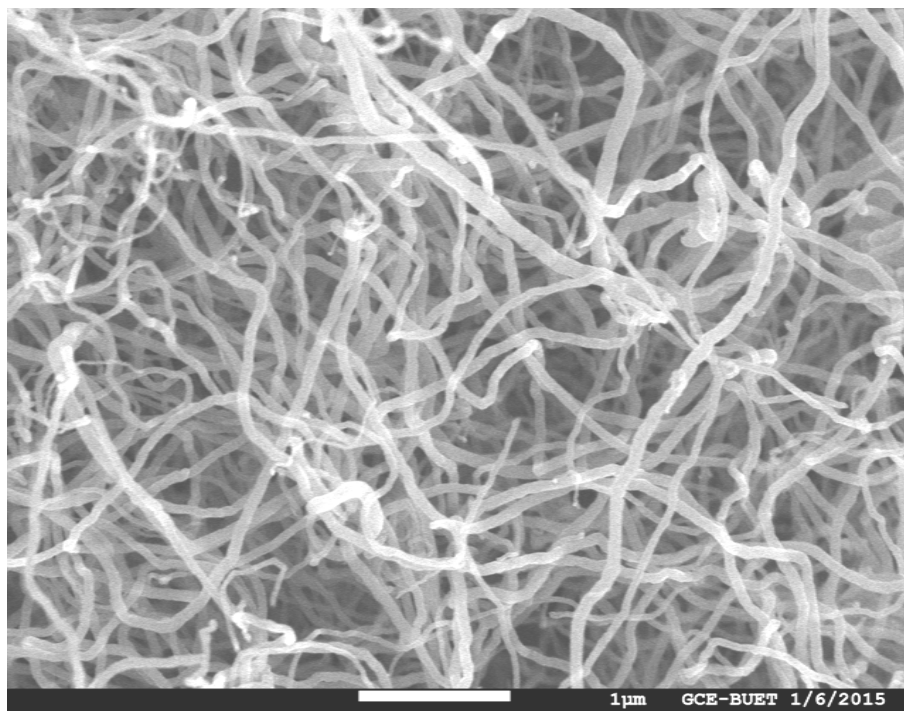
Figure 3.10: SEM image of Mn_3O_4 nanoparticles filled CNTs to observe the percentage of particles attached to the sidewalls of CNTs after filling treatment

The scanning electron microscope (SEM) uses a focused beam of high-energy electrons to generate a variety of signals at the surface of solid specimens. The signals that derive from electron-sample interactions reveal information about the sample including external morphology (texture) to confirm the size and shape of nanoparticles . Modern SEM generates data in digital formats, which are highly portable. The SEM photographs were taken with an average magnification $\times 30000$ and 5-15 kv at room temperature. The study of the SEM images shows the clear size & shape of CNTs and other nanoparticles as well as the filled matrices.   The SEM image for CNT is shown in Figure(3.2), which shows dense and clean nanotubes. Distinguishable CNTs are visible at high resolution and the cross section confirms that CNTs specific diameter.   Obviously, the quality is much better**[60, 61]**. The diameter of the nanotubes are about 70 nanometer on average.

SEM images of other synthesized nanoparticles also revealed specific presentation of their authentic granular sizes. The synthesized nanoparticles were aggregated as common nature of oxides but still provide clear information about their sizes. The size of Ni & NiO   nanoparticles can be confirmed by Figure(3.3, 3.4) respectively. The average granular size is 20 nm -30 nm. Figure(3.5) shows the size of nano MnO_2 as 15 nm- 20 nm. Nano Mn_3O_4 were found with average sizes 20-25 nm for every granules (Figure 3.6). Here we can see that these microscopic views of every synthesized nanoparticles confirm the nanosizes. The aggregated particles are loosely attached to each other and can be easily separated by making suspension.

Encapsulation of CNTs by the synthesized nanoparticles was another challange. As SEM images can only provide the outer morphology of any experimented substances so the inside particles can not be seen from these images. The studies revealed CNTs with a high filling yield. This was confirmed by the weighing difference of initial and final amount of nanoparticles incorporated. From Figure(3.7-3.10) it can be understood that the nanoparticles were perfectly filled in the hollow space of the CNTs. As the size of the synthesized metal species were uniform with nanodimension so percentages of filling were very good. But here it is observed that still very small proportion of nanoparticles which are attached to the side walls can be removed   by electrophoresis as there were a little percentage of particle size discrimination due to agglomeration of the adjacent particles.

3.1.2. EDX spectral anaysis of the synthesized CNTs, nanoparticles and the filled matrices
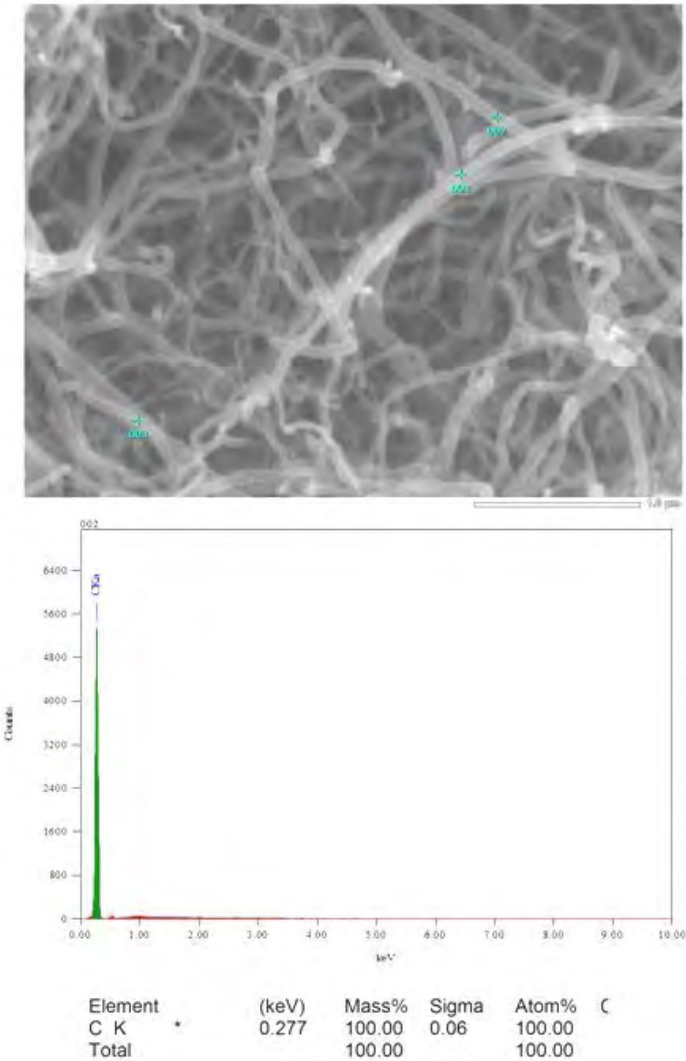
Figure 3.11: EDX data of CNTs to observe the elemental confirmation of synthesized CNTs

Element	(keV)	Mass%	Sigma	Atom%	Compoι
O K	0.525	8.44	0.09	25.27	
Ni K	7.471	91.56	1.18	74.73	
Total		100.00		100.00	
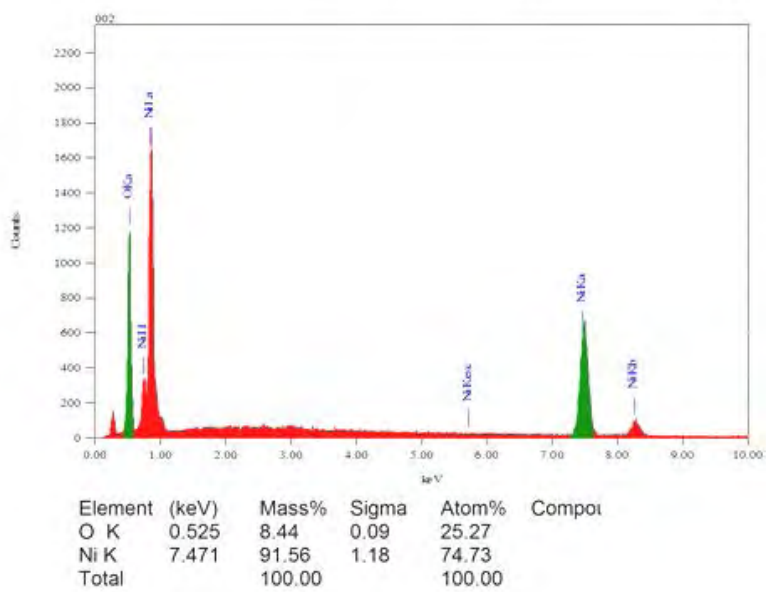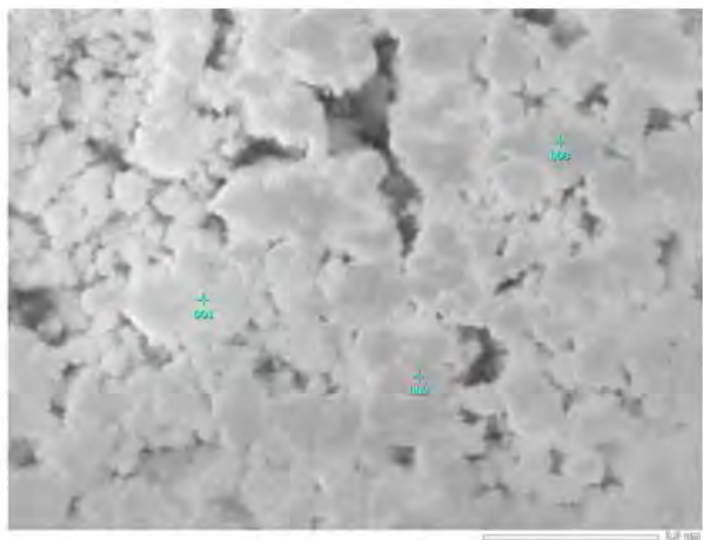
Figure 3.12: EDX data of pure NiO nanoparticles to observe the elemental confirmation of the synthesized nanoparticles
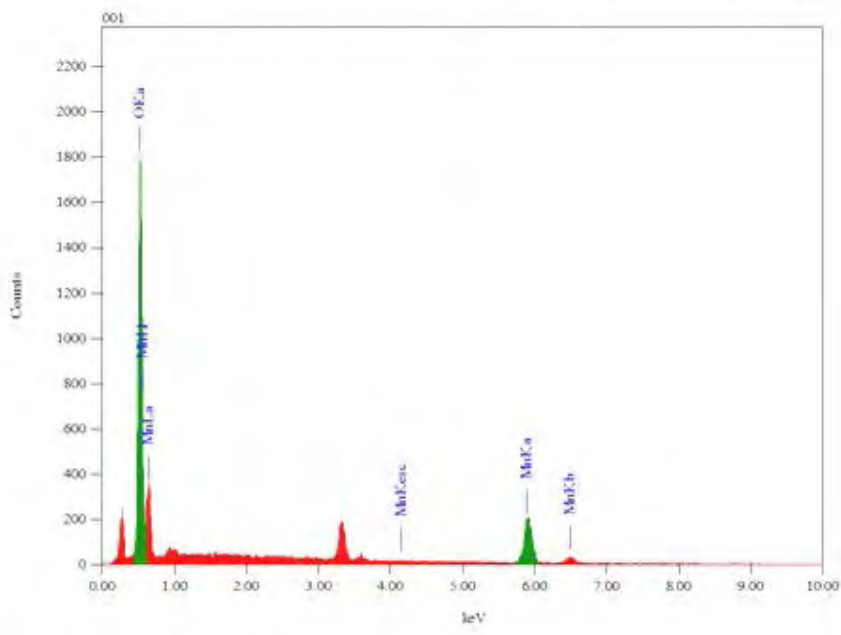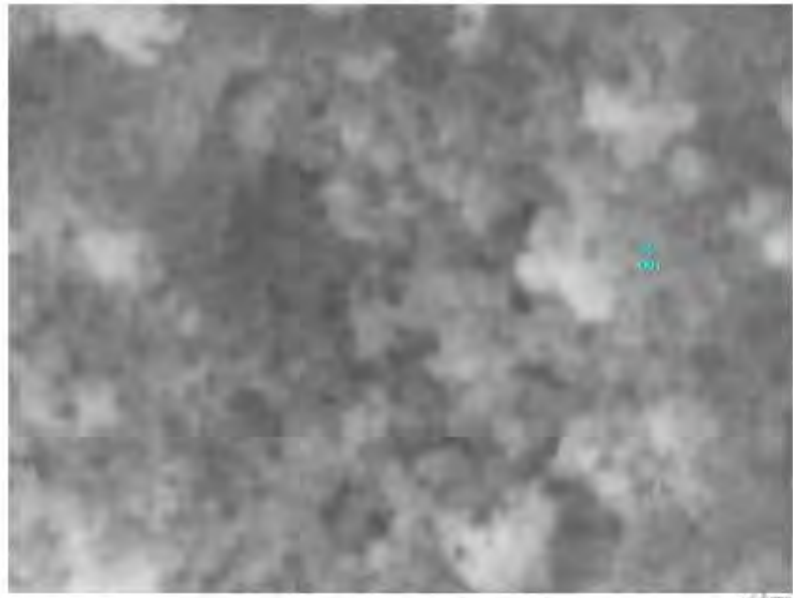
Element	(keV)	Mass%	Sigma	Atom%	Comp
O K	0.525	36.01	0.32	65.90	
Mn K	5.894	63.99	1.56	34.10	
Total		100.00		100.00	

Figure3.13: EDX data of pure MnO_2 nanoparticles to observe the elemental confirmation of the synthesized nanoparticles

Element	(keV)	Mass%	Sigma	Atom%	Compo
O K	0.525	32.34	0.31	62.14	
Mn K	5.894	67.66	1.65	37.86	
Total		100.00		100.00	
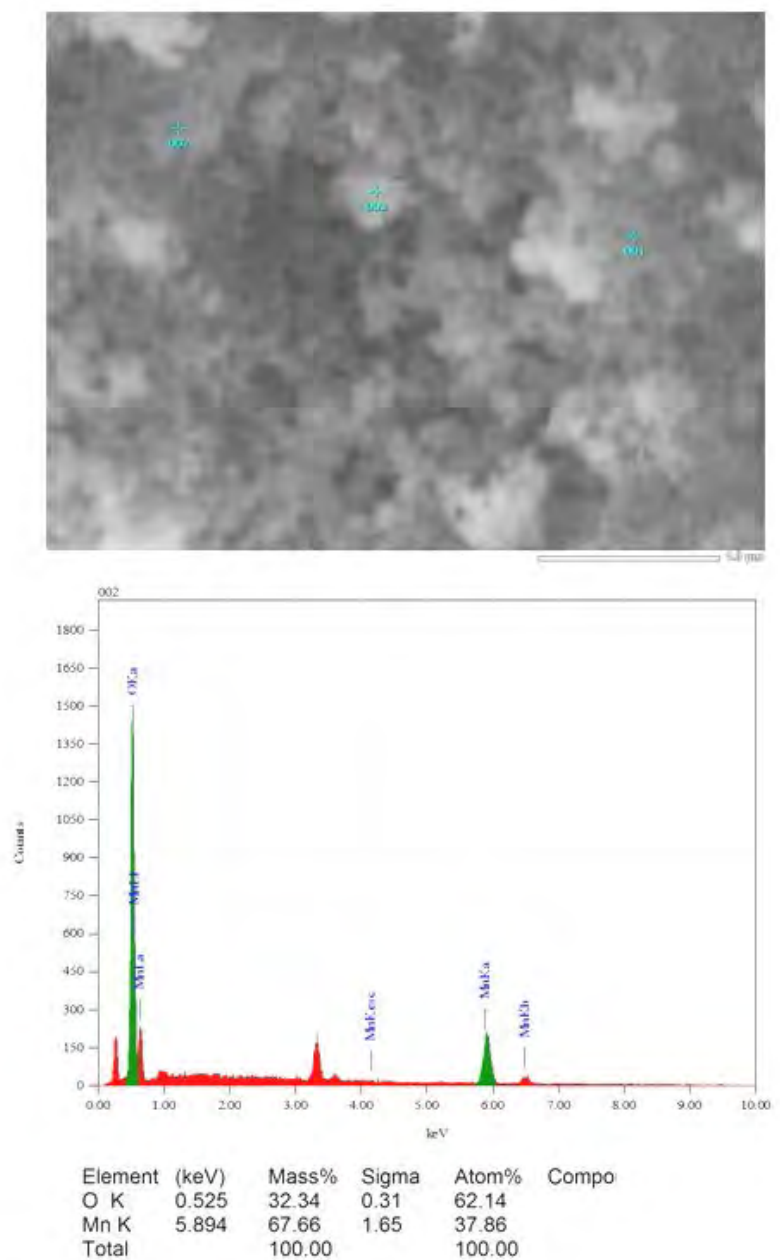
Figure 3.14: EDX data of pure Mn_3O_4 nanoparticles to observe the elemental confirmation of the synthesized nanoparticles

Element	(keV)	Mass%	Sigma	Atom%	Comp
C K	0.277	47.03	8201344.50		69.43
O K	0.525	18.07	25006.05	20.03	
Ni L	0.851	34.89	50412.25	10.54	
Total		100.00		100.00	

Figure 3.15: EDX data of pure NiO filled CNTs to observe the elemental confirmation of the loaded CNTs

Element		(keV)	Mass%	Sigma	Atom%	C
C K		0.277	70.55	0.06	89.98	
O K	*	0.525	3.36	0.07	3.21	
Ni K	*	7.471	26.10	0.47	6.81	
Total			100.00		100.00	
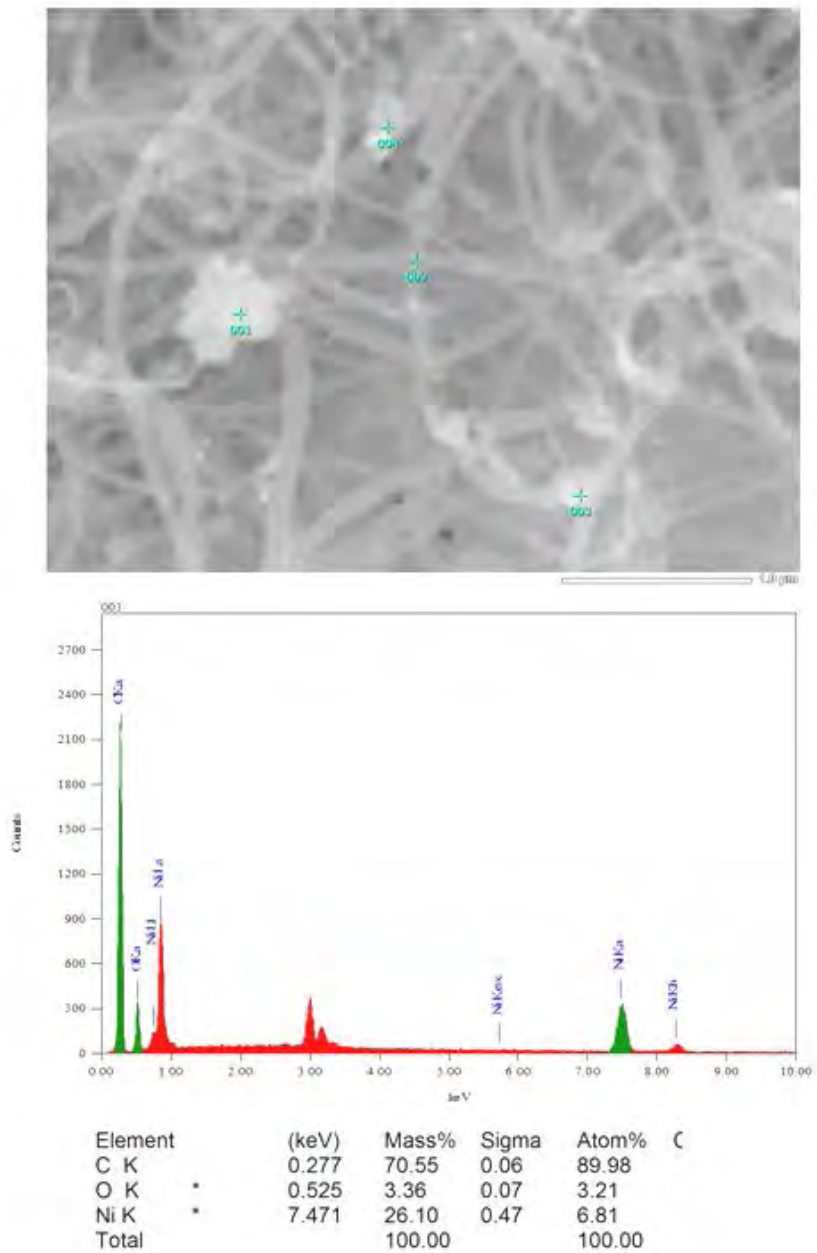
Figure 3.16: EDX data of pure Ni filled CNTs to observe the elemental confirmation of the loaded CNTs
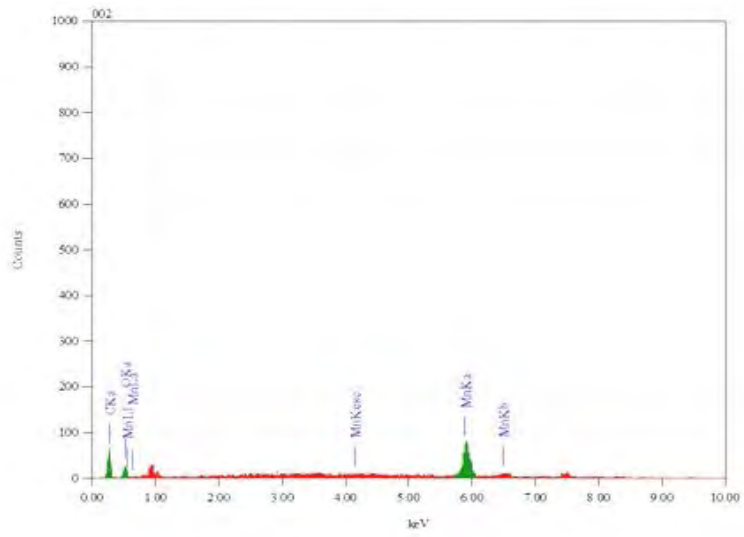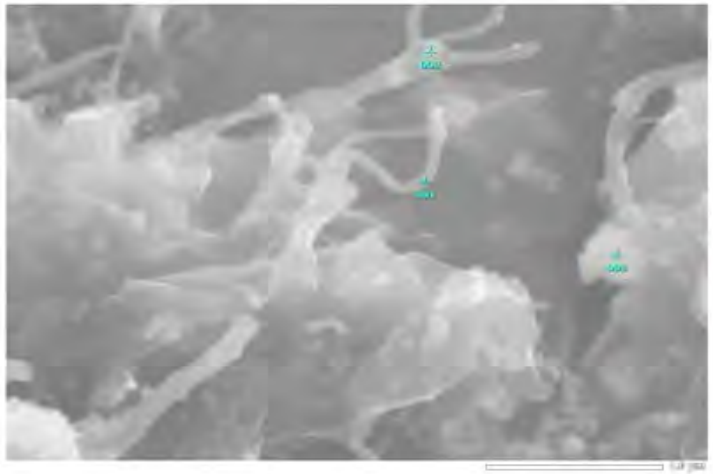
Element		(keV)	Mass%	Sigma	Atom%	
C K		0.277	13.37	0.38	39.84	
O K	*	0.525	2.33	0.18	5.22	
Mn K	*	5.894	84.30	3.64	54.94	
Total			100.00		100.00	

Figure 3.17: EDX data of pure MnO$_2$ filled CNTs to observe the elemental confirmation of the loaded CNTs

Element	(keV)	Mass%	Sigma	Atom%	C
C K	0.277	21.88	0.04	37.93	
O K	0.525	35.17	0.12	45.79	
Mn K	5.894	42.95	0.55	16.28	
Total		100.00		100.00	

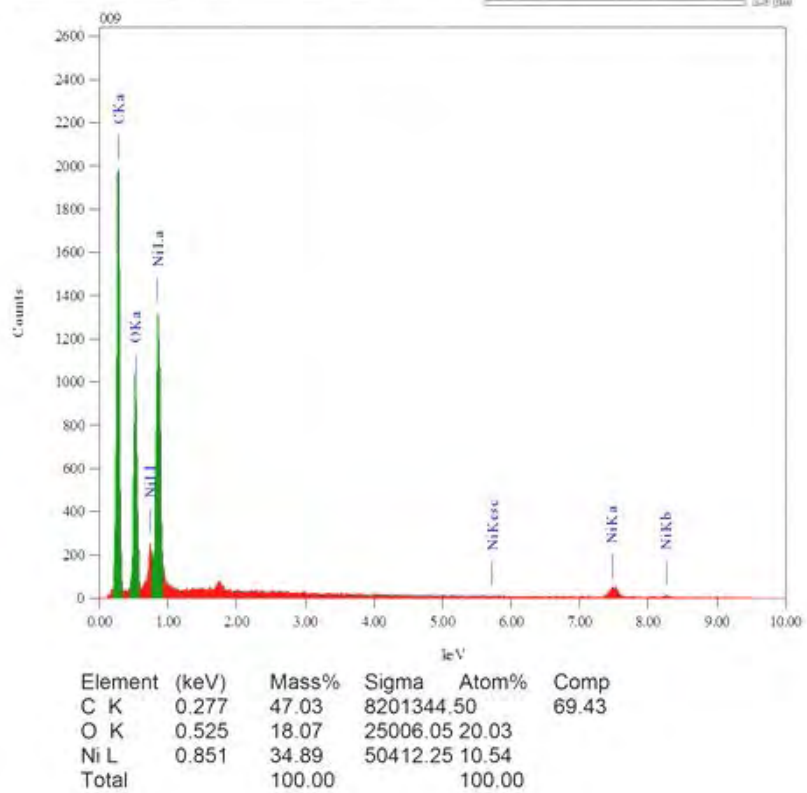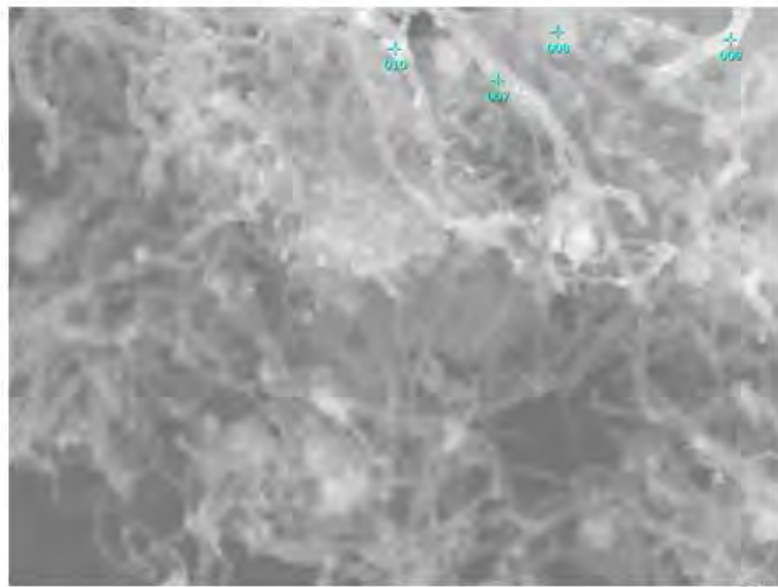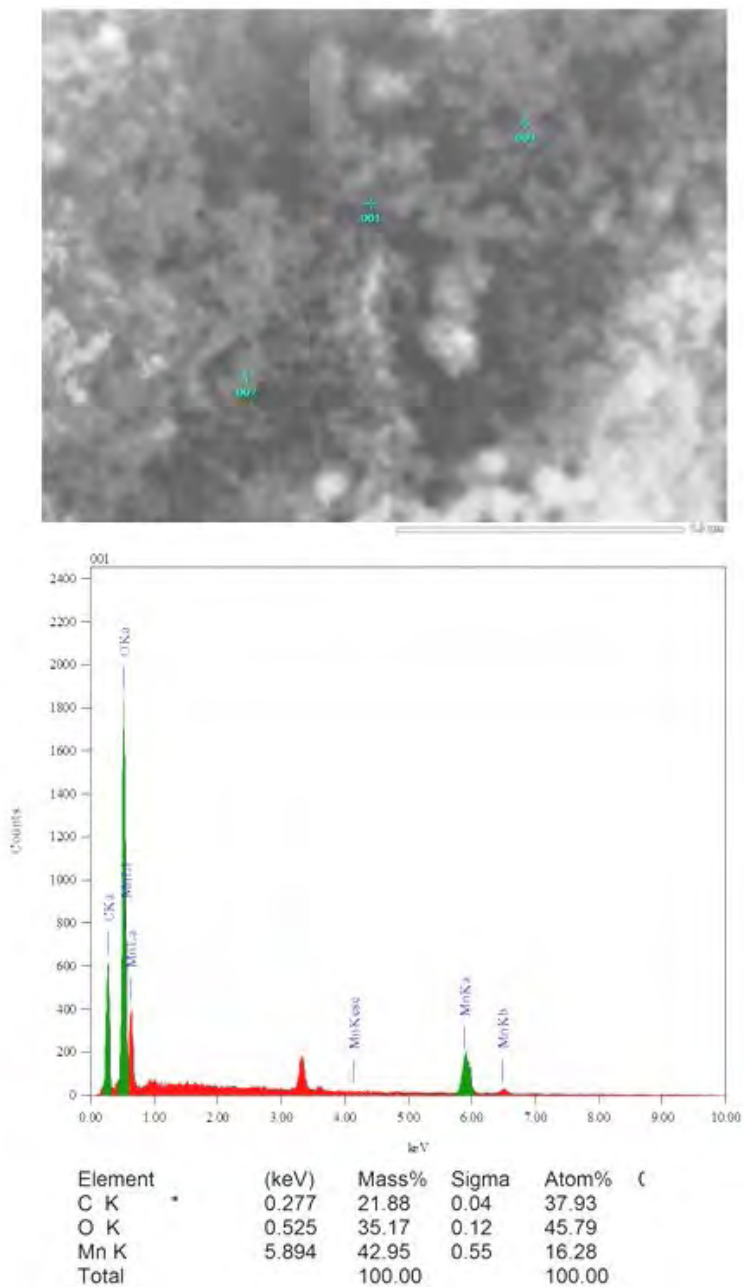**Figure 3.18:** EDX data of pure Mn_3O_4 filled CNTs to observe the elemental confirmation of the loaded CNTs

The elemental analysis was successfully confirmed by energy dispersive X-ray measurment. It's characterization capabilities are due in large part to the fundamental principle that each element has a unique atomic structure allowing unique set of peaks on its X-ray emission spectrum. To stimulate the emission of characteristic X-rays from a specimen, a high-energy beam of charged particles such as electrons or protons, or a beam of X-rays, is focused into the sample being studied. From Figure(3.11) it is observed that there is a clear abundance of carbon element which confirmly supported that CNTs contains only carbons. From Figure(3.11) the abundance simply detected by the k(alpha)shell electrons at 0.3 keV. Percentage by mass and percentage by atomic abundace is 100%. NiO nanoparticles is clearly confirmed by the the Figure(3.12). We can see that the peak for k(alpha) shell electrons of O shows the maximum counts Of NiO at 0.5 keV. From the Figure(3.13) and Figure(3.14) it is confirmed that the MnO_2 and Mn_3O_4 were successfully prepared by following conventional methods. In figure(3.13) Mn was abundantly present at 0.6keV, 5.9keV and 6.5keV comprising L and k shells where O is confirmed at 0.5k eV by K(alpha) shell electrons. As the energy of the X-rays are characterized of the difference in energy between the two shells, and of the atomic structure of the element from which they were emitted, this allows the elemental identification of the specimen to be measured[62]. For Mn_3O_4 nanoparticles we can see that the Mn and O are abundant for the same keV positions but the abundance is different from the Mn_3O_4 constituents.

Figure(3.15-3.18) show the elemental analysis using energy dispersive X-ray measurment for the CNTs encapsulated by the NiO, Ni, MnO_2 and Mn_3O_4 nanoparticles respectively which are assumed as active nanometal species. From Figure(3.15) it is observed that the CNTs as well as encapsulated nano NiO species gives very bright peaks thus it is confirmed there are clear abundance of CNTs and NiO nanoparticles. Figure(3.16) is for the confirmation of the presence of CNTs encapsulated with Ni metal nanoparticles. From this figure we can see that CNTs and Ni nps has significant peaks but there is a presence of a peak for oxygen element at 0.5 keV as an impurity. Figure(3.17) clearly shows about the presence of MnO_2 for the shifting of electron from K (alpha) shell from all the elements and Figure(3.18) is for Mn_3O_4 nanoparticles encapsulated CNTs where K (alpha) shell electrons were shifted for carbon, oxygen and for manganese. Both the K and L shell electrons participeted in shifting to produce X-ray emission.

3.1.3. X-ray crystallographic anaysis of the synthesized nanoparticles and the filled matrices

Main Graphics, Analyze View:
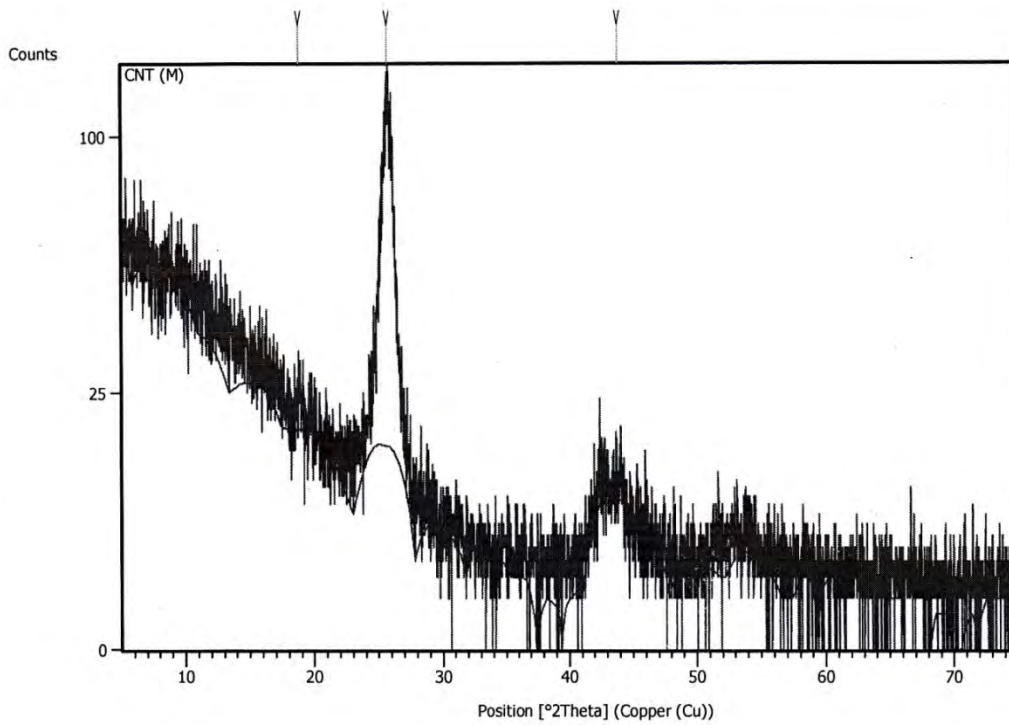
Peak List: (Bookmark 3)

Pos. [°2Th.]	Height [cts]	FWHM Left [°2Th.]	d-spacing [Å]	Rel. Int. [%]
18.8652	7.93	0.4723	4.70406	7.78
25.7250	101.91	0.4723	3.46315	100.00
43.8934	2.94	0.4723	2.06274	2.88

Figure 3.19: X-ray diffraction spectra and resultant data of synthesized CNTs to confirm by matching them with the actual XRD figure and data of CNTs

Main Graphics, Analyze View:
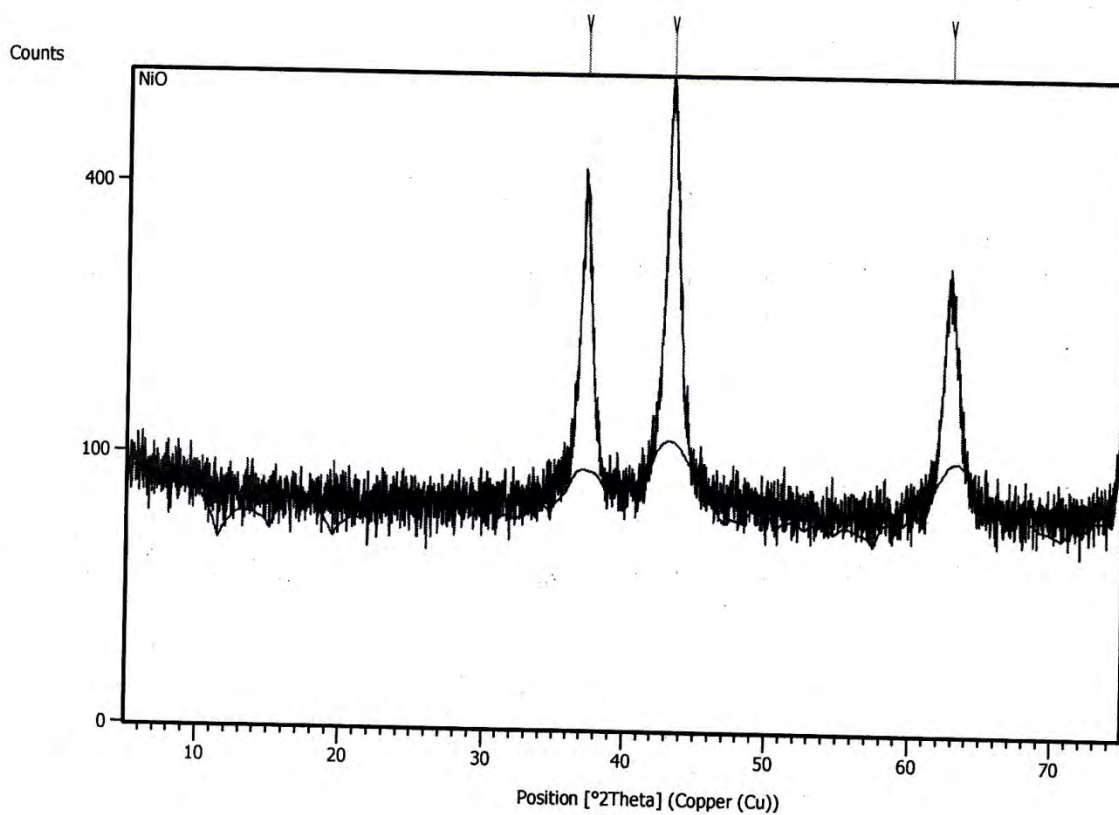
Peak List: (Bookmark 3)

Pos. [°2Th.]	Height [cts]	FWHM Left [°2Th.]	d-spacing [Å]	Rel. Int. [%]
37.1118	310.10	0.2755	2.42258	70.21
43.1587	441.69	0.3149	2.09614	100.00
62.6722	180.28	0.4723	1.48241	40.82

Figure 3.20: X-ray diffraction spectra and resultant data of NiO nanoparticles to find out the crystalline structure and crystal size of the synthesized particles

Main Graphics, Analyze View:
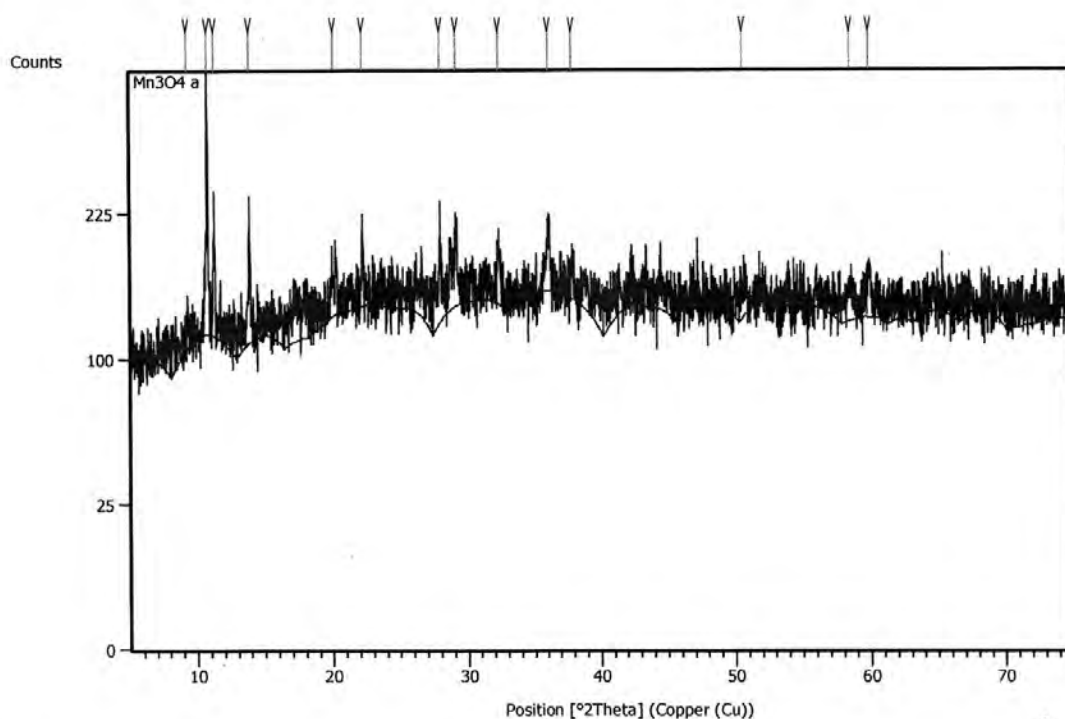
Peak List: (Bookmark 3)

Pos. [°2Th.]	Height [cts]	FWHM Left [°2Th.]	d-spacing [Å]	Rel. Int. [%]
9.3033	33.54	0.1181	9.50634	11.95
10.8140	280.72	0.0787	8.18145	100.00
11.3155	111.47	0.0787	7.81998	39.71
13.8972	112.20	0.0590	6.37248	39.97
20.1286	32.10	0.4723	4.41157	11.43
22.2390	79.82	0.0984	3.99748	28.44
28.0079	107.78	0.0787	3.18583	38.39
29.1780	70.40	0.1574	3.06069	25.08
32.3445	48.26	0.2362	2.76792	17.19
36.0862	51.51	0.2362	2.48904	18.35
37.9534	29.32	0.2362	2.37077	10.45
50.6084	22.54	0.7872	1.80368	8.03
58.5362	27.73	0.4723	1.57689	9.88
59.9033	40.96	0.3936	1.54413	14.59

Figure 3.21: X-ray diffraction spectra and resultant data of Mn_3O_4 nanoparticles to find out the crystalline structure and crystal size of the synthesized particles

Main Graphics, Analyze View:
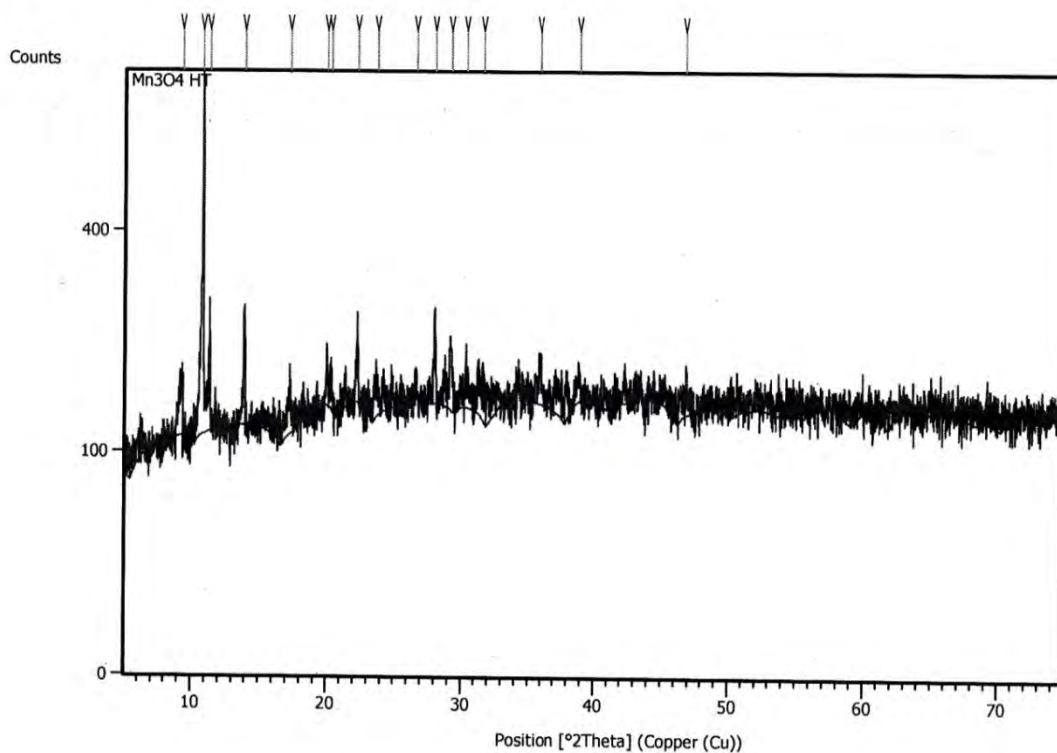
Peak List: (Bookmark 3)

Pos. [°2Th.]	Height [cts]	FWHM Left [°2Th.]	d-spacing [Å]	Rel. Int. [%]
9.2880	79.58	0.0984	9.52190	12.37
10.8200	643.16	0.0590	8.17690	100.00
11.3248	168.61	0.0787	7.81352	26.22
13.8953	152.56	0.0787	6.37334	23.72
17.2770	66.01	0.1181	5.13276	10.26
19.9986	62.51	0.1181	4.43995	9.72
20.2946	60.90	0.1181	4.37587	9.47
22.2539	118.74	0.0590	3.99484	18.46
23.6775	40.90	0.2362	3.75778	6.36
26.6272	34.54	0.1574	3.34781	5.37
28.0013	113.82	0.0787	3.18658	17.70
29.1763	78.46	0.1968	3.06086	12.20
30.3292	31.23	0.4723	2.94709	4.86
31.6137	63.14	0.1181	2.83021	9.82
35.8728	50.93	0.1574	2.50336	7.92
38.8718	34.40	0.1968	2.31685	5.35
46.7860	24.69	0.4723	1.94173	3.84

Figure 3.22: X-ray diffraction spectra and resultant data of Mn_3O_4 synthesized at comparatively high temperature to find out the crystalline structure and crystal size of the synthesized particles

X-ray crystallographer is a tool used for identifying the atomic and molecular structure of a crystal, in which the crystalline atoms cause a beam of incident X-rays to diffract into many specific directions. With specialized techniques, XRD can be used to characterize of crystalline materials, identification of fine-grained minerals such as clays and mixed layer clays that are difficult to determine optically, determination of unit cell dimensions, measurement of sample purity, determine crystal structures using Rietveld refinement etc. Since many materials can form crystals such as salts, metals, minerals, semiconductors as well as various inorganic, organic and biological molecules, X-ray crystallography has been fundamental in the development of many scientific fields.

By measuring the angles and intensities of these diffracted beams, a three-dimensional picture of the density of electrons within the crystal formed. From this electron density, the mean positions of the atoms in the crystal can be determined, as well as their chemical bonds, their disorder and various other information. In Figure(3.19-3.22) X-ray diffraction spectral images and corresponding datas were provided. The height, FWHM(full width at half maxima), d-spacing value and relative intensity at $2\theta^0$ of each nanoparticles give result of high accuracy. The X-ray diffraction image for CNTs (Figure 3.19) displays the clear sharp peak at 25.72 position which clearly confirm the respective compound is CNT [63]. This higher density of electrons at this position is almost identical for every CNTs. The other content of XRD results matches with the standard X-ray powder diffraction values of the respected molecules. Figure(3.21) and Figure(3.22) gives the almost same results for both type of Mn_3O_4 nanoparticles (temperature variation during preparation). Using these XRD data of these nanoparticles the actual crystallite size and shape were determined using scherrer's equation and Nelson Riley (NR) function[$F(\theta)$] [64] respectively.

3.1.3.1. Determination of Crystallite size of nanoparticles and filled matrices

The finite crystallite size is found as a broadening of the peaks in an x-ray diffraction as is explained by the Scherrer 's equation[65].

$$D_g = \frac{0.9\lambda}{\Delta cos\theta}$$

Here, θ=Bragg angle,   λ (default wave legth of x-ray)=0.154060 nm

Δ= Full width at half maxima(FWHM), D_g= cryastalline grain size.

The following results of crystalline size of the nanomaterials were found (Table 3.1).

Table 3.1: Crystal size determination of nanoparticles (diameter of crystal; D_g)

Element	The height of most intensed peak	$2\theta^0$	θ^0	FWHM $[\ ]^0$	λ [Å]	D_g (nm)
NiO	441.69	43.1587	21.57935	0.3149	1.54060	**6.036**
Mn_3O_4	280.72	10.8140	5.407	0.0787	1.54060	**17.697**

The sizes of the crystals were calculated and the values got for the corresponding crystals are excellent. From Table(3.1) the actual crystallite diameter as well as grain diameter of NiO and Mn_3O_4 were found as 6.036 and 17.697 respectively. Here it should be mentioned that these size is for individual crystal, not for the particle. Generally a particle formed consistsisting a number of crystals. The nanoparticle's diameter were confirmed by the SEM analysis.

3.1.3.2. Determination of crystallite parameter to confirm the crystal shape

Nelson Riley (NR) function ; *F(θ)*

$$F(\theta) = \frac{1}{2}\left[\frac{\cos^2\theta}{\sin\theta} + \frac{\cos^2\theta}{\theta}\right]$$

Table 3.2: Crystalline parameters of NiO nanoparticles

$$\frac{1}{d^2} = \frac{h^2+k^2+l^2}{a^2}$$

$2\theta^0$	θ^0	d [Å]	h, k, l (Millar indices)	N.R.	a
37.1118	18.5559	2.42258	111	1.436826	4.1960314
43.1587	21.57935	2.09614	200	1.19562	3.630621
62.6722	31.3361	1.48241	220	0.713044	2.567609
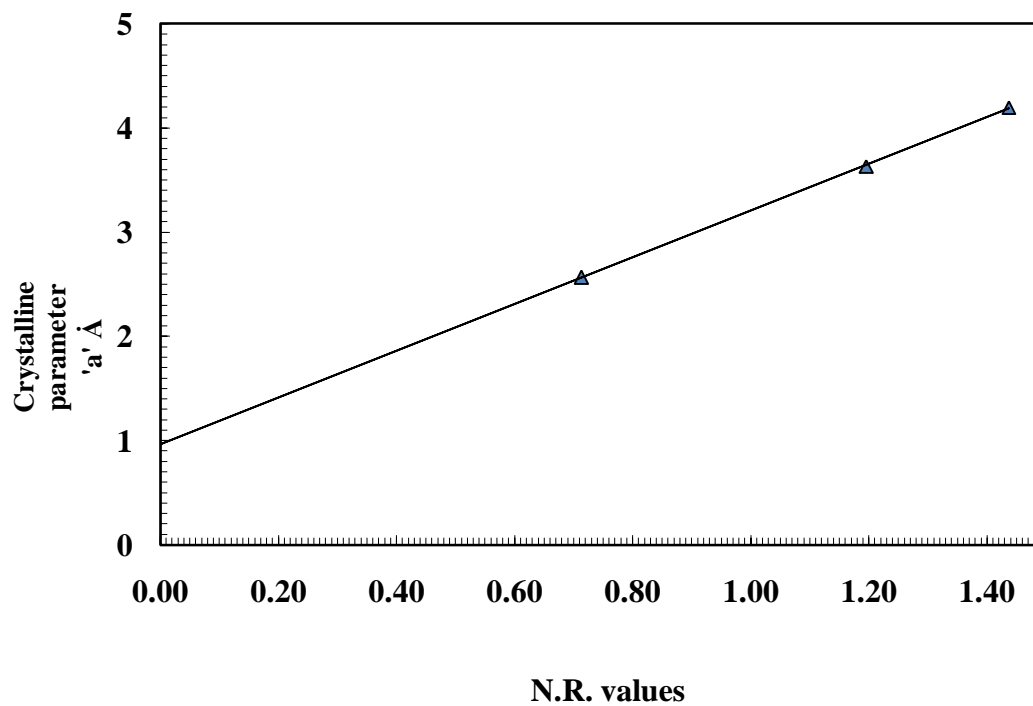
Figure 3.23: Determination of a° value of NiO crystals from graphical presentation to investigate the crystal shape

Table 3.3: Crystalline parameters of Mn$_3$O$_4$ nanoparticles

$$\frac{1}{d^2} = \frac{h^2 + k^2 + l^2}{a^2}$$

2θ^0	θ^0	d [Å]	h, k, l (Millar indices)	N.R.	a
9.3033	4.65165	9.50634	101	6.231637	13.44399
10.8140	5.407	8.18145	100	5.350705	11.57034
13.8972	6.9486	6.37248	111	4.143368	11.03745
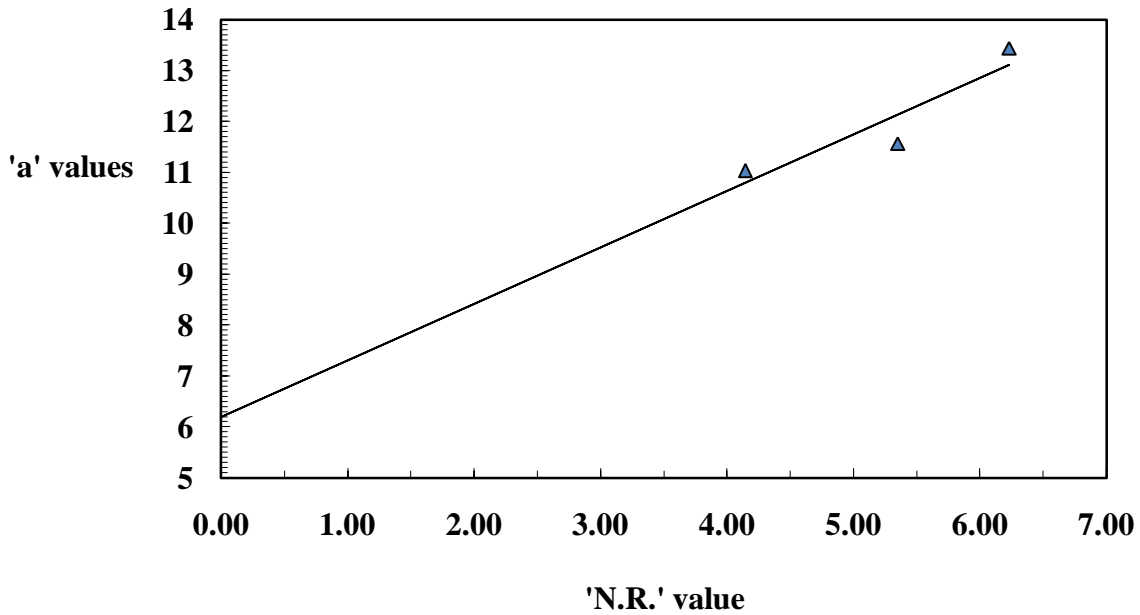
Figure 3.24: Determination of 'a^o' value of Mn$_3$O$_4$ crystal from graphical presentation to investigate the crystal shape

From the literature it is mostly found that NiO and Mn$_3$O$_4$ crystal are cubic shaped and we know the crystalline parameter for the cubic shape is 'a'. Using the XRD parameter the value of 'a' were determined for NiO and Mn$_3$O$_4$ nanoparticles (Table 3.2 & 3.3) and by plotting them against N.R. values (Figure 3.23, 3.24) the a^o values were calculated which were coinsidered standard values. Thus it is confirmed that the NiO and Mn$_3$O$_4$ nanoparticles consist of cubic crystals.

3.1.4. FTIR spectroscopical anaysis of the synthesized CNTs
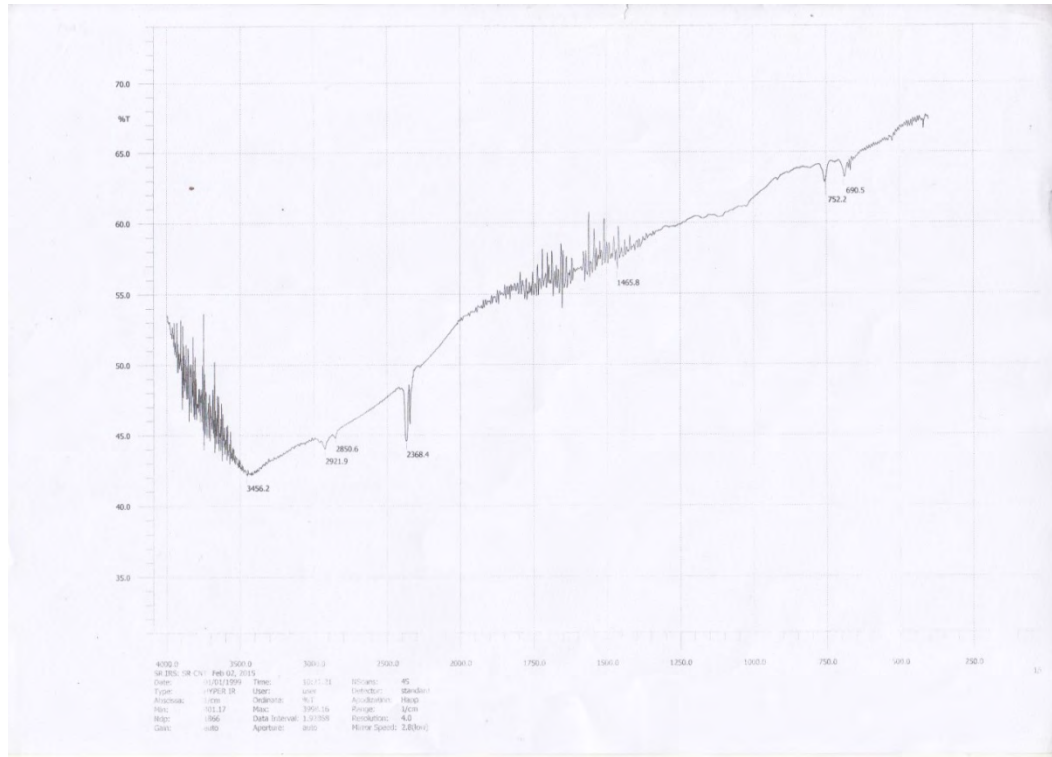
Figure 3.25: FTIR spectra of synthesized CNTs to check the unwanted functional groups if present in the side walls of it

Fourier Transform Infrared Spectroscopy, also known as FTIR Analysis or FTIR Spectroscopy, is an analytical technique used to identify organic, polymeric, and in some cases, inorganic materials. A material's absorbance of infrared light at different frequencies produces a unique identification based upon the frequencies at which the material absorbs infrared light and the intensity of those absorptions. The resulting spectra produce a unique molecular "fingerprint" which can be used to easily screen and scan samples for many different components.

Both qualitative and quantitative information about the test sample can be provided. This profile is in the form of an absorption spectrum which shows peaks representing components in higher concentration.

Figure(3.25) shows the FTIR spectra of CNTs which showed no significant peaks**[66]** except in 2368.4 which might be for –COOH group in the side walls of CNTs due to oxidation. As because there are many C-C single bonds which are homonucliec and we know FTIR absorbance or

transmittence analysis does not preffer any homonuclear single bonds. So it is confirmed that there are no foreign element interactions.

3.2. Adsorption studies

Adsorption of MB dye by CNTs

Table 3.4: Determination of the capacity of adsorption of MB dye by CNTs at any time

Time min	Absorbance	Concentration of MB$\times10^{-6}$ g/50ml	Concentration of MB$\times10^{-7}$ g/l	MB adsorbed$\times10^{-7}$ g	MB adsorbed $\times10^{-4}$ mg	Adsorption at any time : q_t μ g/g
0	3.629	11.710	5.8532	0	0	0
30	3.531	11.390	5.6952	0.1580	0.1580	1.58065
60	3.312	10.680	5.3419	0.5112	0.5112	5.11290
90	2.908	9.381	4.6903	1.1629	1.1629	11.62903
120	2.606	8.406	4.2032	1.6500	1.6500	16.50000
150	1.5247	4.918	2.4592	3.3940	3.3940	33.94032
180	0.371	1.197	0.5983	5.2548	5.2548	52.54839
210	0.155	0.500	0.2500	5.6032	5.6032	56.03226
240	0.156	0.503	0.2516	5.6016	5.6016	56.01613
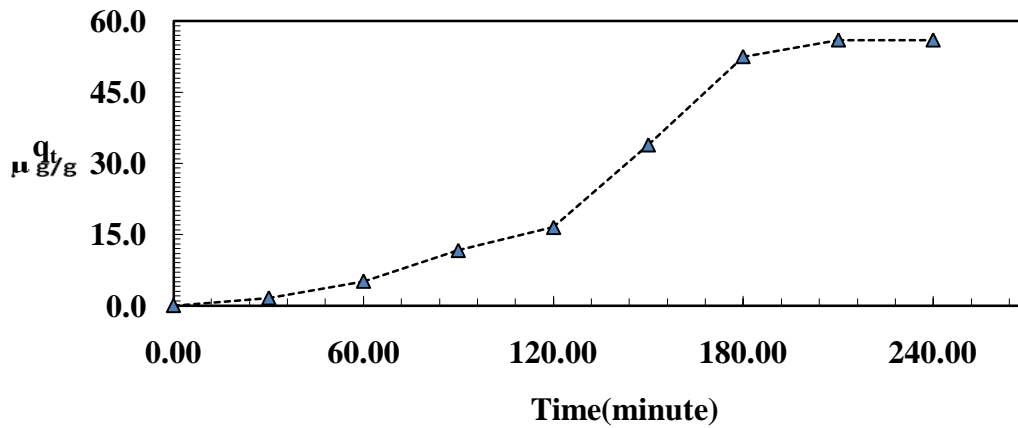
Figure3.26: Plotting of q_t against time(minute) to determine the q_e (adsorption at equilibrium state) and equilibrium time of adsorption for CNTs

Figure 3.27: Plotting of t/q_t against time(minute) to determine the rate constant of adsorption kinetics for CNTs

From the calibration study of MB dye the value of the extinction coefficient was found 310000 in ppm scale. Table(3.4) shows the calculation of adsorptions of MB by CNTs at any time (q_t) in microgram scale. Plotting the values (Figure 3.26) of q_t against times(minute) the adsorption at equilibrium state(q_e) as well as equilibrium time of adsorption were calculated. Then the rate of adsorption were checked out. From the Figure(3.27) it is confirmed that the adsorption by CNTs follows the pseudo-second-order kinectics. The plot shows a descending route which indicates that t/q_t decreases with time. From the graph (Figure 3.27) it is found that the rate constant k_2 is 1.82×10^{-5} $g\mu g^{-1}min^{-1}$ [Eq^{n}1.2(1)].

Adsorption of MB dye by NiO nanoparticles

Table 3.5: Determination of the capacity of adsorption of MB dye by NiO nanoparticles at any time

| Time min	Absorbance	Concentration of MB$\times 10^{-6}$ g/50ml	Concentration of MB$\times 10^{-7}$ g/l	MB adsorbed$\times 10^{-7}$ g	MB adsorbed $\times 10^{-4}$ mg	Adsorption at any time : qt μ g/g
0	3.629	11.706	5.8532	0	0	0
30	3.548	11.445	5.7225	0.1306	0.1306	1.30645
60	3.401	10.971	5.4854	0.3677	0.3677	3.67742
90	3.236	10.438	5.2193	0.6338	0.6338	6.33871
120	3.012	9.716	4.8580	0.9951	0.9951	9.95161
150	2.803	9.041	4.5209	1.3323	1.3323	13.32258
180	2.544	8.206	4.1032	1.7500	1.7500	17.50000
210	2.438	7.864	3.9322	1.9210	1.9210	19.20968
240	2.439	7.867	3.9338	1.9194	1.9194	19.19355
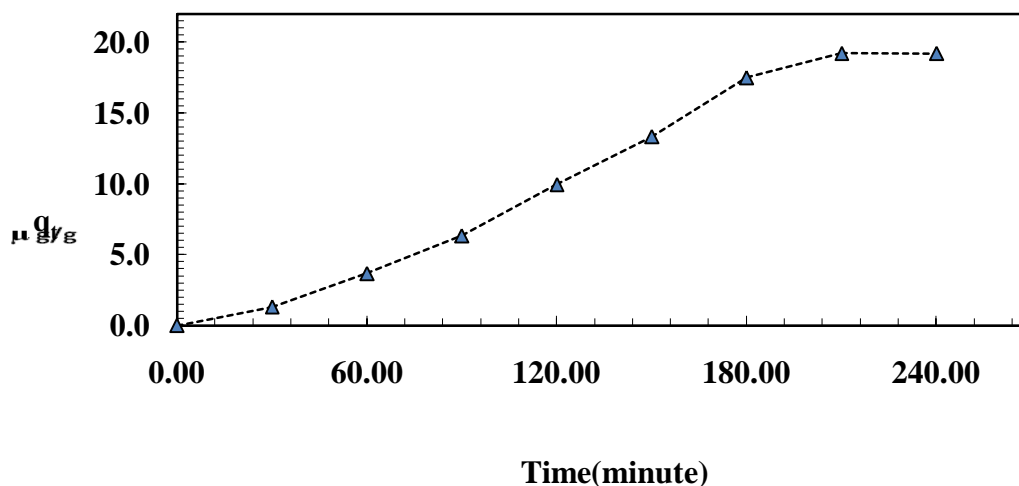
Figure 3.28: Plotting of q_t against time(minute) to determine the q_e (adsorption at equilibrium state) and equilibrium time of adsorption for NiO nanoparticles
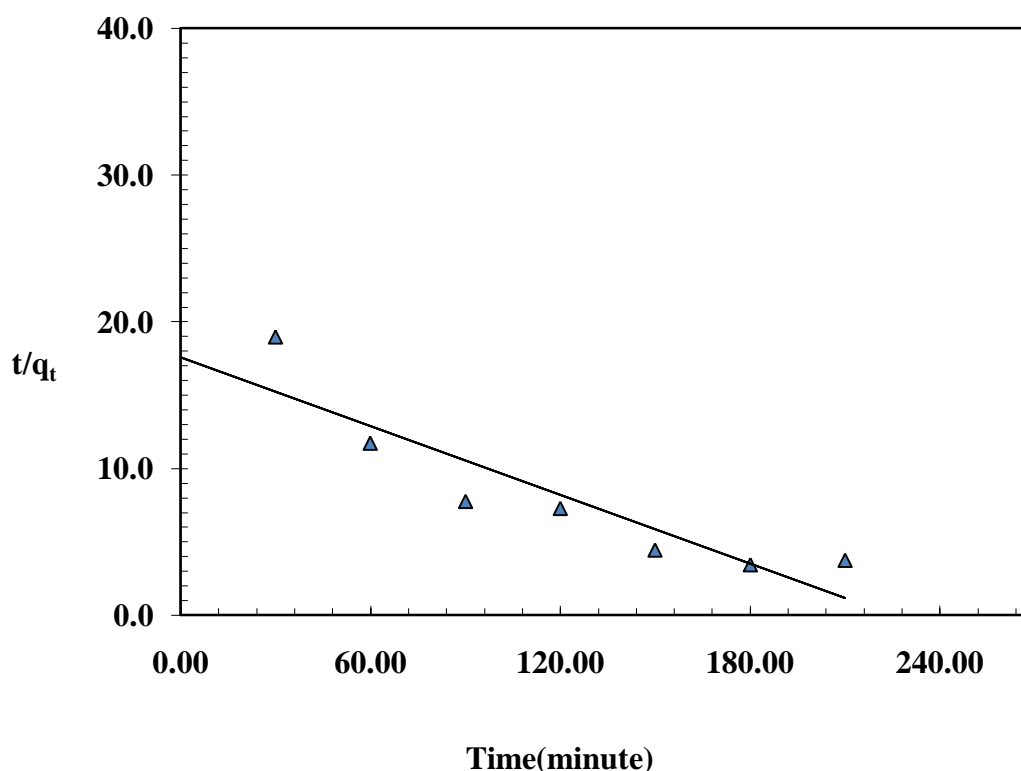
Figure 3.29: Plotting of t/q_t against time(minute) to determine the rate constant of adsorption kinetics for NiO nanoparticles

At present nanoparticles   are the most widely used adsorbent with great success due to its large surface area, microporous structure, and high-adsorption capacity. For that reason adsorption by NiO nanoparticles were studied.   Adsorption at any time q_t was calculated by using MB adsorbed in microgram scale and displayed (Table 3.5). The values of q_t against time(minute) were then plotted (Figure 3.28) and the q_e(adsorption at equilibrium) and equilibrium time of adsorption were notified. Then the rate of adsorption was checkedout. From the Figure(3.29) it is confirmed that the adsorption by NiO nanoparticles follows the pseudo-second-order kinectics. The plot shows a descending route which indicates that t/q_t decreases with time. From the graph it is found that the rate constant k_2 is 1.27×10^{-4} $g \mu g^{-1} min^{-1}$ [$Eq^n 1.2(1)$].

Adsorption of MB dye by NiO nanoparticles loaded CNTs

Table 3.6: Determination of the capacity of adsorption of MB dye by NiO nanoparticles filled CNTs at any time

| Time min	Absorbance	Concentration of $MB \times 10^{-6}$ g/50ml	Concentration of $MB \times 10^{-7}$ g/l	MB adsorbed $\times 10^{-7}$ g	MB adsorbed $\times 10^{-4}$ mg	Adsorption at any time : qt μ g/g
0	3.629	11.700	5.8532	0	0	0
30	3.255	10.500	5.2500	0.6032	0.6032	6.032258
60	2.813	9.070	4.5371	1.3161	1.3161	13.16129
90	2.396	7.730	3.8645	1.9887	1.9887	19.88709
120	1.973	6.360	3.1822	2.6709	2.6710	26.70967
150	1.408	4.540	2.2709	3.5822	3.5823	35.82258
180	0.676	2.180	1.0903	4.7629	4.7629	47.62903
210	0.255	0.823	0.4112	5.4419	5.4419	54.41935
240	0.252	0.813	0.4064	5.4467	5.4468	54.46774
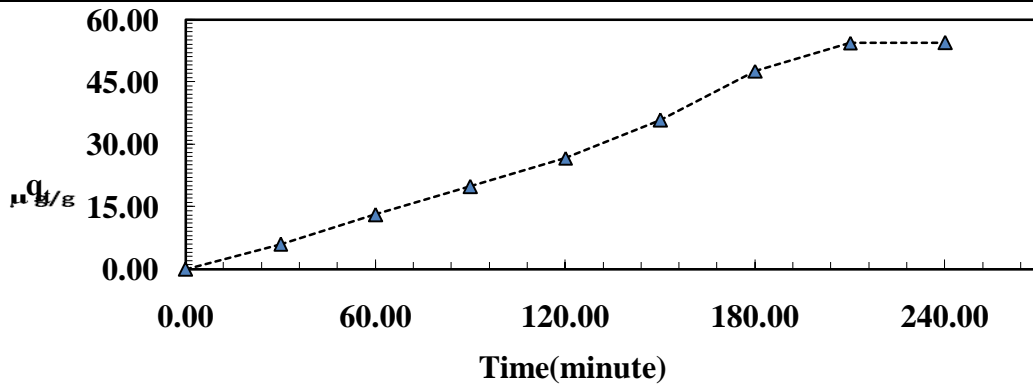
Figure3.30: Plotting of q_t against time(minute) to determine the q_e (adsorption at equilibrium state) and equilibrium time of adsorption for NiO loaded CNTs
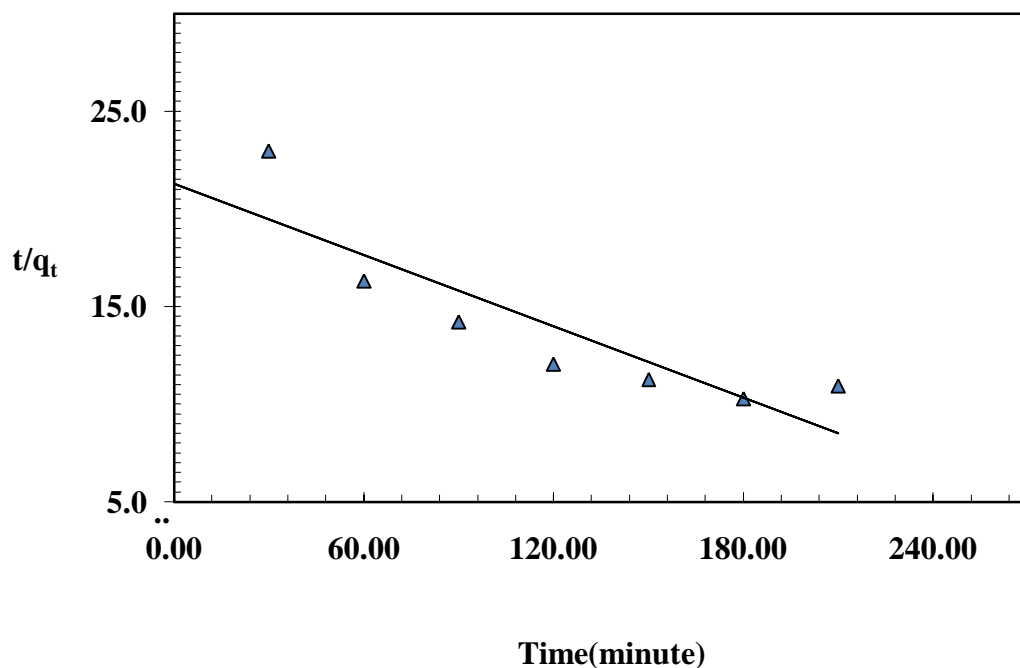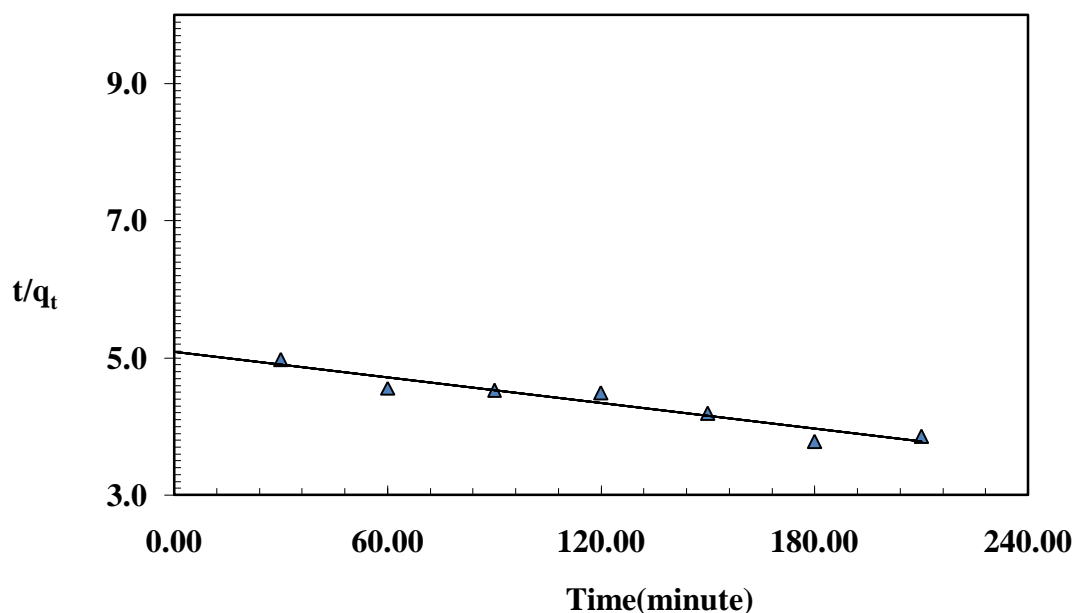
Figure3.31: Plotting of t/q_t against time(minute) to determine the rate constant of adsorption kinetics for NiO loaded CNTs

The adsorption at any time (q_t) was calculated(Table 3.6) by using MB adsorbed in microgram scale. Plotting(Figure 3.30) the values of q $_t$ against time(minute) the equilibrium time and then q_e(adsorption at equilibrium) and equilibrium time of adsorption were calculated. Then the rate of adsorption was investigated. From the Figure(3.31) it is confirmed that the adsorption by NiO nanoparticles loaded CNTs also follows the pseudo-second-order kinectics. The plot shows a descending route which indicates that t/q_t decreases with time. From the graph it is found that the rate constant k_2 is 6.62×10^{-5} gµg^{-1}min^{-1} [Eq^{n}1.2(1)].

From the adsoroption study it can be observed that the adsorption rate of NiO nanoparticles filled CNTs are higher than CNTs. This increase of rate is due to the filling of NiO nanoparticles in the hollow space of CNTs. This is because the total surface area of the NiO filled CNTs is greater than individual CNTs. This excess surface area and intra-particle diffusion did impact on the adsorption rate and they are assumed as principle rate determining steps. As CNT is comperatively costly so filled CNTs can be used in the case of sophisticated dye adsorption.

3.3. Antibacterial activity studies

Antibacterial activity measurement of individual material of pure Mn_3O_4 and Mn_3O_4 nanoparticles loaded CNTs were done by Muller Hinton agar disk diffusion susceptibility testing method according to NCCLS (National Comittee for Clinical Laboratory Standards) **[67]** and international guidelines. A total seven bacterial strains including selected gram positive and gram negative bacteria were selected to success susceptibility pattern.

Experiments were done in single and doublet from two different areas of drug loaded films in the well to find uniform distribution. The measurements of the zones inhibition (including the diameter of the well) were made with a ruler on the undferface of the plate without opening the lid. The zones of growth inhibition were compared with standard drug(ciprofloxacine).
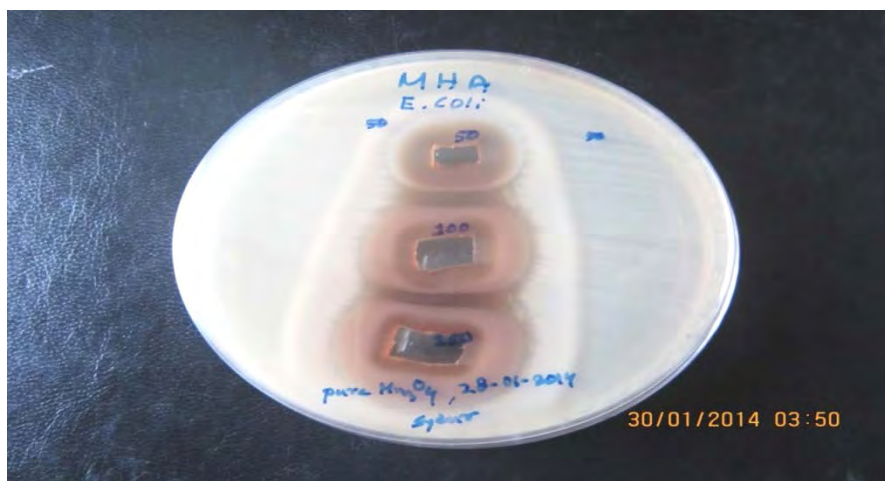
Figure 3.32: Image of zone inhibition for *Escherichia coli* by the pure Mn_3O_4 nanoparticles
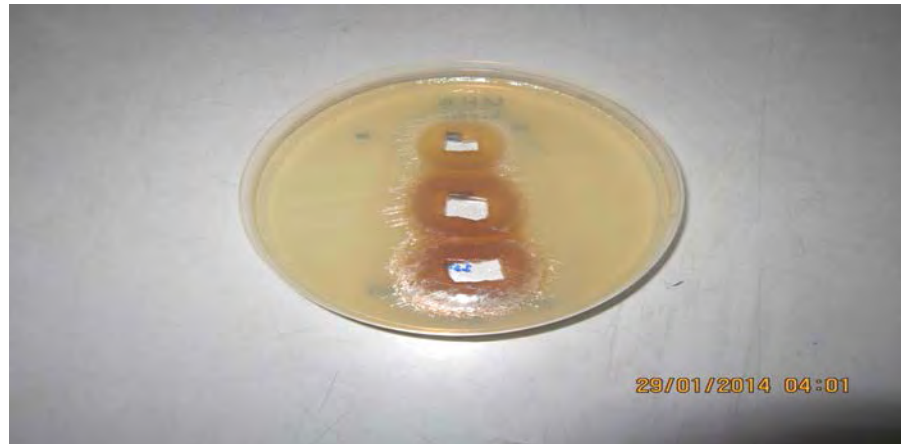
Figure 3.33: Image of zone inhibition for *Pseudomonas aeruginosa* by the pure Mn₃O₄ nanoparticles
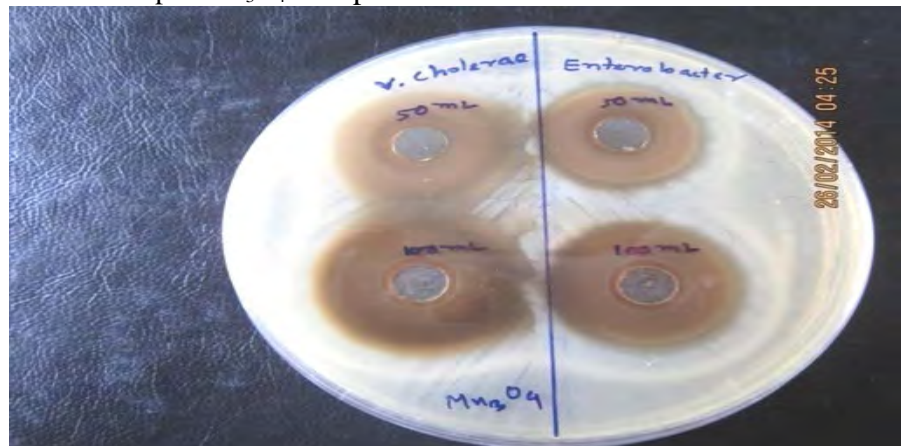
Figure 3.34: Image of zone inhibition for *Vibrio Cholerae*(left) and *Enterobacter cloacae*(right) by the pure Mn_3O_4 nanoparticles

Figure 3.35: Image of zone inhibition for *Salmonella Typhi* (left) and *Acinetobacter baumannii* (right) by the pure Mn₃O₄ nanoparticles

Figure 3.36: Image of zone inhibition for *Streptococcus pneumoniae* by the pure Mn_3O_4 nanoparticles

Table 3.7: Antibacterial activity of the Mn_3O_4 nanoparticles suspension $(0.25gL^{-1})$ against following pathogenic organisms

Name of Bacteria	Comparing the diameter of zone of inhibition of different volumes of pure Mn_3O_4 with standard disk (mm)					
	Pure Mn_3O_4			Standard disk		
	50 μL	100 μL	150 μL	50 μL	100 μL	150 μL
Escherichia coli	30	40	50	33	41	48
Pseudomonas aeruginosa	29	35	38	30.5	36	38
Vibrio cholerae	37	45	-	33	41	-
Enterobacter cloacae	34	40	-	35	42	-
Salmonella typhi	35	44	49	25	33.5	42
Acinetobacter baumannii	30	38	45	31	40	47.5
Streptococcus pneumonia	32	37	41	31	35	41

Antimicrobial activity of Mn_3O_4 nanoparticles was evaluated based on the diameters of clear inhibition zone surrounding the well in the discs . If there is no inhibition zone, it is assumed that there is no antimicrobial activity. Figure(3.32-3.36) shows representative disk diffusion plates with different bacteria after 24 h incubation. The dimeter of the zones were measured and the measured datas were provided by the Table(3.7). Inhibition zone of the well known antibaterial agent ciprofloxacin e were given in the same table simultaneously.   The diameter of inhibition zone of *Pseudomonas ae ruginosa* indicating that it is susceptible to Mn_3O_4 nanoparticles solution. But *Escherichia coli* shows more susceptibility to Mn_3O_4 than *Escherichia coli.* Susceptibility results of other 5 bacterial species (*Streptococcus pneumonia*, V*ibrio cholera*e, <u>*Salmonella Typhi*</u>, *Enterobacter cloacae*, *Acinetobacter baumannii*) are comparatively well . This experiments suggested a moderate antibacterial activity of Mn_3O_4 against these bacteria samples.
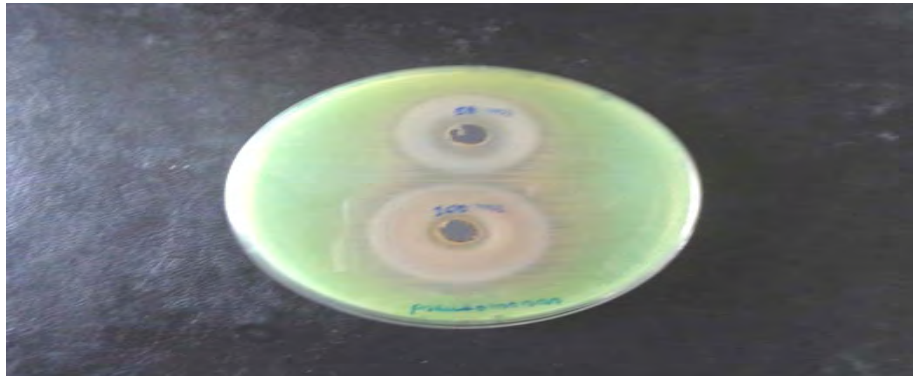
Figure 3.37: Image of zone inhibition for *Streptococcus pneumoniae*
by the Mn_3O_4 nanoparticles loaded CNTs
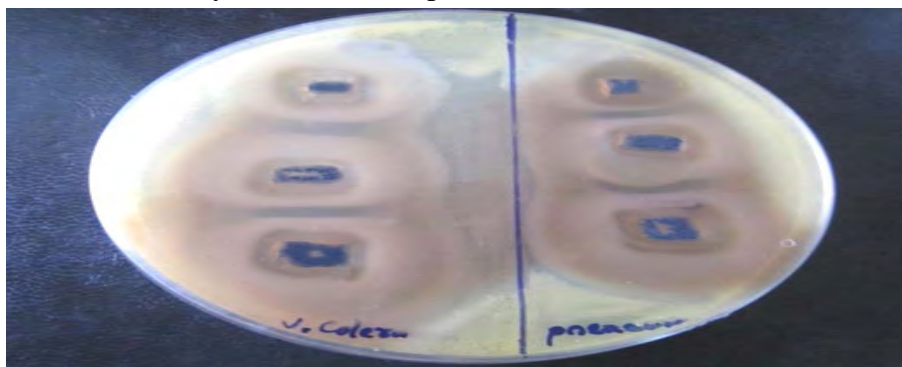
Figure 3.38: Image of zone inhibition for *Vibrio cholerae*(left) and
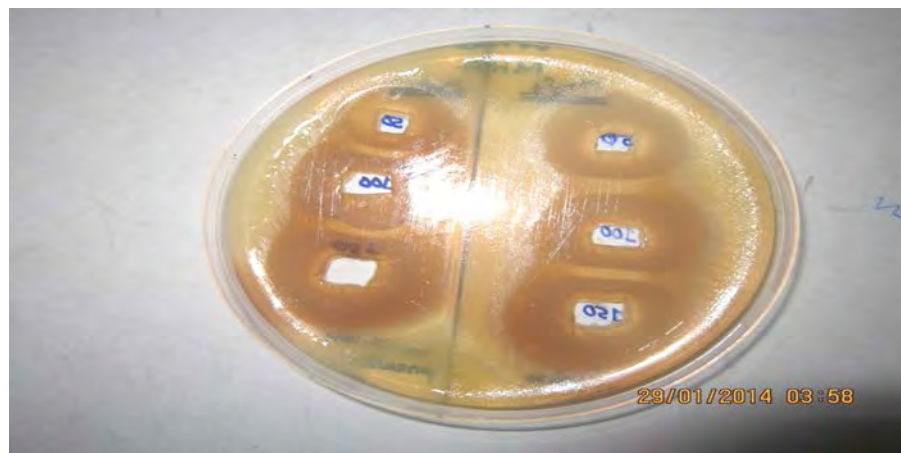*Pseudomonas aeruginosa* (right) by the Mn_3O_4
nanoparticles loaded CNTs
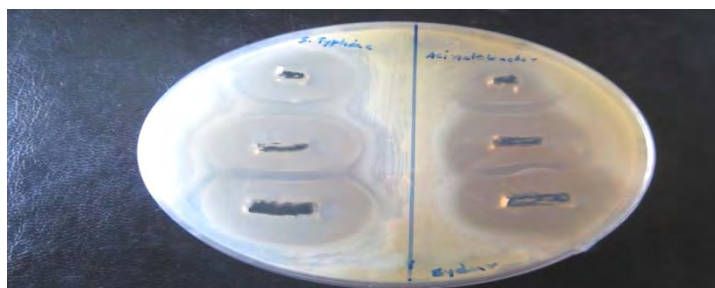
Figure 3.39: Image of zone inhibition for ***Salmonella Typhi*** (left) and ***Acinetobacter Baumannii*** (right) by the Mn_3O_4 nanoparticles loaded CNTs

Table 3.8: Antibacterial activity of Mn_3O_4 loaded CNTs comparing with the Individual Mn_3O_4 itself to check the drug delivery efficiency of CNT

Name of Bacteria	Comparing the diameter of zone of inhibition of different volumes of Mn_3O_4 encapsulated CNTs with pure Mn_3O_4 (mm)					
	Pure Mn_3O_4			**Mn_3O_4 encapsulated CNTs**		
	50 μL	**100** μL	**150** μL	**50** μL	**100** μL	**150** μL
Streptococcus pneumonia	39	42	45	32	39	-
Pseudomonas aeruginosa	29	35	38	27	34	35.5
Vibrio cholerae	37	45	-	35	42	48
Salmonella typhi	35	44	49	32	40	45
Acinetobacter baumannii	30	38	45	27	35	42

Figure(3.37-3.39) displays the effectivity of the Mn_3O_4 when they were encapsulated in the hollow space of CNTs. As there were proper diffusion of Mn_3O_4 nanoparticles so the overall experiment of encapsulated states show very good results and CNTs did not resisist the antibacterial activity of Mn_3O_4. From Table(3.8) we can see that the diameter of zone of inhibition is slightly less of about 1-3 mm which is negligible comparing with the zone diameter of direct Mn_3O_4. One of the most recent strategies proposed to incorporate nanotechnology principles is through the application of CNTs, which leads to the modulation of undesired effects and creating new conjugates with promising and improved pharmacological profiles. CNTs have been proposed and actively explored as multipurpose innovative carriers for drug delivery and diagnostic applications. CNT is a well established drug delivery agent **[68, 69]** and we know it is necessary to maintain many terms and conditions**[70]** for any substance to act as drug delivery agents and CNT satisfys all the required conditions and from our antibacterial experiments the effectivity of drugs are comparatably unchanged so using CNT as a drug delivery agent in the field of antibacterial treatment would be possible in near future.

CHAPTER FOUR

CONCLUSION

CONCLUSION

Although there have been tremendous advances in the fabrication of CNTs, the integration of these nanostructures into successful applications and large-scale production processes depend on the understanding of several fundamental issues, which are yet to be addressed. A few of these issues are briefly discussed below. The carbon arc discharge method is a technique that produces a complex mixture of components and requires further purification to separate the CNTs from the soot and the residual catalytic metals present in the crude product which is vey much complicated.   Producing CNTs in high yield depends on the uniformity of the plasma arc and the temperature of the deposit forming on the carbon electrode that is difficult to maintain.   Another formulation technique of CNTs is laser vaporization method. Arc discharge and laser vaporization methods involve evaporating the carbon source, so it has been unclear how to scale up production to the industrial level using these approaches. The role played by the support in the CVD of CNTs is not yet fully understood. The simplistic view that the support only plays a catalytically passive role in the formation of CNTs requires examination.

In this review, selective growth of CNTs(MWCNTs) by bulk chemical method   has been studied. Evidence of self-assembled carbon nanostructures is presented, In addition, CNTs growth was assumed to be possible from other carbon sources like free long chain hydrocarbons.   The integration of carbon nanotubes in this manufacturing may solve the growth uniformities too.

The simple approach for filling the CNTs with metal species (NiO,Ni)   is boiling of the mixture using capillary forces. Encapsulation of MnO_2 and Mn_3O_4 nanoparticles in CNTs was done following aqueous in-situ CNT cavity stabilization. It was observed a size-dependent filling behavior that indicates a lowering of the cavity–nanoparticles interface energy with decreasing diameter. Filling hollow CNTs with chosen materials opens new possibilities of generating nearly one dimensional nanostrutures. Although, many experimental results have been recently obtained on the filling of nanotubes, there are many aspects to be considered before a comprehensive understanding of nanocapillary could be developed such as the effect of the electronic properties of CNTs or changes of structure or melting point of liquid in nanometric cavities etc.

CNTs hold great promise for use in biomedical fields[71-74]. Among numerous potential applications, including DNA and protein sensors, bioseparators, biocatalysts, and tissue scaffolds, this research work emphasizes the use of CNTs filled with nanoactive species as medical devices, namely, drug delivery vehicles [75-79]. Although it was found that well functionalized CNTs are not toxic[80-82] *in vitro* to cells for limited doses . This work may promote a synergy of techniques and approaches that strongly increases the effectiveness of the antibacterial drugs by deploying to a target site to limit side effect. Special attention should be paid to CNTs with surface functionalization optimized for such applications, with greater chances of minimizing toxic side-effects if any.

The kinetics of adsorption of methylene blue onto nanoparticles(NiO, CNTs) and NiO loaded CNTs were investigated in this research work. The time dependent studies showed a significant adsorption capacity in this study. A batch sorption model based on the assumption of the pseudo-first and second-order mechanism were applied to predict the rate constants. The adsorption process followed a pseudo-second-order kinetic model. The values of the pseudo-second-order rate constants(k_2) were found for three individual adsorption experiments. Increasing MB concentration in solution seems to reduce the diffusion of MB in the boundary layer and to enhance the diffusion in the solid. The increase in value of k_2 of NiO loaded CNTs is due to the greater surface area of the solutes. The result showed that intra-particle diffusion is the principle rate determining steps, as such the adsorption mechanism is controlled by particle diffusion rather than CNTs diffusion for the NiO loaded CNTs.

REFERENCES

1. Yu, F.; "The growth mechanism of single-walled carbon nanotubes with a controlled diameter", *J. Physica,* 2012, 2032–2040

2. Chen, G.; "Diameter control of single-walled carbon nanotube forests from 1.3–3.0 nm by arc plasma deposition" *J. S. reports*, 2014, 3804

3. www. US Research nanometarials, inc

4. Ajayan, P.M.; Iijima, S.; "Capillarity–induced filling of carbon nanotubes". *J. Nature*, 1993, 361, 333

5. Ajayan, P. M.; Ebbesen, T. W.; Ichihashi, T. S.; Iijima; Tanigaki, K.; Hiura; H. Opening carbon nanotubes with oxygen and implications of filling. *J. Nature*, 1993, 362, 522

6. Yang, S.T.; Wang, X.; "Long term accumulation and low toxicity of single walled carbon nanotubes in intravenously exposed mice", *J. ToxicolLett.* 2008; 181, 182-189.

7. Gottardi, R.; Douradinha, B.; "Carbon nanotubes as a novel tool for vaccination against infectious diseases and cancer", *J Nanobiotechnol.*, 2013

8. Iijima, S.; ''Helical microtubules of graphitic carbon'', *J. Nature*, 1991, 354, 56–58

9. Lu, Y.; Jing, L.; Hong, H.; "Electrical Resistivity of Pristine and Functional Singl e-Wall Carbon Nanotubes", *J. Nanomaterials*, 2013, 2013

10. Bucossi, R.A.; Cress, C.D.; "Enhanced Electrical Conductivity in Extruded Single-Wall Carbon Nanotube Wires from Modified Coagulation Parameters and Mechanical Processing", *j. ACS Appl. Mater. Interfaces*, 2015, *7*, 27299–27305

11. Wang, J. N.; Luo, X. G.; Wu, T.; Chen, Y.; "High-strength carbon nanotube fibre-like Ribbon with high ductility and high electrical conductivity", *J. Nature Comm.* 2014, 3848,

12. Che, J.; Tahir; Cagın; William; Goddard; A." Thermal conductivity of carbon nanotubes", *J. Nanotechnol.*, 11, 2000, 65–69

13. Farmany, A.; "High Adsorption Capacity of Multi-Walled Carbon Nanotube as Efficient Adsorbent for Removal of Al(III) from Wastewater", *J. Particulate Science and Technology,* 2015**,** 33, 423-428

14. Mortazav, S. S.; "High Adsorption Capacity of Multi-Walled Carbon Nanotube as Efficient Adsorbent for Removal of Al(III) from Wastewater"**,** *J. Particulate Science and Technology*, 2015. 423-428

15. Barkaline, V. V.; "Adsorption properties of carbon nanotubes from molecular dynamics viewpoint", *J. Rev.Adv.Mater.Sci.*, 2009, 20, 21-27

16. Nam, D.H; Kim, J.H; Cha, S.I; Jung, S.I; Lee, J.K; Park, H.M; Park, H.D.; Hong, H.; "Hardness and wear resistance of carbon nanotube reinforced aluminum-copper matrix composites", *J. Nanosci Nanotechnol.*, 2014, 14, 9134-9138.

17. Orth, R. N.; "Creating biological membranes on the micron scale: Forming patterned lipid bilayers using a polymer lift-off technique", *J. Biophys.*, 2003, 85, 3066–3073

18. Fandiño; R.G, Membrane Perturbation by Embedded Nanopores: A Simulation Study", *J. ACS Nano*, 2016, *10*, 3693–3701

19. Dobson, J.; "Gene therapy progress and prospects: magnetic nanoparticle-based gene delivery" *J. Gene Therapy*, 2006,13, 283–287

20. Durham, E.; "Using carbon nanotubes for drug delivery" *j. nanomaterials***,** 2017, 2016

21. Ciobotaru, C.C.; Damian, M.;" Drug delivery study of single wall carbon nanotubes covalently functionalized with cis-platin", *J. Nanomater. and Biostr.*, 2014, 9, 859 - 868

22. Abdelbary, M. A.; Ahmed, W.; Hassan, I.; Dhanak, V. R.; "Nanotubes in Cancer Therapy and Drug Delivery". *J. Drug Delivery*. 2012, 2012

23. Kostarelos, K.; Lacerda, L.; Partidos, C.D.; Prato, M.; Bianco, A.; "Carbon nanotube-mediated delivery of peptides and genes to cells: translating nanobiotechnology to therapeutics", *J. Drug Deliv Sci Technol*, 2005, 15 16.

24. Bianco, A.; "Carbon nanotubes for the delivery of therapeutic molecules" *J. Expt Opin Drug Deliv*, 2004, 1, 57-65.

25. Lim, Y. T.; Kim, S.; Nakayama, A.; Stott, N. E.; Bawendi, M. G.; Frangioni, J. V.; "Selection of quantum dot wavelengths for biomedical assays and imaging," *J. Mol. Imaging*, 2003, 2, 50–64

26. Kong, Y.; Cui, D.; Ozkan, C. S.; Gao, H; "Modeling carbon nanotube based bio-nano systems: A molecular dynamics study," *J. Proc. Materials Research Soc. Symp.*, 2003, 773, 111–116.

27. Tan, G.; Mieno, T.; ''Experimental and numerical studies of heat convection in the synthesis of single-walled carbon nanotubes by arc vaporization'', *Jap. J. Appl. Phys.*, 2010, 49, 045102/1–045102/6.

28. Keidar, M.; Shashurin, A.; Volotskova, O.; Raitses, Y.; Beilis, I.I.; ''Mechanism of carbon nanostructure synthesis in arc plasma'', *J. Physics of Plasmas*, 2010, 17, 057101/1–057101/9.

29. Volotskova, O.; Fagan, J.A.; Huh, J.Y.; Phelan Jr., F.R.; Shashurin, A.; Keidar, M.; ''Tailored distribution of single-wall carbon nanotubes from arc plasma synthesis using m agnetic fields'', *j. ACS Nano*, 2010, 4, 5187–5192.

30. Escobar, M.; Giuliani, L.; Candal, R. J.; Lamas, D.G.; Caso, A.; Rubiolo, G.; Grondona, D.; Goyanes, S.; Marquez, A.; ''Carbon nanotubes and nanofibers synthesized by CVD on nickel coatings deposited with a vacuum arc'', *J. Allo. and Comp.*, 2010, 495, 446–449.

31. Zhao, T.; Liu, Y.; Li, T.; Zhao, X.; ''Current and arc pushing force effects on the synthesis of single-walled carbon nanotubes by arc discharge'', *J. Nanosci. and Nanotech.*, 2010, 10, 4078–4081.

32. Qiu, J.; Chen, G.; Li, Z.; Zhao, Z.; ''Preparation of double-walled carbon nanotubes from fullerene waste soot by arc-discharge'', *Carbon*, 2010, 48, 1312–1315.

33. Nikolaev, P.; Holmes, W.; Sosa, E.; Boul, P.; Arepalli, S.; Yowell, L;. ''Effect of vaporization temperature on the diameter and chiral angle distributions of single-walled carbon nanotubes'', *J. Nanosci. and Nanotech.*, 2010, 10, 3780–3789

34. Marchiori, R.; Braga, W.F.; Mantelli, M.B.H.; Lago, A.; ''Analytical solution to predict laser ablation rate in a graphitic target'', *J. Mater. Sci.*, 2010, 45, 1495–1502.

35. Li, Z.; Xu, Y.; Dervishi, E.; Saini, V.; Mahmood, M.; Oshin, O.D; Biris, A.S.; ''Spectroscopic characteristics of differently produced single-walled carbon nanotubes'', *J. Mater. R es. S oc. Symp.* Proceed

36. Stuerzl, N.; Lebedkin, S.; Malik, S.; Kappes, M.M.; ''Preparation of 13C single-walled carbon nanotubes by pulsed laser vaporization'', *J. Basic Solid State Phys.*, 2009, 246, 2465–2468.

37. Lu, X.Y.; Qiu, T.; Liu, J.Y.; Wu, B.H.; Weng, J.; ''Growth of carbon nanotubes in calcium phosphate matrix with different Ca/P molar ratio'',*J.Mater. Sci. Forum,* 2011, 688, 141–147.

38. Kumar, M.; Ando, Y.; ''Chemical vapor deposition of carbon nanotubes: a review on growth mechanism and mass production'', *J. Nanosci. and Nanotec.*, 2010, 10, 3739–3758.

39. Kumar, M.; Zhao, X.; Ando, Y.; Iijima, S.; Sharon, M.; Hirahara, K.; ''Carbon nanotubes from camphor by catalytic CVD'', *J. Molec. Cryst. and Liq. Cryst.*, 2002, 387, 117–121.

40. Hosseini, A.A.; Taleshi, F. ''Large diameter MWNTs growth on ironsprayed catalyst by CCVD method under atmospheric pressure'', *Ind. J. Phys.*, 2010, 84, 789–794.

41. Liu, Q.X.; Ouyang, Y.; Zhang, L.Y.; Xu, Y.; Fang, Y.; ''Effects of argon flow rate and reaction temperature on synthesizing single-walled carbon nanotubes from ethanol'', *J. Physica E: Low-Dimen. Syst. & Nanostruc.*, 2009, 41, 1204–1209.

42. Biris, A.R.; Lupu, D.; Misan, I.; Dervishi, E.; Li, Z.; Xu, Y.; Trigwell, S.; Biris, A.S.; ''High crystallinity multi wall carbon nanotubes synthesized by inductive heating CCVD'', *J. Optoelectr. and Adv. Mater.*, 2008, 10, 2311–2315.

43. Abechi E.S.; Gimba C.E; Uzairu A.; Kagbu J.A.; "Kinetics of adsorption of methylene blue onto activated carbon prepared from palm kernel shell" *Archives of Applied Science Research, www.scholarsresearchlibrary.com*, 2011, 3, 154-164

44. Dresselhauss, M.S.; Eklund, P.C.; "Phonons in carbon nanotubes" *J. Adv Phys.* 2000, 49, 705–814.

45. Bandow, S.; Asaka, S.; "Effect of the growth temperature on the diameter distribution and chirality of single-wall carbon nanotubes", *J. Phys Rev Lett.*,1998, 80, 3779.

46. Duha, S. A.; Adawiya, J.;" Compare ion of functionalization of multiwalled carbon nanotubes treated by oil olive and nitric acid and their characterization ",*Sci. Direc.*, 2013, 36, 1111 – 1118.

47. Maxim, N.; "Effect of Mild Nitric Acid Oxidation on Dispersability, Size, and Structure of Single-Walled Carbon Nanotubes" *J. Chem Mattr*, 2007, 19, 5765-5772

48. Yakub, M.T.; "Dye and its removal from aqueous solution by adsorption: a review", *J. Adv. Colloid Interface Sci.*, 2014, 209, 172-184.

49. Farooqui, M.; Sultan, S.; "Adsorption studies of Methylene Blue dye from aqueous solution onto *phaseolus aureus* biomaterials", *Ind. J. of Chem. Technol.*, 2004 *11*, 190-193

50. Bello, O. S.; "Adsorption of Dyes Using Different Types of Sand: A Review" , *J. Chem. S. R.*, 2013, 66, 117–129

51. Abechi, E.S.; Gimba, C.E; Uzairu, A.; Kagbu, J.A.; "Kinetics of adsorption of methylene blue onto activated carbon prepared from palm kernel shell" *Archives of Applied Science Research, www.scholarsresearchlibrary.com*, 2011, 3, 154-164

52. Ho, Y. S.; "Pseudo-second-order model for lead ion sorption from aqueous solutions onto palm kernel fiber", *J. Hazard. Mater.*, 2006, B12, 9137–142

53. Uddin, I.; Venkatachalam, S.; Mukhopadhyay, A.; Usmani, M.A.; "Nanomaterials in the Pharmaceuticals: Occurrence, Behaviour and Applications", *J. Curr. Pharm. Des.*, 2016, 22, 1472-84.

54. Chen, Y.; Liu, C.; Li, F.; Cheng, H.; "Preparation of single-crystal α- MnO_2 nanorods and nanoneedles from aqueous solution", *J. Alloys Compd.*, 2005; 397, 282-285.

55. Yuan, A.; Wang, X.; Wang, Y.; Hu, J.; "Textural and capacitive characteristics of MnO_2 nanocrystals derived from a novel solid-reaction route", *J. Electrochim Acta*, 2009, 54, 1021-1026.

56. Zhang, X.; Duan, Y.; Guan, H.; Liu, S.; Wen, B.; Effect of doping MnO_2 on magnetic properties for M-type barium ferrite. *J. Magn. Mater.*, 2007; 311: 507-511.

57. NCCLS, National Committee for Clinical Laboratory Standards. www.en.wikipedia.com/NCCLS

58. Treacy, M.M.J.; Ebbessen, T.W.; Gibson, J.M.; "Exceptionally High Young's Modulus Observed for Individual Carbon Nanotubes," *J. Nature London*, 1996, 381, 678–680.

59. Li, C.; Chou, T.W.; "A Structural Mechanics Approach for the Analysis of Carbon Nanotubes," *Int. J. Solids Struct*.", 2003, 40, 2487–2499.

60. https://en.wikipedia.org/wiki/Carbon_nanotube

61. Hoyos-Palacio, L.M; "Catalytic effect of Fe, Ni, Co and Mo on the CNTs production", IOP Conf. Ser., 2014 Mater. Sci. Eng.

62. http://www.shimadzu.com.br/analitica/produtos/elemental/raios_x/eds/catalogos/edx.pdf

63. Sahu, S.; "Preparation of long aligned carbon nano tubes and study its physical properties", *Dept. of Physics, National institute of Technology, Udissa*, 2012-2014

64. http://alternativeartsproject.net/readpdf/nelson-advanced-functions-chapter-2-solutions.pdf

65. http://www.eng.uc.edu/~beaucag/Classes/XRD/Chapter3html/Chapter3.html

66. Misra, A.; "FTIR spectroscopy of multiwalled carbon nanotubes: a simple approach to study the nitrogen doping", *J. nano sci nanotech*, 2007, 7, 1820

67. NCCLS, National Committee for Clinical Laboratory Standards. www.en.wikipedia.com/NCCLS

68. Pastorin, G.; "Crucial Functionalizations of Carbon Nanotubes for Improved Drug Delivery".*J. Pharmaceutical Research.* 2009, 26, 746–769.

69. Hilder; Tamsyn, A*.;* Hill, James, M. "Modeling the Loading and Unloading of Drugs into Nanotubes". 2009, 5 , 300–308

70. www.drugdel.com

71. Davalapalli, H.; "Role of nanotechnology in pharmaceutical product development" *J pharm sci.*, 2007, 96, 2547-65

72. Harris, P.J.F; "Carbon nanotube science: Synthesis, Properties and Applications", *Cambridge University Press, Cambridge,* 2009

73. . Liu, Z.; Davis, C.; "Circulation and long-term fate of functionalized, biocompatible single-walled carbon nanotubes in mice probed by Raman spectroscopy" *ProcNatlAcadSci USA.* 2008; 105, 1410-15.

74. Yang, S.T.; Wang, X.; "Long term accumulation and low toxicity of single walled carbon nanotubes in intravenously exposed mice", *J. ToxicolLett.* 2008; 181, 182-189.

75. Kam, N.W.S.; Jessop, T.C.; Wender, P.A.; "Nanotube molecular transporters: internalization of carbon nanotube-protein conjugates into mammalian cells", *J. Am. Chem. Soc.*, 2004126, 6850-6851

76. O'Connell, M.; Wisdom, J.A.; Dai, H.J.; "Carbon nanotubes as multifunctional biological transporters and near-infrared agents for selective cancer cell destruction", *Proc. Natl. Acad. Sci.*, 2005 102, 11600- 11605

77. Kang, B.; YU, D.C.; Chang, S.Q.; Chen, D.; Dai, Y.D.; Ding, Y.T. "Intracellular uptake, trafficking and subcellular distribution of folate conjugated single walled carbon nanotubes within living cells. *J. Nanotechnology*, 2008, 19, 375103-375110

78. Kim, S.N.; "Carbon nanotubes for electronic and electrochemical detection of biomolecules", *J. Adv. Mater.,* 2007, 19, 3214- 3228

79. Kolosnjaj-Tabi; "In vivo behavior of large doses of ultrashort and full-length single-walled carbon nanotubes after oral and intraperitoneal administration to Swiss mice. *J. ACS Nano*, 2010, 4, 1481-1492

80. Khalid, P.; Hossain, M.A.; "Toxicology of Carbon Nanotubes - A Review", *Int. J. of Appl. Eng. Res.*, 2011, 11, 148-157

81. Sun, Z.; "Carbon Nanotubes release Cytotoxicity Mediated by Human Lymphocytes In Vitro", *j.Plos one* 2011, 0021073

82. Elkin, T.; Jiang, X.; Taylor, S.; Lin, Y.; Gu, L.; Yang, H.; Brown, J.; Collins, S.; Sun, Y.P.; "Immuno carbon nanotubes and recognition of pathogens. *J. ChemBiochem*. 2005; 6, 640-43